ABSTRACT

MILLER, ANTHONY D. Repair of Impact-Damaged Prestressed Concrete Bridge Girders Using Carbon Fiber Reinforced Polymer (CFRP) Materials. (Under the direction of Dr. Sami Rizkalla).

Over-height vehicles impacting prestressed concrete (PS) and reinforced concrete (RC) bridge girders is a frequent problem experienced by the majority of transportation departments all over the world. The most common practice used to restore a damaged bridge is to cut out the damaged girder and replace it with a new one. More recently, alternative methods have been examined to help decrease the costs of replacing damaged girders and minimizing closure time. The research reported in this thesis considered three scenarios to examine the effectiveness of using Carbon Fiber Reinforced Polymers (CFRP) to restore impact-damaged PS girders to their original capacity. The first scenario investigated the effectiveness of CFRP sheets to repair a 54 ft (16.4 m) long girder with one ruptured prestressing strand caused by an over-height vehicle impact. The second scenario investigated the effectiveness of CFRP sheets to repair two 54 ft (16.4 m) long girders with various numbers of prestressing strands ruptured artificially at midspan. The final scenario examined the effectiveness of CFRP sheets to repair a shear-critical specimen with four prestressing strands artificially ruptured near the support.

The design of all CFRP repair systems was conducted using a cracked section analysis and/or guidelines for shear capacity of prestressed members. The predictions according to the two approaches compared well with the measured values. The designs were compared to current codes and a recently developed debonding model. All of the repaired girders were able to reach and surpass their respective undamaged capacities. All of the flexural tests failed due to crushing of concrete.

REPAIR OF IMPACT-DAMAGED PRESTRESSED CONCRETE BRIDGE GIRDERS USING CARBON FIBER REINFORCED POLYMER (CFRP) MATERIALS

by

ANTHONY DAVID MILLER

A thesis submitted to the Graduate Faculty of
North Carolina State University
in partial fulfillment of the requirements for
the Degree of Master of Science

Civil Engineering

Raleigh, NC

2006

Approved By:

Dr. Sami Rizkalla (Chair)

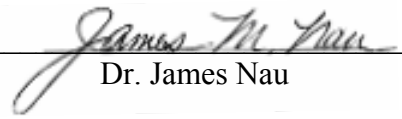

Dr. James Nau

Dr. Emmett Sumner

To all my family and friends;
past, present and to come

BIOGRAPHY

Anthony Miller began his study of Civil Engineering in 2000 at the Virginia Military Institute. In 2004, he obtained his Bachelor of Science in Civil Engineering with a minor in mathematics. Anthony enrolled at North Carolina State University in 2004 in pursuit of a Master's of Science degree in Civil Engineering with an emphasis on structural engineering. Upon completion of his MS degree, he intends on working in the corporate sector in pursuit of his Professional Engineering license.

ACKNOWLEDGMENTS

I would like to acknowledge the generous financial support as well as the donation of material and manpower that have made this project possible. First, I would like to thank the North Carolina Department of Transportation for their financial support and guidance throughout the project. Special thanks are extended to Ed Fyfe, Sarah Witt, and Tyler Maas of Fyfe, Inc. for all of their various contributions.

Dr. Rizkalla, I not only would like to thank you for all the invaluable help and guidance you have given me as an advisor and mentor, but also thank you for entrusting me with a project of this magnitude. I shall never forget the lessons I have learned from you that affect every aspect of my life. I would also like to extend a special thanks to Dr. Emmett Sumner and Dr. James Nau for graciously accepting to be members of my advisory committee.

I would next like to thank the staff of the Constructed Facilities Laboratory. Without your knowledge and expertise of the testing facility, equipment, and administrative duties, I would still be lost. I would especially like to thank Jerry Atkinson. You were always willing to lend a hand every time I was struggling.

Thanks are also extended to all of my fellow CFL graduate students for their endless help and friendship. A very special thanks is extended to Owen Rosenboom who not only laid the foundation for this project, but also kept me on track and constantly ensured that everything ran relatively smooth. I would also like to thank Trina Walter for assisting me with all of the never-ending lab duties this project required. Lastly, I would like to thank Matthew Boylan for always giving up his hopes and dreams for everyone.

Lastly I would like to thank my family and friends, who have always supported me throughout all of my endeavors. Mom and dad, your love, patience, and generosity will never be forgotten.

TABLE OF CONTENTS

LIST OF TABLES

LIST OF FIGURES

REPAIR OF IMPACT-DAMAGED PRESTRESSED CONCRETE BRIDGE GIRDERS USING CARBON FIBER REINFORCED POLYMER (CFRP) MATERIALS

By

Anthony David Miller

Under the guidance of Dr. Sami Rizkalla

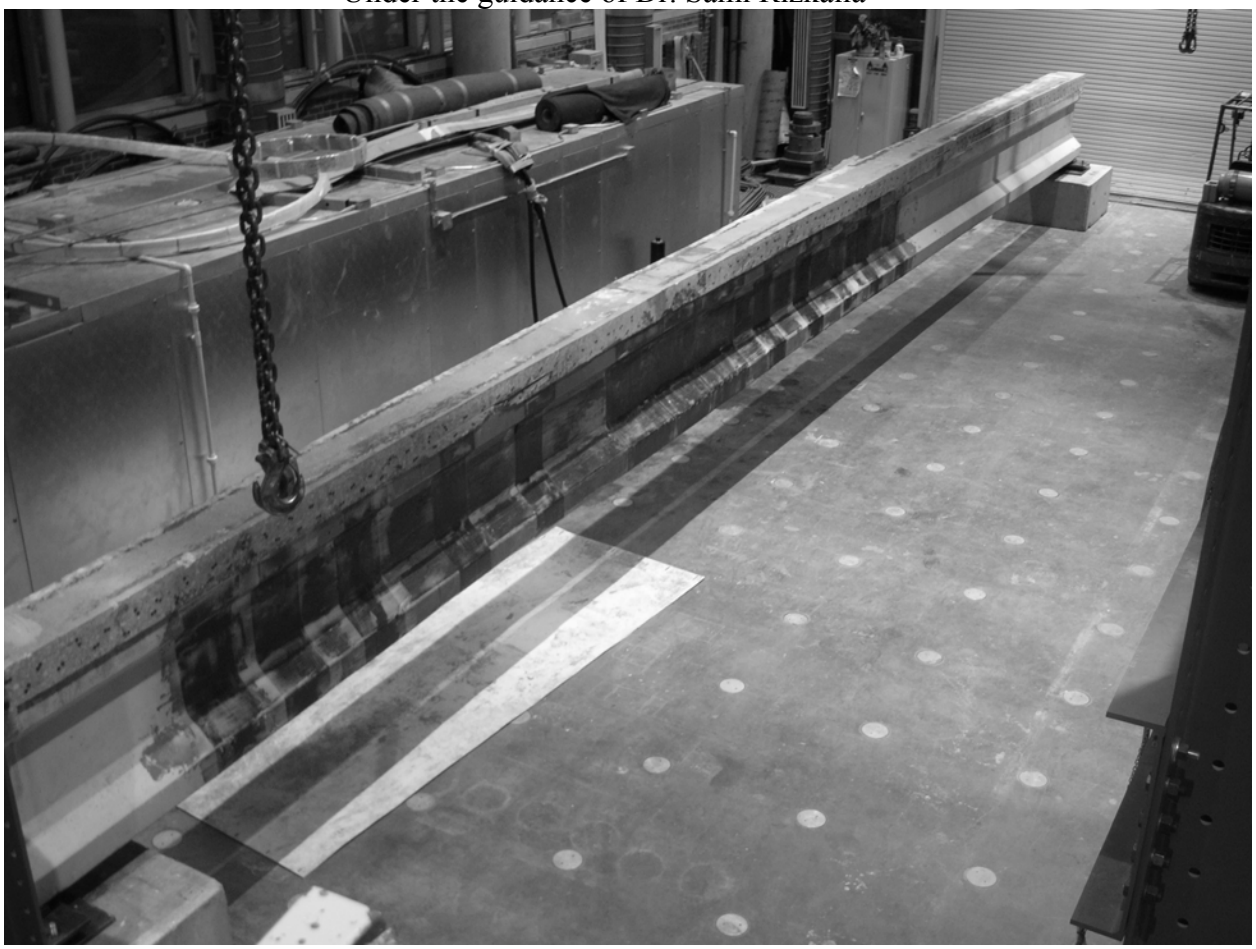

North Carolina State University
Raleigh, North Carolina

2006

1. Introduction

1.1 Background

Impact damage by over-height vehicles to reinforced concrete (RC) and prestressed (PS) concrete bridge girders is an ever recurring problem facing bridge maintenance departments throughout the United States, and in the rest of the world. According to one report, 81 percent of damaged prestressed girders were caused by lateral overheight vehicular loads (Shanafelt and Horn 1980). Aside from the obvious structural damage to the bridge resulting from the impact, the damage also results in long traffic delays during maintenance, potential safety hazards, large financial burdens on maintenance budgets, and negative psychological effects on highway users.

As much of a problem as impact damage may be, roughly 86 percent of the occurrences only cause minor to moderate damage to the girder. Minor to moderate damage can be defined as anything ranging from isolated cracks and shallow spalls, up to large spalls that expose undamaged prestressing stands. Only approximately 14 percent of impact damage occurrences are severe enough that they cut prestressing strands and remove large portions of the concrete section (Feldman et al 1998). The current research was focused on these severe cases.

For most transportation departments, the common practices for dealing with severely impact-damaged bridge girders is to saw-cut the deck, remove the girder, and replace with a new girder. Several options have been examined in the past, as well as new solutions proposed and researched by transportation departments, to eliminate the need for complete removal of severely impacted PS girders. This research project was proposed to evaluate the

effectiveness of externally bonded Carbon Fiber Reinforced Polymer (CFRP) sheets as a repair system for impact-damaged PS bridge girders.

The use of CFRP materials began after WWII primarily in military applications. Significant use then expanded within the aerospace and automotive industries. The use of FRP materials within the transportation infrastructure, either as a retrofit material or in construction of new structures, gained popularity in the 1980's. Today, CFRP bars, strips, tendons, and wet lay-up sheets are commonly used in the repair and retrofit of concrete structures. Some of the major benefits of CFRP include its high strength to weight ratio, high fatigue endurance and the ease of fabrication, manufacturing, handling and installation.

One of the most common uses of CFRP materials is to externally bond the material directly to the concrete surface. The sheets are typically bonded to the tension side of the members to increase the flexural strength and/or on the sides of the member to improve the shear capacity. Installation of this technique is relatively simple and can be achieved in a very short time. The system must be designed to avoid premature failure due to possible delamination or debonding of the CFRP material from the concrete surface, a failure mode that many researchers are currently investigating (Teng et al 2001, Oehlers and Seracino 2004, Rosenboom 2006).

1.2 Objectives

The primary objective of the research project is to evaluate the feasibility of using CFRP sheets as a repair system for severely laterally impact-damaged girders. The secondary objective of the research is to evaluate existing design methods for application to FRP repair systems for impact-damaged prestressed bridge girders.

1.3 Scope

To complete the primary objective, the scope of the investigation included the following:

1) A comprehensive state-of-the-art literature review of CFRP strengthening and repair systems. The review included published reports and field applications pertinent to the use of CFRP systems for shear and flexural behavior.
2) Repair of an impact damaged AASHTO Type II bridge girder with a CFRP system to restore its original capacity. The girder was tested under fatigue loading conditions and loaded monotonically to failure.
3) Two AASHTO Type II girders underwent simulated impact damage and subsequent repair with a CFRP system to restore their original flexural capacity.
4) Damage and repair two AASHTO Type II girders to restore their original shear capacities using CFRP.
5) Determine the mechanical properties of the CFRP sheets, prestressing tendons and concrete for each test specimen.
6) Test the above girders to determine and evaluate the behavior up to failure. This included the fatigue behavior of the structural system, as well as the behaviors prior to cracking, post-cracking, at yielding, and at ultimate. Each specimen was compared with its respective prediction and/or undamaged behavior.
7) Prepare an analytical model to provide an in-depth understanding of the behavior of the repaired girders. The analytical modeling was performed using RESPONSE© 2000, a cracked section analysis program, PCI design guidelines, as well as design guidelines presented by ACI Committee 440.

8) Compare the measured behavior to the predicted values using various common design codes. Where applicable, experimental results of the repaired girders were compared to initial tests performed on the same girders prior to damage and repair.
9) Perform both a flexure and shear parametric study to predict the repair systems necessary while changing several variable, such as the number of ruptured prestressing strands, amount of concrete damage, as well as different types of AASHTO girders.

2. Literature Review

2.1 Overview

A literature survey was conducted during the course of this research project. The survey included published experimental, analytical studies, and field applications, of using FRP for repair and strengthening of structures. FRP composites are characterized by excellent tensile strength in the direction of the fibers and by negligible strength in the transverse direction of the fibers. They are lightweight, easily installed, and very resistant to corrosion. FRP composites are relatively new in the transportation industry, but have been used in the aerospace, automotive, and military industries since the 1940's. This chapter provides a summary of the survey including: 1) FRP strengthening of reinforced and prestressed concrete girders, 2) repair of reinforced and prestressed concrete girders using traditional techniques, 3) repair of reinforced and prestressed concrete girders using FRP, 4) field applications of RC and PS concrete bridge girder repairs, and 5) current FRP flexure and shear design guidelines.

2.2 Strengthening of Reinforced and Prestressed Concrete Girders with FRP

Strengthening of both reinforced and prestressed concrete girders with Fiber Reinforced Polymers (FRP) materials has become increasingly widespread in many laboratory settings and field applications. A wide array of research exists on the strengthening of reinforced concrete (RC) members with CFRP, however there has been little research until recently involving the strengthening of prestressed (PS) members using FRP materials. This section will discuss the failure modes of RC and PS concrete girders

strengthened with CFRP and the behavior of concrete members strengthened with flexure and/or shear CFRP systems.

Failure Modes

The three types of failure modes of RC and PS members strengthened with CFRP materials are flexure, shear, and debonding of the FRP. Flexure failure includes concrete crushing and rupture of longitudinal steel/FRP reinforcement. Shear failure includes inclined failure near the support and horizontal splitting anywhere along the member length. FRP debonding failures include plate-end debonding and intermediate crack debonding.

Concrete crushing in the compression zone of any member is the desired mode of failure, and is recognizable either by localized or global crushing of the concrete in the compression zone. In order for this to occur, proper design and detailing of the CFRP strengthening system must be performed. Rupturing of the FRP reinforcement is caused by the strain in the FRP exceeding the maximum allowable strain. This results in a sudden and brittle failure of the FRP. The rupturing of prestressing strands or reinforcing bars results in ductile flexural failure. However, in most cases rupture of the longitudinal steel occurs as a result fatigue rupture during service loading levels. The other mode of failure that can occur in concrete members strengthened with FRP is shear failure. Shear failure is a result of the shear demand on a section being greater than the shear capacity of that same section. This brittle failure usually occurs in short-span members near the supports and is recognizable by a large inclined crack forming near the support.

Lastly, two different debonding failure modes exist within concrete members strengthened with FRP. These debonding failures don't allow the FRP material to utilize its full strength capacity. The first is plate-end debonding, which is characterized by the peeling

off of a chunk of concrete attached to the FRP material starting at the termination point and propagating toward midspan. This results from a stress concentration at the termination point of the FRP. Plate end debonding can be minimized with the usage of transverse U-wraps (Rizkalla et al. 2005). The second debonding failure mode of FRP is known as intermediate crack debonding. Intermediate crack debonding is caused by a localized stress concentration at a flexural crack that leads to peeling of the FRP through the concrete substrate, propagating toward the support. As with plate end debonding, this effect can be minimized with the usage of transverse U-wraps (Rizkalla et al. 2005).

Flexural Strengthening

There are many papers that exist which deal with the flexural strengthening of concrete members using FRP materials. Only several of those papers will be discussed here; first RC strengthening and then PS concrete strengthening.

CFRP flexurally strengthened reinforced concrete beams were tested by Ceroni et al. (2004) to examine their cracking behavior. Ten 15.75 by 7.87 by 145 in (400 by 200 by 3700 mm) beams were statically tested to failure, with crack widths and patterns measured at intervals until yielding of the reinforcing steel. One specimen was a control specimen; two were strengthened with CFRP sheets, one specimen with two layers and one specimen with three layers. The last seven members were strengthened with Steel Reinforced Fibers (SRP) to investigate the behavior of this new material. The crack spacing was not affected by the presence of external reinforcing, but flexural crack widths were much smaller in the strengthened specimens. The experimental cracking patterns and crack widths corresponded well to analytical model predictions using an approach that allows for non-linear constitutive relationships and bond laws.

Arduini et al. (2002) tested several severely degraded reinforced concrete bridge girders that had been decommissioned. Four girders were strengthened with several layers of FRP sheets and transverse U-wraps. Failure of one girder was due to debonding of the longitudinal CFRP sheets between U-wraps. Two other girders failed as a result of CFRP rupture and the last girder failed by crushing of the concrete. The research concluded that the CFRP flexural design guidelines produced by the ACI Committee 440 (2002) adequately corresponded to the observed flexural behavior of the strengthened specimens.

Flexurally strengthening prestressed concrete girders was examined by Reed and Peterman (2004). Two longitudinal layers of CFRP sheets were able to increase the flexural capacity of two single-T prestressed members by 20 percent over the control specimen. The single-T sections were each 36 in (915 mm) wide, 23 in (585 mm) deep, and 40 ft (12.2 m) long. The longitudinal CFRP sheets for the first strengthened specimen extended the entire length of the girder with one 12 in (305 mm) wide transverse U-wrap at each termination point. This strengthened specimen achieved a 23 percent increase in load capacity versus the control specimen before a horizontal shear crack occurred in the tension zone at midspan and extended toward the support. Failure resulted from the horizontal shear crack because of the narrow web of the single-T section. Rupture or debonding of the longitudinal CFRP did not occur. The longitudinal CFRP sheets of the second strengthened member also extended the full length of the girder, however in addition to the 12 in (305 mm) U-wrap located at the ends of the longitudinal sheets, eleven additional U-wraps, each one of which is comprised of two 6 in (152 mm) layers, were spaced at 18 in (458 mm) along the length of the girder. This second specimen achieved a 25.6 percent increase in capacity versus the control specimen with rupturing of the longitudinal CFRP sheets being the mode of failure. The presence of

the U-wraps not only aided in preventing debonding failure, but also prevented the formation of the horizontal shear crack that had led to the failure of the first strengthened specimen.

Another experimental program performed by Rosenboom and Rizkalla (2006) examined the strengthening of six prestressed concrete C-channel type girders, each 30 ft (9.14 m) in length. The longitudinal strengthening system for each girder was extended the full length of the girder with 6 in (152 mm) wide transverse CFRP U-wraps located at each termination point as well as spaced at 3 ft (914 mm) intervals along the length of the longitudinal CFRP. The U-wraps were provided to prevent plate end debonding at the termination points as well as intermediate crack debonding at midspan. A maximum increase in the flexural capacity of 73 percent over a control specimen was achieved using externally bonded CFRP sheets.

Shear Strengthening

Research on CFRP shear strengthening of RC/PS members is less common than CFRP flexural strengthening research. Research strengthening RC structures will be presented first, followed by CFRP strengthening of prestressed members.

Li et al. (2001) reported on the effects of varying the amount of flexure and shear CFRP reinforcement for 4.5 ft (1350 mm) long RC beams. Five girders, four of which were strengthened, were all tested in 4-point bending. They concluded that in order to strengthen an RC beam in shear, it is necessary to first provide flexural strengthening because the first cracks always form in the flexural tension zone.

In order to determine the effectiveness of various CFRP shear strengthening schemes, Adhikary and Mutsuyoshi (2004), tested eight RC beams. Each beam was 6 in (150 mm) wide by 8 in (200 mm) deep by 8.5 ft (2.6 m) in length. Steel shear reinforcement was not

provided to ensure that shear failure occurred in the strengthened members. After testing one control specimen and seven strengthened sections with CFRP sheets, it was concluded that transverse U-wraps extending to the top of the member are more effective than vertical sheets not extending to the top of the member or horizontal sheets. U-wraps alone also achieved a higher loading level than a combination of horizontal and vertical CFRP sheets.

Micelli et al. (2002) examined the shear behavior of twelve RC joist beams strengthened with various CFRP strengthening schemes. The T-section RC beams were 26 in (660 mm) wide by 15 in (381 mm) deep by 108 in (2740 mm) in length. Each specimen was statically loaded to failure near the support to compare the ultimate load capacities of each strengthening scheme. The variables studies in this research were number of layers of U-wraps and the use of FRP shear anchorage systems. It should be noted that FRP flexural reinforcing was required to ensure shear failure in all the members. The experimental results showed that using more than one unanchored U-wrap in the same location does not proportionally increase the shear capacity based on the number of layers, but only increases the overall shear contribution of the system by a negligible percentage. This was because debonding failure controlled both the one and two layer U-wrap systems. It was also concluded that using an end anchorage system greatly increased the capacity of U-wraps when compared to those without anchorage.

De Lorenzis and Nanni (2001) tested six shear-critical reinforced concrete girders strengthened with NSM CFRP bars. The 10 ft (3.05 m) long T-section girders were tested in four-point bending to failure, with an a/d ratio of 3.0. Inclining the FRP rods at 45 degrees was found to increase the effectiveness of the FRP rods versus vertical rods by as much as 43 percent over a girder with the same amount of FRP oriented in the vertical direction. The

two failure modes observed were debonding of the FRP rods in one or more test and splitting of the concrete cover of the longitudinal reinforcement. Debonding of the FRP rods could be prevented by inclining the rods at 45 degrees or decreasing the spacing between rods. In the absence of steel stirrups, an increase of 105 percent over the control girder load capacity was achieved using inclined rods. The increased shear contribution of inclined shear reinforcing versus vertical shear reinforcing was taken into consideration during the design of the CFRP sheet repair system discussed in Section 3.4.

Very little research is available utilizing the shear strengthening of prestressed concrete members with CFRP. One possible explanation is that most prestressed members are extremely long with a high a/d ratio, making them shear-critical only in rare cases. One study, performed by Reed and Peterman (2004), examined the shear strengthening of single-T sections using CFRP sheets. Each specimen was 16 ft (4.88 m) in length and strengthened with transverse U-wraps at the end and evenly spaced at 18 in (457 mm) intervals throughout the length of the member. The one variable introduced in this study was the presence of an overhang, a 2 ft (0.61 m) long cantilevered section beyond the support, or lack thereof. The load was applied to both sets of girders 4 ft (1.22 m) from the right support, with the overhang 2 ft (0.61 m) beyond the right support, where applicable. Both the control specimen and the strengthened specimen without an overhang failed as a result of strand debonding in the transfer region. This occurred because the shear capacity of a section is less in the transfer zone where the prestressing strands have not fully developed versus the same section with fully developed strands (PCI 2006). The control specimen and two strengthened specimens with an overhang failed due to web shear and flexural failure. The presence of the overhang enabled the prestressing strands to fully develop in the shear-critical region of the

member. The presence of CFRP shear reinforcing increased the capacity of girders without overhangs and with overhangs by 16 and 30 percent, respectively.

Hutchinson and Rizkalla (1999) strengthened seven scaled down models of AASHTO girders using CFRP sheets. The members were strengthened near the support using vertical, diagonal, or a combination of diagonal and horizontal CFRP sheets, and tested to failure. Each specimen failed as a result of an inclined crack at 30 degrees from the support. Straightening of the CFRP sheets at the interface between the bottom flange and web exceeded the bond capacity between the CFRP and concrete and was a common failure mode. Several of the conclusions were: 1) when using diagonal sheets, a second layer did not greatly increase the shear capacity of the member because straightening of the sheets led to failure of the specimen, 2) all diagonal specimens failed due to straightening of the sheets, prevent full development of the FRP strength, 3) a horizontal sheet placed over a diagonal sheet increased the load capacity of the member by 16 percent over diagonally strengthened members without external horizontal reinforcement, and 4) failure of the CFRP sheets may initiate prior to yielding of the steel stirrups.

2.3 Repair of Reinforced and Prestressed Concrete Members

The repair of damaged reinforced and prestressed concrete girders is an ever-growing practice in the US and around the world. Early methods such as external post-tensioning, strand splicing, and steel plates were used prior to the advent of FRP materials. This section will discuss a wide array of research performed during laboratory tests as well as field applications of both traditionally repaired and FRP repaired RC and PS concrete members. Lastly, existing FRP design guidelines will be presented.

Traditional Repair Methods

Extensive research literature is available for traditional repair methods of reinforced and prestressed concrete members. Several articles for various repair methods will be described; first for RC structures then for PS structures.

The use of bonding steel plates to RC members was reported by Aboutaha (1998). The advantages of using steel plates were: 1) improved serviceability and increased ultimate strength, 2) causes minimum changes to member dimensions and weight, and 3) they are cost effective and easy to maintain. Steel plates were also able to increase the flexural stiffness and reduce cracking of the test specimens. However, the largest drawback for the use of steel plates in strengthening concrete members is their poor resistance to corrosion.

Another traditional method of repairing shear-deficient RC members was examined by Khaloo (2000) using external post-tensioning. Twenty four members were tested to failure under shear-critical loading. Steel plates, bolts, and angles were used to achieve vertical post-tensioning of the members near the supports. The research was able to increase the shear capacity enough to change the mode of failure from shear failure to flexural failure, as well as increase the ductility of the post-tensioned member versus the control specimen.

The most common traditional repair method for damaged prestressed concrete bridge members is strand splicing. Two research studies by Olsen et al. 1992 and Zobel et al. 1998 found that severed prestressing strands could be effectively repaired using strand splicing. They both concluded that in many cases the strand splices were unable to restore the ultimate strength of the girder but were found to perform poorly during fatigue loading of the specimens. A more innovative technique was needed that could not only restore the ultimate

strength capacity of the damaged girder, but withstand the repetitive service loadings that all bridge girders undergo.

CFRP Repair Methods and Field Applications

The advantage of using CFRP materials is not only can they restore the ultimate flexural or shear capacity of damaged sections, but they perform extremely well under repetitive service loading and in corrosive environments. Examples of reinforced and prestressed concrete members repaired using CFRP materials are presented below.

In Alabama, one span of a reinforced concrete bridge was chosen to repair damage due to aging (Stallings et al. 2000). CFRP precured laminates along with Glass FRP sheets were used to restore the repaired sections beyond their original capacities to increase posted load restrictions. Before installation of the repair systems designed by the researchers, load tests were performed to measure the behavior of the bridge superstructure under various static and dynamic loads. The same static and dynamic tests were performed after the completion of the FRP repair systems to compare with the prior results. The results of these load tests demonstrated that the FRP repair system reduced girder deflections ranging between 2 to 12 percent, as well as reducing rebar stresses by an average of 8 percent. The usage of CFRP plates to repair and strengthen reinforced concrete bridge girders was successfully installed and verified by field loading tests.

Three separate prestressed concrete bridges were repaired with CFRP systems in repair projects sponsored by the Missouri Department of Transportation. In the first project, eleven prestressed concrete bridge girders located on a bridge in Independence, MO were impact damaged due to an overheight vehicle and repaired with CFRP wet lay-up sheets (Schiebel et al. 2001). Although no prestressing strands were ruptured, all eleven girders had

large cracks and spalling of concrete exposing prestressing strands. The CFRP repair system was designed using a simple section analysis procedure to ensure that the new flexural strength was equal to or greater than that of the original girder. Detailing of the CFRP repair system followed industry standards and provided transverse U-wraps at 15.75 in (400 mm) spacing and extension of the CFRP well away from the damaged concrete area. Experimental testing was limited to bond and adhesion tests to ensure proper bond of the CFRP to the concrete substrate. In the second project, a prestressed concrete bridge girder was repaired in-situ with CFRP wet lay-up sheets after impact damage ruptured two prestressing strands (Tumialan et al. 2001). The design of the repair system was determined by the rectangular stress block approach. Two layers of CFRP sheets were applied to the tension face, extending past the damaged location. CFRP U-wraps were also applied to prevent debonding failure. Following current industry standards, the CFRP repair system was successfully installed by a contractor. Field testing was not performed, however the repaired girder is performing well in service.

A third project sponsored by the Missouri DOT, repaired impact damage caused by a contractor who struck a girder during construction of a new bridge (Ludovico 2003). Two prestressing strands were ruptured and a significant loss of concrete occurred. The concrete section was restored and the girder repaired using CFRP sheets in both the longitudinal and transverse directions. Load testing was not performed on the repaired section, but the girder is currently performing well under traffic loading.

The Iowa Department of Transportation has sponsored several research projects that involved the use of CFRP to repair impact damaged prestressed concrete bridge girders. In the first project, several overheight impacts damaged all the girders on a bridge (Klaiber et al.

1999). Although no prestressing strands were ruptured, one girder had two prestressing strands which were visibly relaxed. The girders were load tested in-situ to examine their respective load-deflection behaviors. Two damaged girders were then cut out of the deck, replaced with new ones, and transported to a testing facility. The more severely damaged girder with two relaxed prestressing strands was tested to failure to observe the behavior of a beam with significant concrete loss and relaxed strands. The second girder, with only moderate damage, was then loaded to simulate service load conditions. The girder was then damaged to simulate a larger loss of concrete and rupturing of two prestressing strands. Following the simulated damage, the girder was then repaired by first restoring the concrete section using a cementitious mortar. CFRP plates were then bonded to the bottom flange of the beam to restore the flexural capacity of the member. CFRP sheets were added in the transverse direction to prevent debonding. Load tests after the CFRP installation indicated that the repaired girder exhibited 27 percent less deflection than the damaged girder. The repaired girder also exhibited a higher ultimate load capacity over the control specimen previously mentioned.

A second project, sponsored by the Iowa DOT, included the testing of a bridge before and after the installation of a CFRP repair system. All six prestressed concrete girders on one span of a bridge were damaged as a result of an overheight impact; however most damage only occurred to the first two girders. The first girder sustained spalled concrete as well as one ruptured prestressing strand. The second girder was damaged more significantly with a much larger loss of concrete, five prestressing strands visible and two of those ruptured. After restoration of the section was completed with patching material, CFRP plates were attached to the bottom flange of the beams. The researchers demonstrated through the

before and after load tests that the midspan bridge deflections decreased following the installation of the CFRP plates. The researchers concluded that flexural strengthening of impact damaged PC girders is possible when up to 15 percent of the strands are severed. Higher ratios may be possible, but tests have not been performed to validate this assumption.

An experimental project was sponsored by the Florida Department of Transportation to create guidelines, standard practices, and experimental data for the repair of impact-damaged bridge girders using CFRP systems. The FDOT had previously repaired a damaged prestressed bridge girder on an acitive bridge, but did not have any design guidelines at the time to follow. All they had were the manufacturers engineeers to assist in the repair. In Green et al. (2004), six 44 ft (13.41 m) long AASHTO Type II girders were tested in four point bending to examine effectiveness of various CFRP systems to restore the capacity of damaged girders back to their original strengths. The experiment was comprised of one control specimen, a second control specimen with simulated damage, and four specimens with simulated damage all repaired with different CFRP systems. All test results compared well with analytical predictions. The results show that one of the four repaired girders was able to achieve its orignial capacity. Wet lay-up CFRP sheets were used in the first repaired specimen. The girder failed prematurely, at 91 percent of the control specimen's ultimate strength, due to plate-end debonding. The researchers did not provide any U-wraps along the length of the longitudinal CFRP. It is believed that the presence of U-wraps would have prevented the plate-end debonding. The second repaired specimen was repaired using pre-impregnated CFRP fabric sheets. Four layers of pre-preg sheets were installed in the longitudinal direction, along with bi-directional CFRP sheet U-wraps which were bolted into the web. The girder achieved 92 percent of the experimental capacity of the control girder,

with failure due to adhesive failure immediately followed by rupture of the longtitudinal CFRP. The third girder incorporated a spray-on FRP repair system. This system achieved 95 percent of the original capacity, with failure caused by FRP rupture. The researchers found after the failure that the desired thickness of the spray was 0.50 in (12.7 mm) but the actual thickness as 0.27 in (6.86 mm). The final repaired girder emplyoyed the usage of wet lay-up CFRP sheets. One transverse U-wrap was provided at the end of the longitudinal sheets to provide achorage. The girder failed after the longitudinal FRP pulled away from the U-wraps, leading to an achorage failure, but not until after the girder had achieved a 7 percent increase in strength over the control specimen. The researchers concluded that FRP can be used to restore a significant portion of the strength capacity of an impact damaged girder, however they observed that proper detailing at termination points is critical to any FRP system.

In Di Ludovico et al. (2005), three 36 ft (11 m) prestressed concrete Missouri Type II bridge girders, with a 32 in (810 mm) composite cast-in-place slab, were tested monotonically to failure to assess the flexural behavior of repaired damaged sections with CFRP wet lay-up laminates. After the first girder was tested as a control specimen, the other two were damaged at midspan by removing the concrete cover and rupturing two and four prestressing strands, respectively. They were then repaired with cementitious mortar and repaired with two or three layers of longitudinal CFRP sheets below numerous transverse CFRP U-wraps. The results show that the CFRP system can restore the ultimate capacity and stiffness of the original girder, but the two repaired girders could not match the original serviceability. The failure mode observed for both of the repaired girders was rupture of a U-wrap on the undamaged side followed by intermediate crack debonding of the longitudinal

CFRP system. The researchers provided numerous CFRP U-wraps throughout the repaired area, but they only extended around the bottom flange of the girder to the bottom of the web. It is possible that this detailing led to the premature debonding failures at 56 and 46 percent of the ultimate nominal FRP strain. The authors also provide an analysis procedure to calculate the prestress force, the cracking moment and the ultimate moment based on strain compatibility and equilibrium. For the design of the CFRP system, they applied the bond reduction factor (κ_m) from ACI Committee 440 (2002), but not the environmental reduction factor (C_E).

Existing CFRP Design Guidelines

The American Concrete Institute produced a document to provide guidelines for the design and construction of externally bonded FRP systems for strengthening reinforced and prestressed concrete structures (ACI Committee 440 2002). The document addresses various aspects of FRP use from surface preparation, installation guidelines, up to field inspection procedures during and post-installation. Design limits to protect against fire damage or sudden rupture of FRP due to impact are discussed. CFRP detailing concerns are discussed in conjunction with FRP anchorage and lap splice recommendations. Lastly, detailed design examples for complete shear and flexure FRP strengthening are provided.

As for the actual design process using FRP materials, reduction factors are introduced to take into account degradation due to environmental effects (C_E) over time. For flexural strengthening systems, an empirical bond reduction coefficient (k_m) is used to determine the effective bond between the concrete and FRP. This bond coefficient is currently being examined by Rosenboom (2006) to be based on experimental test results. For shear

strengthening, a bond reduction coefficient (k_v) is also introduced. However, this coefficient is based on material properties and type of strengthening system used. For shear applications only, an additional reduction factor (ψ) equal to 0.85 is multiplied by the total shear force contribution of the FRP strengthening system. This is to account for the brittle nature of FRP failure.

3. Experimental Program

3.1 Introduction

In October 2003, a tractor trailer carrying improperly secured excavating equipment impacted the prestressed concrete superstructure of NC Bridge 169 shown in Figure 3.1, in Robeson County, North Carolina. The impacted bridge was located on Green Springs Road (SR 1718) over Interstate 95. Originally built in 1959, the bridge consisted of four 55 ft (16.8 m) long spans. Each span was made up of four AASHTO Type II prestressed concrete girders spaced at 7 ft (2.13 m) intervals. The impact of the excavating equipment heavily damaged the first exterior girder by nearly severing it in half. The second and third girders were missed, and the last girder was then struck, causing a large loss of the concrete section and rupturing one prestressing strand.

This was not the first time that the bridge had been hit; therefore the bridge maintenance engineers with the North Carolina Department of Transportation decided to replace all four girders in the eastern span with cored slab units. The cored slab units would provide more ground clearance and therefore reduced the probability of future impacts. The bridge girders were identified by members of the North Carolina State University Civil Engineering Department as a potential research source. These girders were then transported to the NCDOT Bridge Maintenance Facility in Raleigh, NC for future repair work. Figure 3.2 shows the three girders at the DOT maintenance facility. The first phase of the project focused on repairing the severely damaged girder with rupture of one prestressing strand. The other two structurally sound interior girders were set aside for phase two of the project, which involved simulating varying degrees of impact damage and then repairing them.

Figure 3.1 Undamaged eastern span of NC Bridge 169

Figure 3.2 AASHTO Type II girders at the NCDOT maintenance facility

During the first phase, the impact damaged AASHTO Type II girder previously described was repaired using a polymer modified cementitious material to rebuild the concrete section and CFRP wet lay-up sheets to restore the nominal section capacity. The second phase included simulating damage to the two 55 ft (16.8 m) long specimens by removing part of the concrete section and rupturing three or four prestressing strands, respectively. The girders were damaged at midspan to simulate a flexurally critical situation. The girders were then repaired in the same manner as the first AASHTO girder. Following the completion of testing these two girders, one girder was then cut into thirds in order to create short spans, which is typically critical for shear resistance. One of these short spans was tested as a control specimen and the second was damaged to simulate an impact near the girder's support. This girder was then repaired, using PCI and ACI Committee 440 design guidelines, and tested statically to failure. This chapter presents the experimental program for the five test specimens. Complete test results and discussion are given in Chapter 4.

3.2 Test Girders

Three Type II AASHTO girders (AASHTO1, AASHTO2, and AASHTO3) were tested to examine the flexural behavior of CFRP repaired girders damaged by vehicular impact. The girders were damaged, either accidentally or artificially, near midspan location to examine different damage scenarios, including varying the amount of prestressing strands ruptured. This chapter will provide details and descriptions of the various tests conducted in this study.

Two short span girders were tested under shear-critical loading conditions. Following the flexural testing of AASHTO2, the girder was saw-cut into thirds, with the two identical end pieces used for the shear study. One section of the girder was used as a control specimen

(AASHTO2C), while the other specimen was damaged near the support and repaired with CFRP sheets (AASHTO2R). AASHTO3 was saw-cut in a similar manner and saved for future research. This chapter will provide details and descriptions of the individual tests. Complete test results are discussed in Chapter 4.

AASHTO1

AASHTO1 was the first girder tested in this research project. The test girder was an AASHTO Type II girder prestressed with sixteen 0.5 in (12.7 mm) – 7 wire 270 ksi (1862 MPa) straight prestressing strands, as shown in Figure 3.3. The total length of the tested girder was 54.84 ft (16.71 m) with a center-to-center support span of 53.34 ft (16.26 m). The girder after impact damage from an overheight vehicle is shown in Figure 3.4. The cross section and elevation of AASHTO1 are shown in Figure 3.3. The loss of concrete section extended a length of 11.9 ft (3.63 m) on the front side and 6.0 ft (1.83 m) on the back side with an approximate volume of damaged concrete equal to 4.8 ft^3 (0.1 m^3). In addition to the loss of concrete, one prestressing strand on the bottom layer was ruptured on the front side, resulting in a 6.3 percent loss of prestressing force. The full 7 ft (2.13 m) composite bridge deck was not part of the test specimen since it was cut through in order to remove the damaged girder from the bridge superstructure. The average width of the composite deck of the test girder was 14.9 in (388 mm), ranging from 16.9 in (430 mm) to 13.9 in (353 mm). Several transverse cuts were located along the length of the composite deck. These cuts, originating during the cutting of the cast in place diaphragms, were approximately 0.4 in (10 mm) in width.

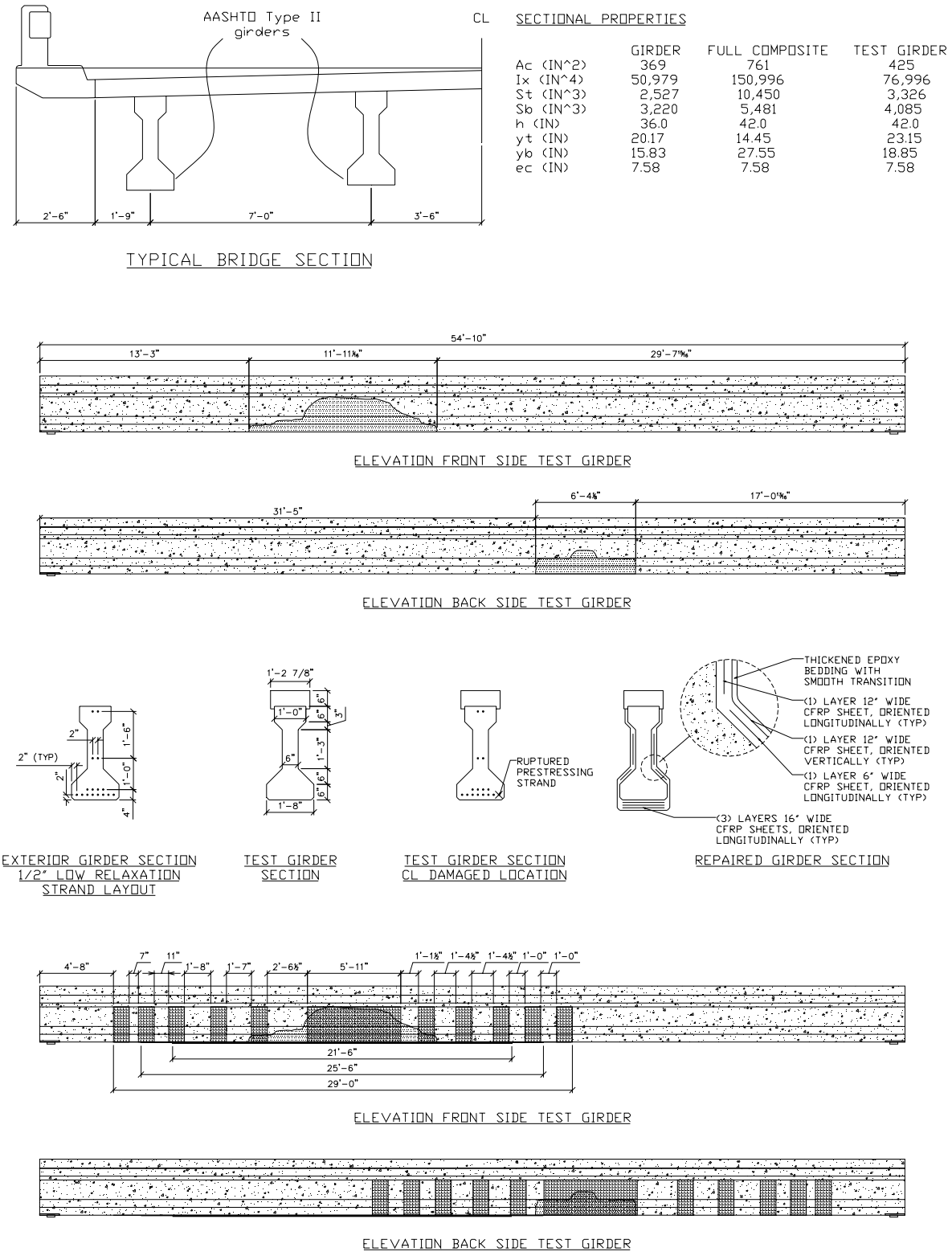

Figure 3.3 AASHTO1 girder cross section, elevation, and CFRP design details

Figure 3.4 AASHTO1 at NCDOT yard after impact damage

Design drawings provided by the NCDOT specified the 28 day concrete strength for the girder was 5000 psi (34.5 MPa) as well as the concrete strength of the deck was 3000 psi (20.7 MPa). Material test results of the prestressing strands and concrete core samples taken after testing are presented in Section 3.3

AASHTO2

The second test girder, AASHTO2, was an interior girder of the bridge and therefore was not damaged like AASHTO1. This AASHTO Type II girder was older than the others; based on the presence of a large endblock and 28-7/16 in (11.1 mm) diameter 250 ksi (1724 MPa) prestressing strands it was determined the girder was cast in the 1960's. The girder was prestressed with twenty four straight and four harped prestressing strands using a hold

down system at midspan. The total length of the girder was 54.5 ft (16.61 m), with a span length of 53.06 ft (16.17 m) from center-to-center of the supports. Based on measurements taken at two foot intervals, the average width of the composite deck was determined to be 16.5 in (419 mm). Cross section and elevation drawings of AASHTO2 are shown in Figure 3.5.

As previously mentioned in Section 3.1, AASHTO2 was received by the researchers undamaged, except for several transverse cuts approximately 0.4 in (10 mm) wide in the composite deck after the removal of the diaphragms. In order to simulate impact damage, a large portion of the tension flange of the girder was removed (Figure 3.6), and four prestressing strands were ruptured (Figure 3.7), corresponding to a reduction in prestressing force of 14.3 percent. The length of the damage was extended to a total of 2.0 ft (0.61 m) on either side of midspan on the front side of the girder only. Approximately 2.2 ft^3 (0.06 m^3) of concrete was removed, as shown in Figure 3.7.

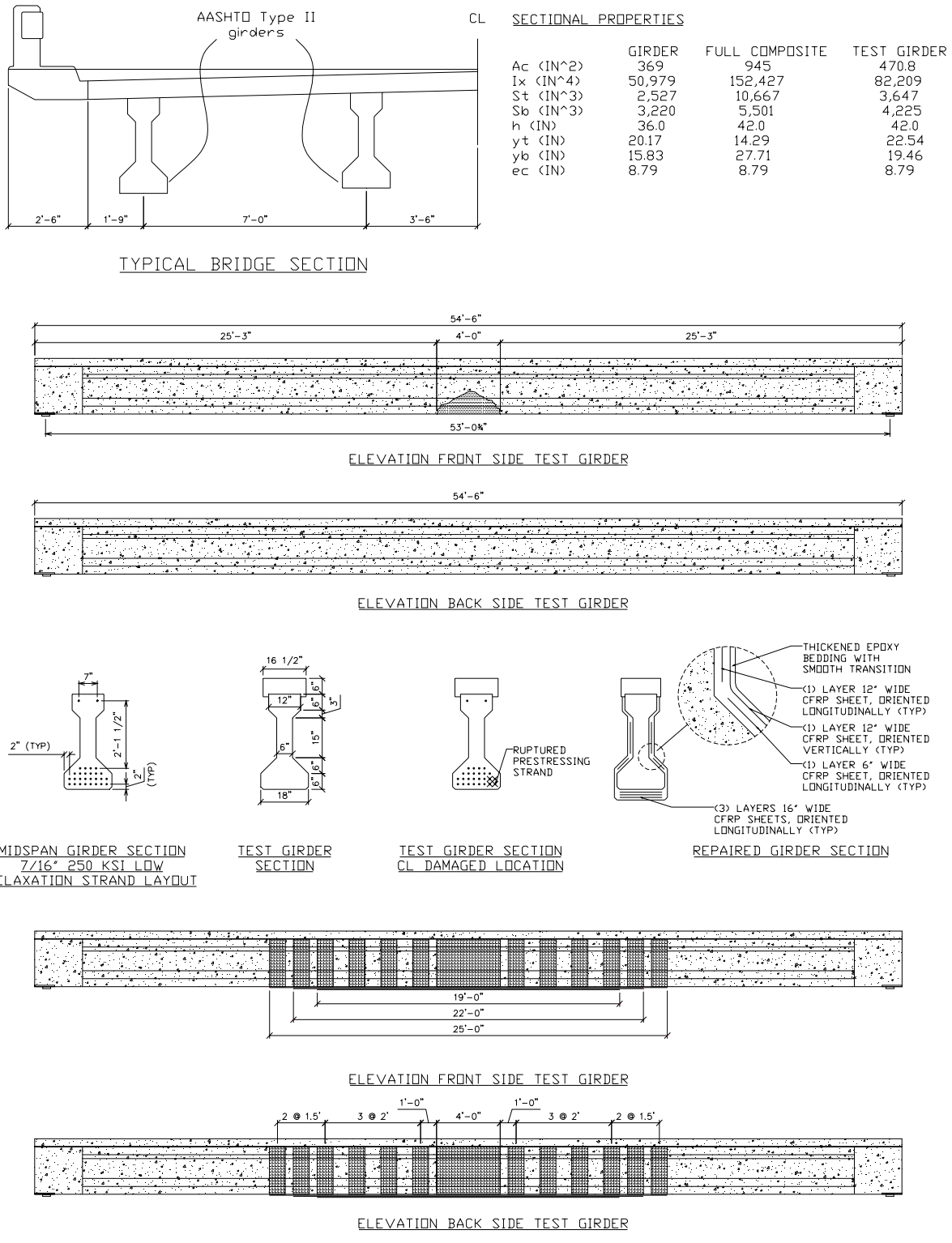

Figure 3.5 AASHTO2 girder cross section, elevation, and CFRP design details

Figure 3.6 AASHTO2 during removal of concrete

Figure 3.7 Simulated damage of AASHTO2 girder

Design drawings were provided by the NCDOT; however they were illegible and it was difficult to discern most information. Initially it was assumed that the concrete strength for the girder was 5000 psi (34.5 MPa) when it was first erected 40 some years ago. For preliminary calculations, a girder concrete strength of 6000 psi (41.4 MPa) was used to reflect the age of 40 years plus. The composite deck slab was estimated at 3000 psi (20.7 MPa). Material test results of the prestressing strands and concrete core samples taken after testing girder AASHTO2 are presented in Section 3.3.

AASHTO3

The third girder tested in flexurally critical conditions was AASHTO3. This exterior girder was an AASHTO Type II girder, but was only 10 years old because a previous girder in the same location had been struck by an overheight vehicle and required replacement. AASHTO3 was comprised of 16-0.5 in (12.7 mm) diameter 270 ksi (1862 MPa) straight prestressing strands. The total length of the girder was 54.5 ft (16.61 m). The testing span length of this girder had to be shortened to avoid the damage at one end of the girder, caused during transportation, as shown in Figure 3.8. The center-to-center length between the testing supports was 49.0 ft (14.94 m). Based on measurements taken at two foot intervals, the average width of the composite deck was determined to be 13.5 in (343 mm). Cross section and elevation drawings of AASHTO3 are shown in Figure 3.9.

Figure 3.8 Damage to right support of AASHTO3 caused during transportation of girder

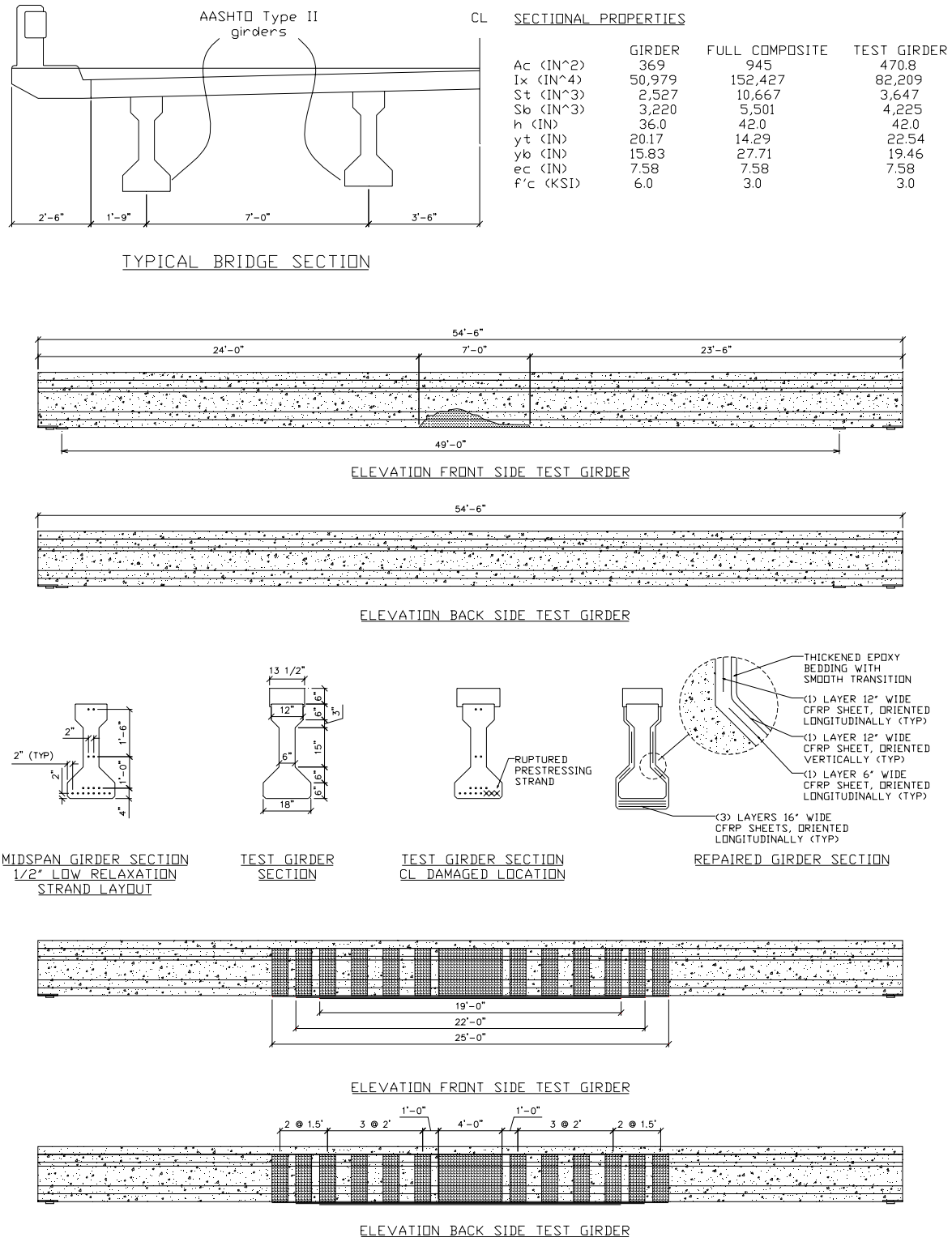

Figure 3.9 AASHTO3 girder cross section, elevation, and CFRP design detail

AASHTO3 had been impacted several times prior to being removed from the bridge. Figure 3.10 shows one section where an earlier concrete repair had been performed along with epoxy injection of the cracks caused by vehicular impacts. In order to simulate impact damage to this girder, a large portion of the tension flange was removed, similar to girder AASHTO2, and three prestressing strands were ruptured (Figure 3.11), corresponding to a reduction in prestressing force of 18.8 percent. The length of the damage was 2.0 ft (0.61 m) to the left of midspan and approximately 5.0 ft (1.52 m) to the right on the front side only. It was intended for the damage to be symmetrical about midspan, but the presence of earlier repairs made it difficult to cut as planned. A total of approximately 2.4 ft^3 (0.07 m^3) of concrete was removed, as shown in Figure 3.11.

Figure 3.10 AASHTO3 defects after arriving at the testing facility

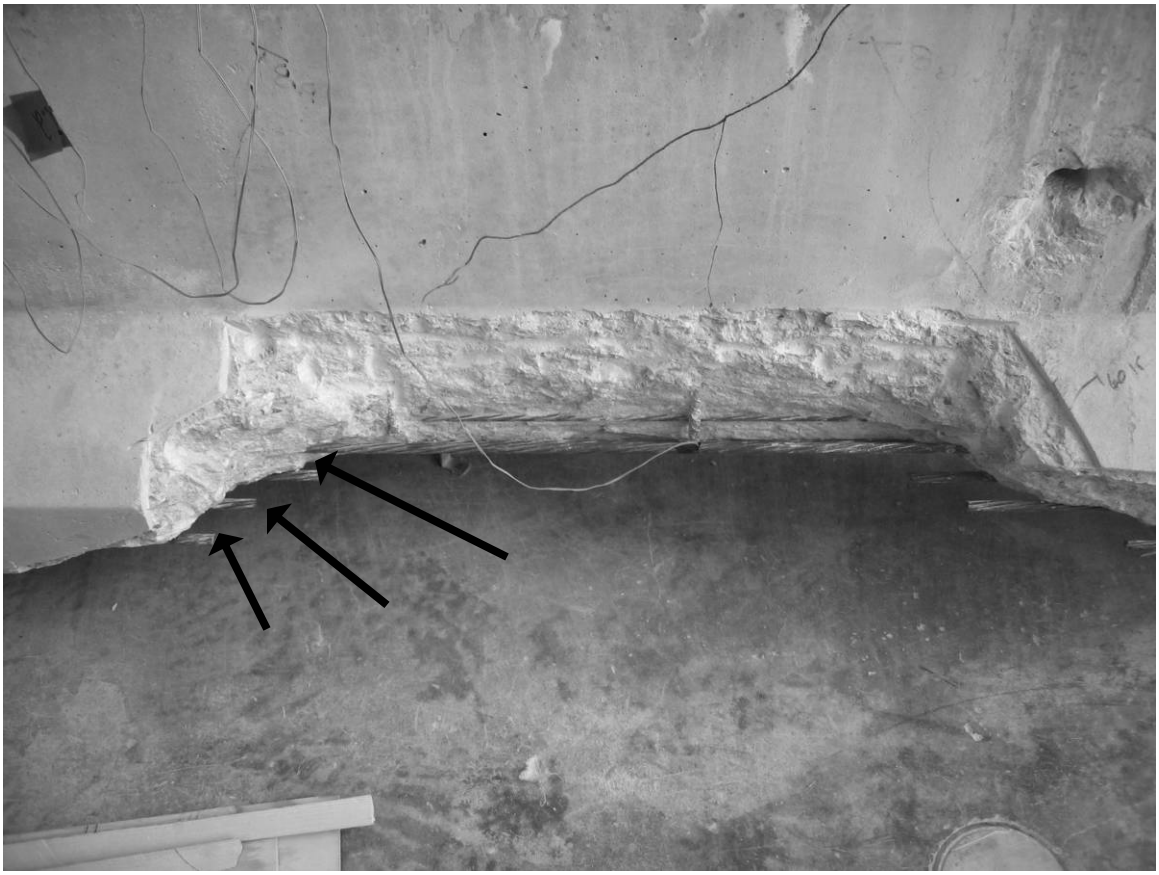

Figure 3.11 Simulated damage of AASHTO3 girder

Design drawings provided by the NCDOT indicated that the concrete strength for the girder was 5000 psi (34.5 MPa) and 3000 psi (20.7 MPa) for the bridge deck. Material test results of the prestressing strands and concrete core samples taken after testing girder AASHTO3 are presented in Section 3.3.

AASHTO2C

The first girder tested during the shear study, AASHTO2C, was tested monotonically to failure as a control specimen. The girder, shown in Figure 3.12 was prestressed with 28-7/16 in (11.1 mm) diameter 250 ksi (1724 MPa) strands. The total length of the girder was 20.67 ft (6.30 m), with a span of 17.83 ft (5.43 m) from center-to-center of the supports.

Based on measurements taken at two foot intervals, the average width of the composite deck was determined to be 16.5 in (419 mm). Cross section and elevation drawings of AASHTO2C are shown in Figure 3.13.

Figure 3.12 AASHTO2C test specimen

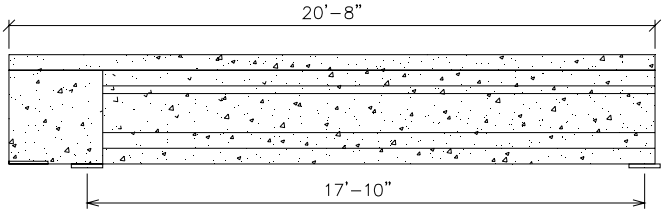

ELEVATION FRONT SIDE CONTROL SPECIMEN

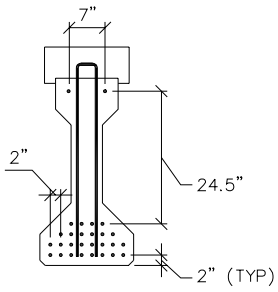

MIDSPAN GIRDER SECTION
7/16" 250 KSI LOW
RELAXATION STRAND LAYOUT

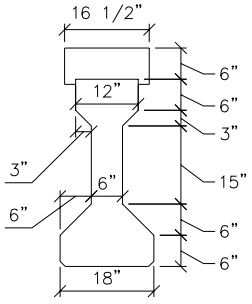

TEST GIRDER
SECTION

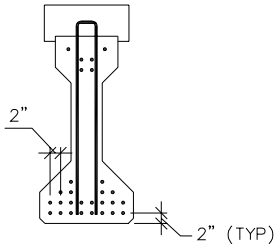

END GIRDER SECTION
7/16" 250 KSI LOW
RELAXATION STRAND LAYOUT

SECTIONAL PROPERTIES

	GIRDER	TEST GIRDER
Ac (IN^2)	369	470.8
Ix (IN^4)	50,979	82,209
St (IN^3)	2,527	3,647
Sb (IN^3)	3,220	4,225
h (IN)	36.0	42.0
yt (IN)	20.17	22.54
yb (IN)	15.83	19.46
ec (IN)	8.79	8.79

Figure 3.13 AASHTO2C girder cross section and elevation

AASHTO2 was received by the researchers undamaged, except for several transverse cuts which were repaired as mentioned previously in Section 3.2. Concrete strengths were the same as those specified for girder AASHTO2. Material test results of the prestressing strands and concrete core samples are presented in Section 3.3.

AASHTO2R

AASHTO2R was tested monotonically to failure as a shear critical member with simulated damage repaired with CFRP sheets as shown in Figure 3.14. The girder was prestressed with 28-7/16 in (11.1 mm) diameter 250 ksi (1724 MPa) strands. The total length of the girder was 20.67 ft (6.30 m), with a span of 17.83 ft (5.31 m) from center-to-center of the supports. Based on measurements taken at two foot intervals, the average width of the composite deck was determined to be 16.5 in (419 mm). Cross section and elevation drawings of AASHTO2R, including CFRP repair details, are shown in Figure 3.15. It should be noted that the section properties for AASHTO2R are the same as AASHTO2C but were not included for clarity.

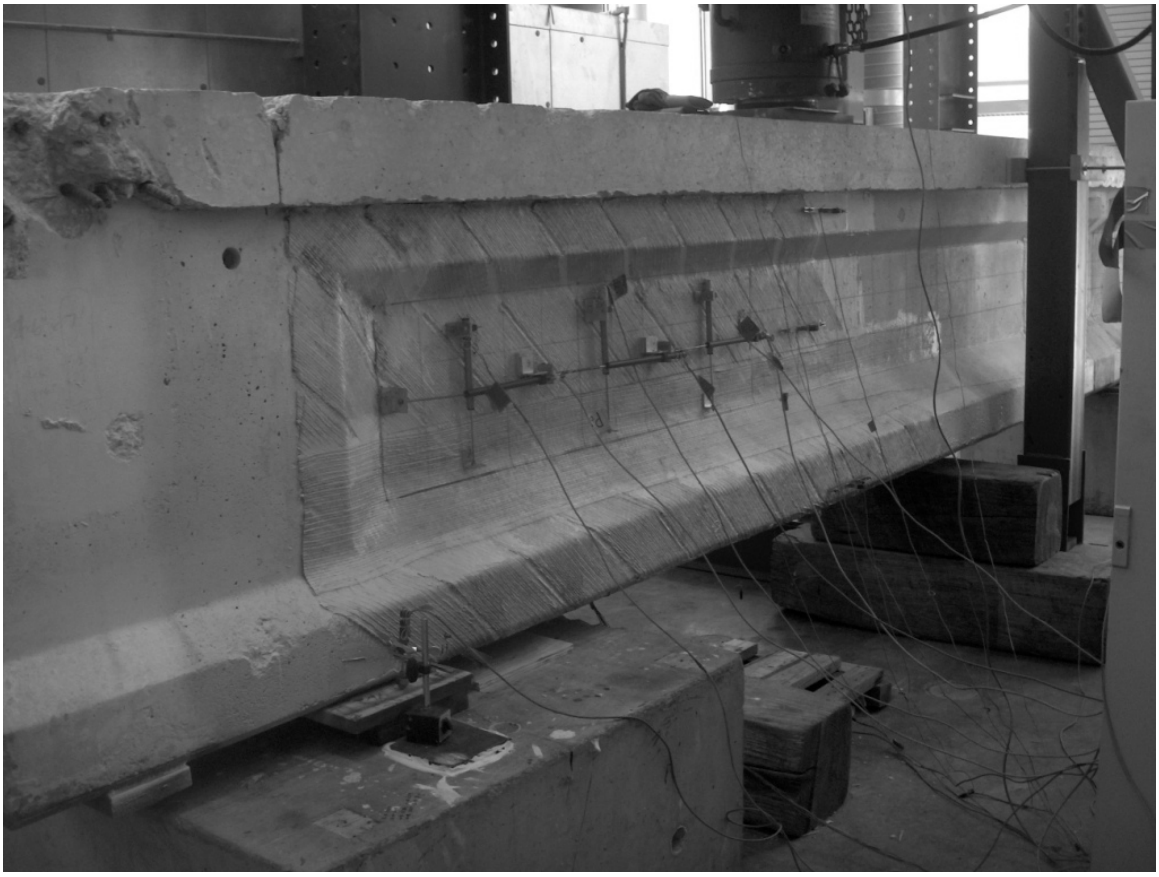

Figure 3.14 AASHTO2R test specimen

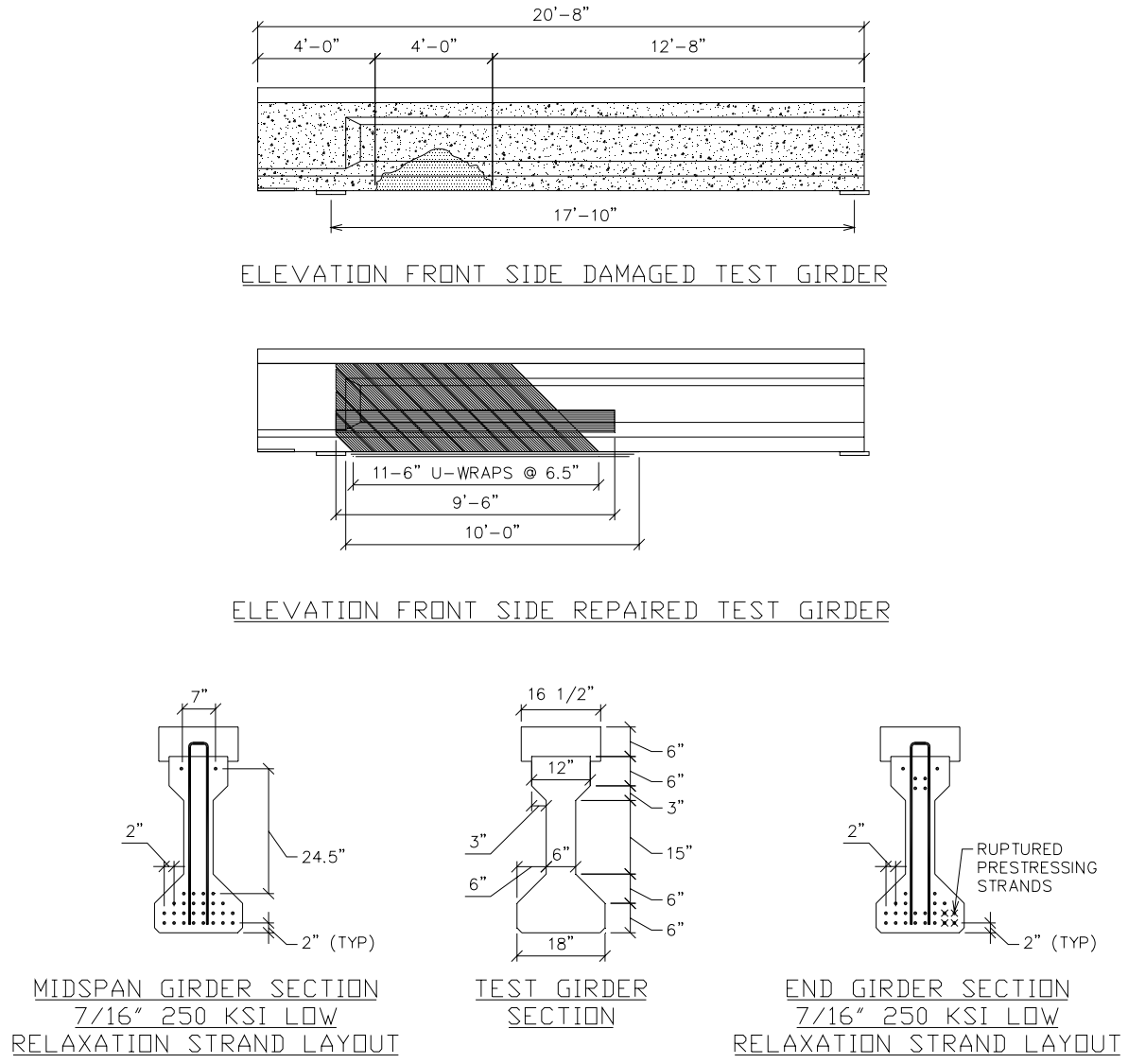

Figure 3.15 AASHTO2R girder cross section, elevation, and CFRP design details

In order to simulate impact damage, a large portion of the tension flange of the girder was removed, and four prestressing strands were ruptured (Figure 3.16), corresponding to a reduction in prestressing force of 14.3 percent. The length of the damage began 1 ft (305 mm) past the face of the left support and extended 4 ft (1.22 m) to the right. A total of approximately 1.5 ft^3 (0.04 m^3) of concrete was removed, as shown in Figure 3.16.

Figure 3.16 AASHTO2R after completion of simulated damage

3.3 Material Properties

This section will present testing methods and results of material tests performed on prestressing strands, concrete core samples, and CFRP sheets.

Prestressing Strands

Two different types of prestressing strands were encountered during the experimental program of this research project. Specimens AASHTO1 and AASHTO3 utilized the same prestressing strand pattern with 270 ksi (1862 MPa) strands, while specimens AASHTO2, AASHTO2C, and AASHTO2R utilized the same prestressing strand pattern with 250 ksi (1724 MPa) strands. The 270 ksi (1862 MPa) strand pattern (Figure 3.17 left) consisted of

16-0.5 in (12.7 mm) straight prestressing strands. The 250 ksi (1724 MPa) strand pattern (Figure 3.17 rigtht) consisted of 28-7/16 in (11.1 mm) prestressing strands, 24 of which were straight and four of which were harped with a hold-down system located at midspan.

Material testing was carried out on prestressing strands encountered in each of the three main girders, after testing of each girder was complete. In order to test the strands, several were extracted from the bottom layer as close to the supports as possible. The strands were removed from the supports to ensure the strands had not yielded under the effect of loading. Special care was taken during removal of the strands to prevent unraveling.

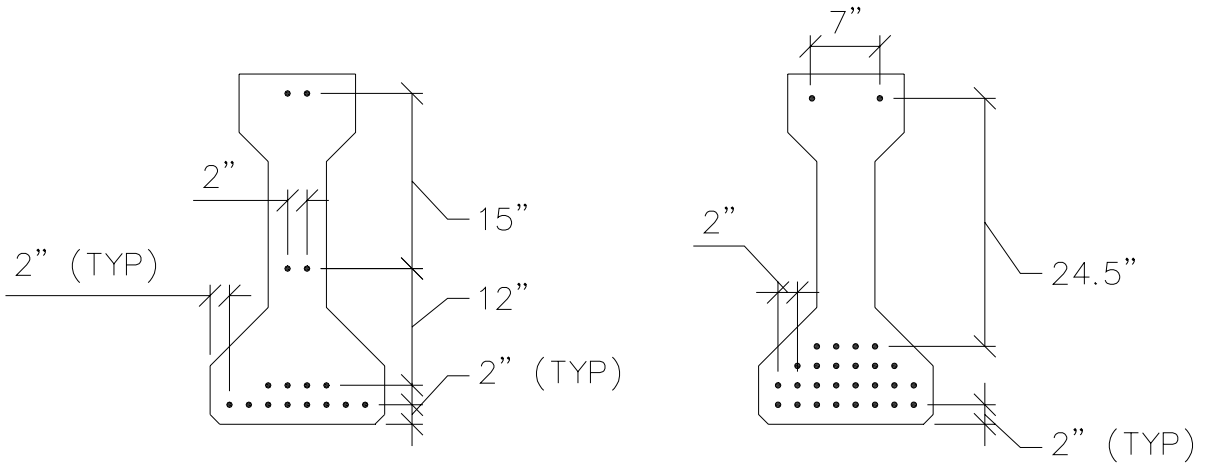

Figure 3.17 270 ksi (left) and 250 ksi (right) midspan strand patterns

The prestressing strands were tested in tension according to ASTM A416 specifications using a 220 k (979 kN) MTS closed-loop universal testing machine used to apply a constant rate of displacement. The prestressing strands were clamped into the MTS grips using multiple-use super chucks. A 1 in (25 mm) extensometer was placed at the middle of the specimen during the test to measure displacement and to obtain modulus of elasticity measurements. Figure 3.18 shows a typical prestressing strand specimen. Prior to rupture of the strand, the extensometer was removed to prevent any damage caused by the violent nature of the failure. The stroke of the MTS machine was then used to determine the

rupture strain of the specimens. Table 3.1 shows the average yield strength, ultimate strength, modulus of elasticity, and rupture strain for each set of tested prestressing strands.

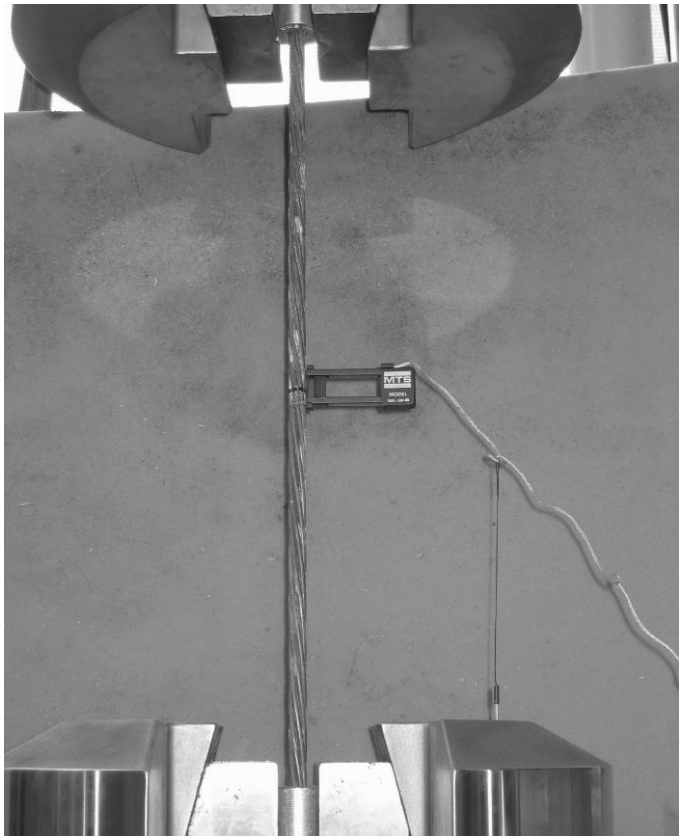

Figure 3.18 Typical prestressing strand test setup

Table 3.1 Prestressing steel properties

Specimen Designation	Strand Type, ksi	σ_y, ksi	σ_u, ksi	ε_u, %	E, ksi
AASHTO1 and AASHTO3	270	262	279	5.10	28,500
AASHTO2	250	210	255	5.62	28,900

The Ramberg-Osgood function (Collins and Mitchell 1991) was used to match the stress-strain behavior of the prestressing strands with material constants.

$$f_p = E_p \varepsilon_{ps} \left[A + \frac{1 - A}{\left[1 + \left(B\varepsilon_{ps}\right)^C\right]^{1/C}} \right] \tag{3.1}$$

where f_p is the prestressing strand stress, E_p is the modulus of elasticity of the prestressing strand, ε_{ps} is the strain in the prestressing strand, and A, B, C are material constants.

Constants A, B, and C were determined by fitting the stress-strain curve generated by the Ramberg-Osgood equation with the stress-strain curve generated from the tension tests. For the 270 ksi (1862 MPa) strands, the average values for A, B, and C were 0.015, 108, and 10 respectively. These values compared well with similar test values obtained from previous research by Rizkalla (2005). For the 250 ksi (1724 MPa), strands the average values for A, B, and C were 0.025, 139, and 6 respectively, which also compared well with the values from earlier research by Rizkalla (2005). Figure 3.19 shows the measured stress-strain behavior compared to the Ramberg-Osgood function for both types of prestressing strands encountered.

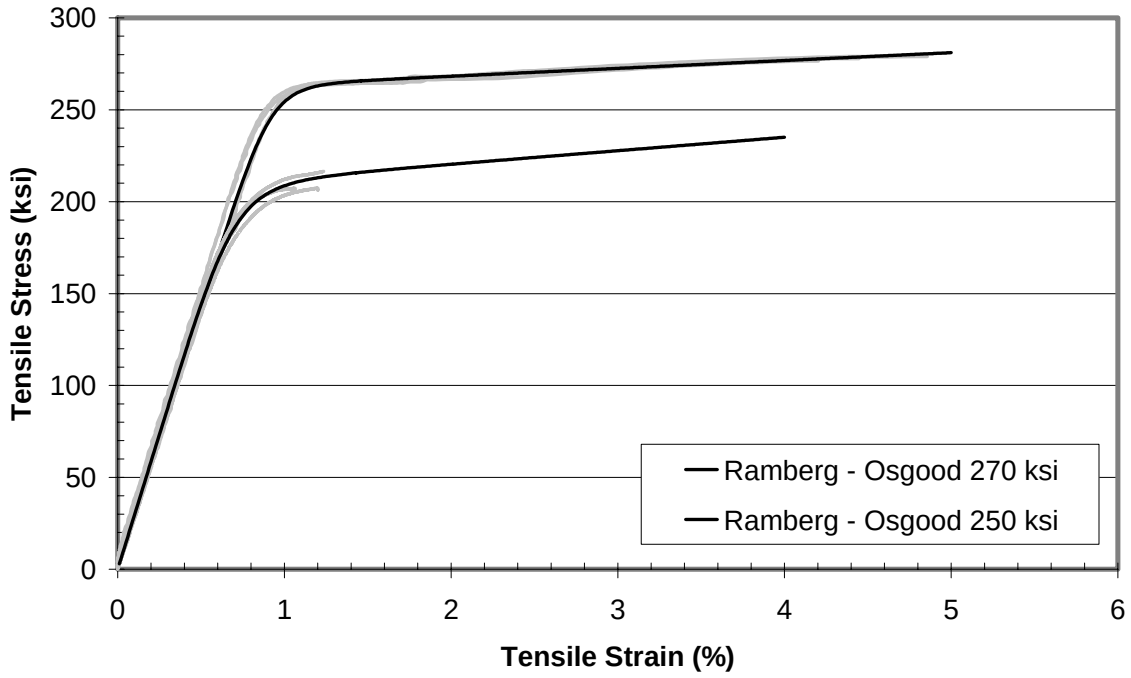

Figure 3.19 Stress-strain behavior of 270 ksi and 250 ksi prestressing strands

Reinforcing Bars

Due to the difficulty to extract any straight reinforcing bars, no tests were conducted to examine the characteristics of the reinforcing bars in the deck or the stirrups of each girder. The material properties used in the analysis were based on the specifications provided on the design drawings provided by NCDOT.

Concrete

The specified nominal concrete strength for all of the AASHTO girders was 5000 psi (34.5 MPa) at time of erection. The design strength of these girders, as described in Section 3.2, was estimated to increase by at least 1000 psi (6.9 MPa) as a result of the significant aging of the concrete. The following equation proposed by MacGregor (2005) accounts for the strength increases due to aging:

$$f'_{c(t)} = f'_{c(28)}\left[\frac{t}{4+0.85(t)}\right] \tag{3.2}$$

where $f'_{c(t)}$ is the concrete compressive strength as a function of time and t is time in days.

Several core samples were taken from both the girders and deck slab by qualified NCDOT personnel (Figure 3.20). The cores were then tested in accordance with ASTM C42 in an MTS closed-loop universal testing machine used to apply a constant rate of displacement. Concrete strains were measure using the stroke of the MTS machine. Eight inch long (203 mm) core samples were not able to be obtained due to the configuration of the AASHTO girders. The cores taken from the deck slab were approximately 5 in (127 mm) in length. Likewise, the only feasible place to take cores from the girder itself was from the web, which was 6 in (152 mm) in width. 4 in by 8 in (102 mm by 203 mm) cylinders were

also cast of the various concrete repair materials used during the research. Table 3.2 lists the average results of all concrete testing for each AASHTO girder.

Figure 3.20 NCDOT personnel removing core samples

Table 3.2 AASHTO core sample test results

Specimen Designation		Compressive strength of concrete, f'c, ksi	Aggregate description
AASHTO1	**girder**	7.1	Crushed and round ¼" – 1"
	deck	6.7	Gritty ¼" – ½"
	repair mortar	6.3	N/A
AASHTO2	**girder**	6.8	1" rounded quartz and river rock
	deck	5.1	½" – ¾" crushed sandstone
	repair mortar	6.3	3/8" crushed
AASHTO3	**girder**	6.6	Crushed and round ¼" – 1"
	deck	7.1	¾" crushed
	repair mortar	6.3	3/8" crushed

Carbon Fiber Reinforced Polymers (CFRP)

Carbon Fiber Reinforced Polymer (CFRP) wet lay-up sheets were used in the repair of every specimen, as mentioned in Section 3.1. The design of the repair systems are presented in Section 3.4. Although several girders were repaired using the same CFRP system, samples were made during installation and kept at the same location as the girder to determine their tensile strength, modulus of elasticity, and rupture strain. All tests were performed in accordance with ASTM D3039 specifications and tested using the MTS equipment described previously in Section 3.3. Test results for each girder, along with the manufacturer's specifications, are shown in Table 3.3.

Table 3.3 CFRP tension test results

Specimen Designation	CFRP system		Tensile strength, ksi	E, ksi	ε_u, %	Avg. thickness, in
AASHTO1	Tyfo SCH-41 Composite	Test	76	6,350	1.2	.08
		Manufacturer	143	13,890	1.0	.04
AASHTO2		Test	109	9,730	1.08	.096
		Manufacturer	143	13,890	1.0	.04
AASHTO3		Test	109	9,730	1.08	.096
		Manufacturer	143	13,890	1.0	.04
AASHTO2R		Test	98	8,480	1.12	.099
		Manufacturer	143	13,890	1.0	.04

All CFRP samples were cut out of witness panels to a width of 1 in (25.4 mm) and a length of 17.5 in (445 mm). The samples were then bonded to aluminum tabs using Wabo MBrace© Saturant (Wabo 2002) to produce a gauge length of 6 in (152 mm). Figure 3.21 shows a typical CFRP tension test setup. The strain of the CFRP was measured using a 0.236 in (6 mm) TML FLA-6-11 120 Ω electric resistance strain gauge placed at the center of the width and gauge length of the specimen. The primary mode of failure was the sudden and brittle rupture of the fibers in the CFRP, as shown in Figure 3.22 (left). The second, and

less frequent mode of failure, was rupturing of the CFRP matrix through the cross section, as shown in Figure 3.22 (right).

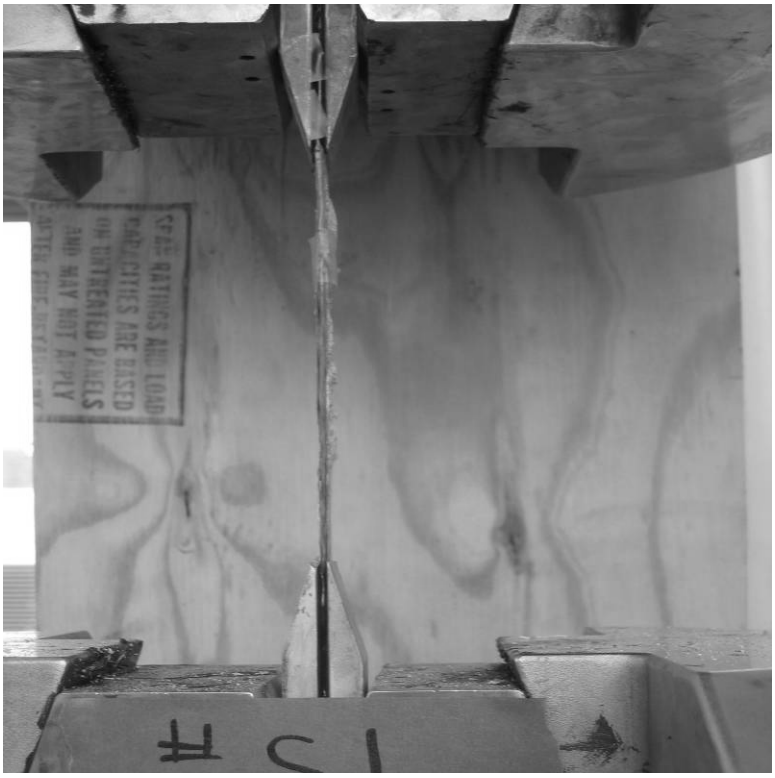

Figure 3.21 Typical CFRP tension test setup

Figure 3.22 Failure through the fibers (left) and failure through cross section (right)

3.4 Design of CFRP Repair Systems

The purpose of applying CFRP to the various damaged AASHTO girders was to restore their original ultimate flexural and shear strengths. Based on previous research by Rizkalla et al. (2005), it was decided to use externally bonded CFRP wet lay-up sheets to restore the original flexural and shear capacity of all the girders. The wet lay-up sheets were chosen for two reasons: 1) transverse U-wraps would be needed to encapsulate the restored concrete section to stabilize crack growth, thus meaning that two CFRP systems would be needed if wet lay-up sheets were not chosen as the main longitudinal reinforcement and 2) based on previous research by Rizkalla et al. (2005), and in consultation with NCDOT officials, CFRP wet lay-up sheets were found to be the most cost-effective repair system, and thus most likely to be used by the NCDOT in future field applications.

AASHTO1

The first task in the design of the CFRP repair system was to determine the original flexural capacity of the girder, prior to the impact damage. The undamaged behavior of the girder was determined using RESPONSE 2000©, a cracked section analysis program (Bentz 2000). The base curve of the concrete model used in the cracked section analysis program was the Popovics curve, which included compression softening based on the Vecchio-Collins model, as well as tension stiffening based on the Bentz model (Bentz 2000).

By inspection, it was apparent that one prestressing strand was ruptured as a result of the lateral impact load. It was also apparent that all of the other prestressing strands were corroded as a result of six months of exposure to the weather. Although research by Klaiber et al. (1999) and Shanafelt and Horn (1980) concluded that no additional loss of prestressing force need be considered for exposed and corroded strands, an additional prestressing strand was considered to be missing in the design of the CFRP repair system to be on the conservative side.

To restore the lost concrete of the girder, a two part repair mortar was chosen. After consultation with the contractor, Tyfo© Type P, two-component, polymer modified cementitious mortar (Fyfe 2002) was selected based on its rapid setting properties, good bond performance to sound concrete, and ability to be placed using your hands rather than being cast into formwork. Partway through the restoration process the contractors exhausted their supply of this material. It was agreed to finish the repair using SikaTop© 123 Plus (Sika 2003), a material very similar to the previous. As previously shown in Section 3.3, the compressive strength of the SikaTop© 123 Plus material was 6300 psi (43.4 MPa).

The type of wet lay-up system used was Fyfe© CH-41 composite and Tyfo© S two part epoxy (Fyfe 2006). The amount of CFRP repair material required to restore the original capacity of AASHTO1 was determined using the RESPONSE 2000© program previously described. The compressive strength of the girder was assumed to be 6000 psi (41.4 MPa), and 3000 psi (20.7 MPa) for the deck. The 270 ksi (1862 MPa) prestressing strands were modeled using the Ramberg-Osgood function (Equation 3.1) for low relaxation strands. The design material properties for the CFRP system were provided by the manufacturer's data sheet:

Ultimate tensile strength for design laminate:	143,000 psi (986 MPa)
Laminate thickness:	0.04 in (1 mm)
Tensile Modulus:	13.9 x 10^6 psi (95.8 GPa)
Ultimate elongation:	1.0%

To restore the original ultimate flexural capacity of the girder, a procedure similar to the one described in Appendix A was used. The analysis concluded that three layers of 16 in (406 mm) wide longitudinal CFRP layers were required. In order to minimize the initiation of new cracks in the repaired concrete, additional longitudinal sheets were installed; a 6 in (152 mm) wide sheet was placed on the top of the bottom flange and a 12 in (305 mm) wide sheet was placed in the middle of the web. These additional longitudinal sheets were placed on both sides of the girder to ensure symmetry of the section. In order to ensure proper utilization of the CFRP's strength and strain capacity, adequate development length of the sheets was provided. The full details of the CFRP reinforcement are described below, as well as a full schematic shown in Figure 3.3:

1) The three bottom layers of longitudinal CFRP reinforcement were extended 6 ft (1.83 m) past the location of the ruptured prestressing strand. This length was chosen based on the full development length of a 0.5 in (12.7 mm) diameter prestressing strand (PCI 2006).
2) The termination points of the longitudinal CFRP were staggered at a distance of 2 ft (610 mm) to prevent plate-end debonding.
3) Two 6 in (152 mm) sheets and two 12 in (305 mm) sheets were installed on the top face of the bottom flange and middle of web, respectively. These four sheets were used to control cracking in the non-prestressed, damaged location. These sheets extended the same length as the longest longitudinal CFRP sheet.
4) 12 in (305 mm) wide transverse CFRP U-wraps were spaced along the entire length of the longitudinal CFRP reinforcing sheets including at the termination point of each longitudinal CFRP sheet, as well as at two other locations beyond the damaged region. The U-wraps extended from the top flange of the girder on one side, down to the bottom of the girder and back up to the top flange of the other side.
5) An additional three U-wraps, 2 ft (610 mm) in width, were provided to completely encapsulate the area of repaired concrete. The sheets were overlapped by 1 in (25 mm) to prevent the formation of cracks between the sheets. These three sheets were provided to control crack growth within the non-prestressed repair mortar. It should be noted that completely encapsulating the entire length of the girder should be avoided because of the concern of moisture build-up between the CFRP and concrete.

The completed installation of the CFRP system for AASHTO1 is shown in Figure 3.23.

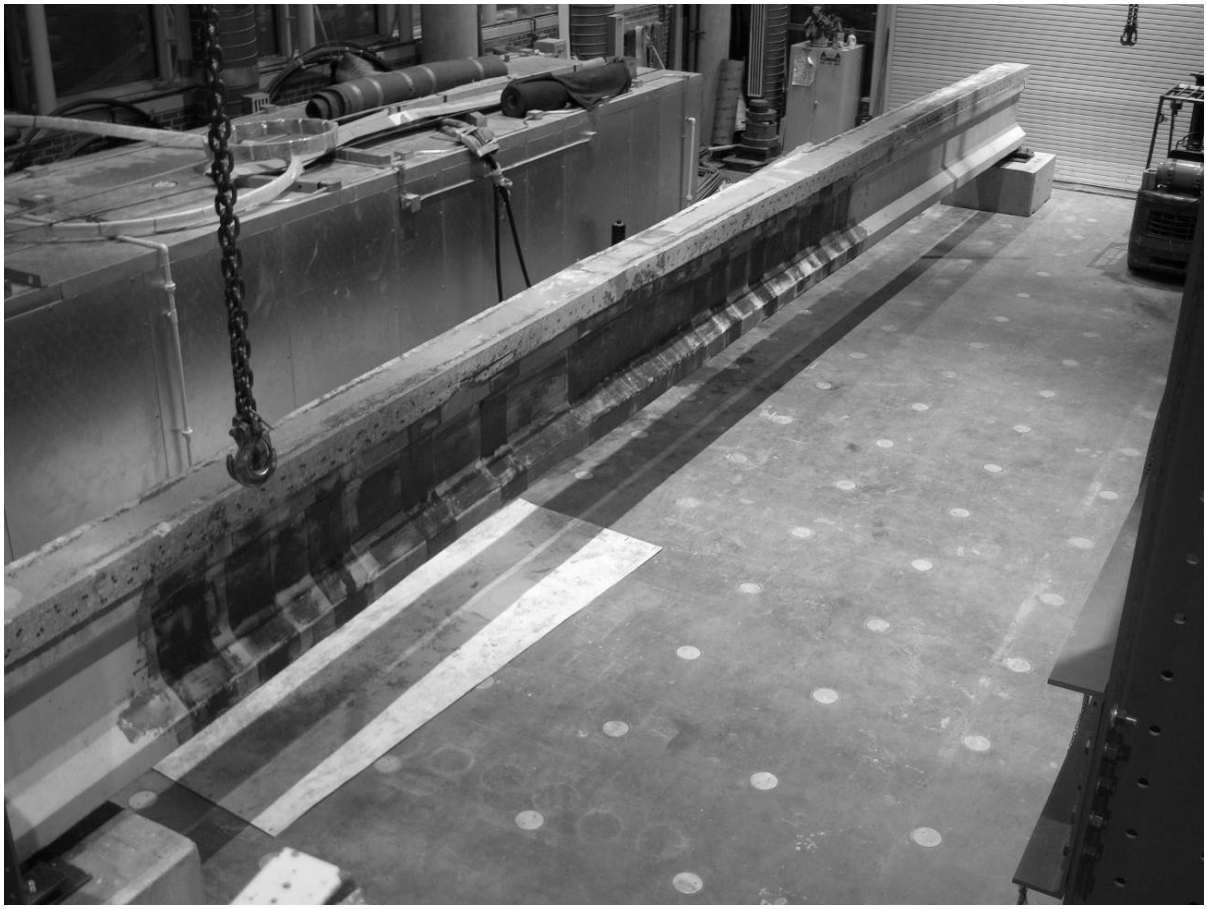

Figure 3.23 CFRP repaired AASHTO1 girder

AASHTO2

As with AASHTO1, the first task in the design of the CFRP repair system for AASHTO2 was to determine the ultimate flexural strength and load vs. deflection behavior of the undamaged specimen. The ultimate capacity of the section was predicted using the previously described cracked section analysis program RESPONSE 2000© and was verified by loading the girder as described in Section 3.6.

Following the simulated impact damage described earlier, the concrete section was restored using Emaco® T430 rapid-strength repair mortar with extended working time (ChemRex 2002). Due to the vast size of the damaged region, 3/8 in (9.5 mm) rounded aggregate was added to increase the strength of the mortar, minimize shrinkage, and maintain an equivalent modulus of elasticity value. The compressive strength of the repair mortar was 6300 psi (43.4 MPa), as shown in Section 3.3.

To restore the loss of four prestressing strands, or 14.3 percent of prestressing, in AASHTO2, the Fyfe© CH-41 composite and Tyfo© S two part epoxy system were again chosen. The amount of CFRP repair material required to restore the original capacity of AASHTO2 was determined using RESPONSE 2000©. Several of the input parameters follow: 1) the compressive strength of the girder was estimated to be 6000 psi (41.4 MPa), and 3000 psi (20.7 MPa) for the deck and 2) the 250 ksi (1724 MPa) prestressing strands were modeled using the Ramberg-Osgood function (Equation 3.1) for low relaxation strands. Material properties for the CFRP system were previously shown in design of AASHTO1 repair system.

Following a procedure similar to that described in Appendix A, it was concluded that three layer of 16 in (406 mm) wide longitudinal CFRP sheets were needed to restore the original ultimate flexural capacity of the girder. In order to minimize the initiation of new cracks in the repaired concrete, addition longitudinal sheets were provided; a 6 in (152 mm) wide sheet was placed on the top of the bottom flange and a 12 in (305 mm) sheet was placed in the middle of the web. These sheets were provided on both sides of the girder to ensure symmetry of the section. In order to ensure proper utilization of the CFRP's strength and strain capacity, adequate development length of the sheets was provided. Twelve 12 in (305

mm) wide transverse CFRP U-wraps were provided along the repaired section to prevent interfacial debonding of the longitudinal sheets. Full details of the CFRP reinforcement are described below, as well as a full schematic shown in Figure 3.5:

1) The three bottom layers of longitudinal CFRP reinforcement were extended 7.5 ft (2.29 m) past the location of the ruptured prestressing strand. This length was chosen to ensure full development of a 0.5 in (12.7 mm) diameter prestressing strand, as well as full development of the CFRP sheet.
2) The termination points of the longitudinal CFRP were staggered at a distance of 1.5 ft (457 mm) to prevent plate-end debonding.
3) Two 6 in (152 mm) sheets and two 12 in (305 mm) sheets were installed on the top face of the bottom flange and middle of web, respectively. These four sheets were to control cracking in the non-prestressed, damaged location. These sheets extended the same length as the longest longitudinal CFRP sheet.
4) 12 in (305 mm) wide transverse CFRP U-wraps were spaced along the entire length of the longitudinal CFRP reinforcing sheets. The U-wraps were placed at the termination point of each longitudinal CFRP sheet, as well as at three other locations beyond the damaged region. The U-wraps extended from the top flange of the girder on one side, down to the bottom of the girder and back up to the top flange of the other side.
5) An additional two U-wraps, 2 ft (610 mm) in width, were provided to completely encapsulate the area of repaired concrete. The sheets were overlapped by 1 in (25 mm) to prevent the formation of cracks between the sheets. These two sheets were provided to control crack growth within the non-prestressed repair mortar.

It should be noted that completely encapsulating the entire length of the girder should be avoided because of the concern of moisture build-up between the CFRP and concrete.

The completed installation of the CFRP system for AASHTO2 is shown in Figure 3.24.

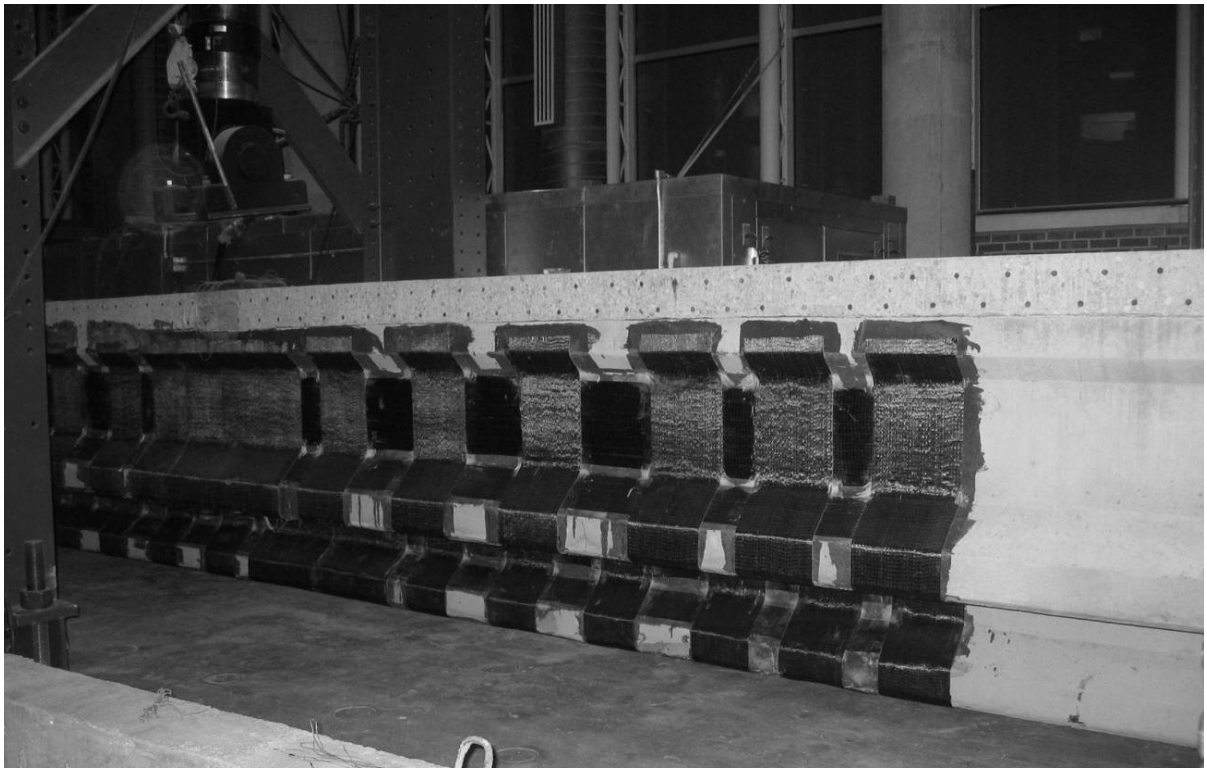

Figure 3.24 CFRP repaired AASHTO2 girder

AASHTO3

As with AASHTO2, the first task in the design of the CFRP repair system for AASHTO3 was to determine the ultimate flexural strength and load vs. deflection behavior of the undamaged specimen. The ultimate capacity of the section was predicted using the

previously described cracked section analysis program RESPONSE 2000© and was verified by loading the girder as described in Section 3.6.

The restoration of the concrete section was performed in the same manner previously described for AASHTO2. Likewise, the same design procedure and same CFRP materials were used in AASHTO3. However, unlike AASHTO2, AASHTO3 was comprised of 270 ksi (1862 MPa) prestressing strands.

Following a procedure similar to that described in Appendix A, it was concluded that three layers of 16 in (406 mm) wide longitudinal CFRP sheets were needed to restore the original ultimate flexural capacity of the girder. The full details of the CFRP reinforcement are the same as those previously described for AASHTO2. The CFRP repair details are shown in Figure 3.9.

AASHTO2R

The purpose of applying CFRP to the damaged AASHTO2R girder was to restore the original ultimate shear strength, as well as the flexural capacity of the section. Wet lay-up sheets were chosen as the CFRP repair system for the reasons previously described in Section 3.4. The shear and longitudinal CFRP sheets were designed according to the analysis procedures outlined in Chapter 4. The full CFRP repair system is outlined below:

1) Three 16 in (406 mm) longitudinal sheets were installed on the bottom flange of the girder to restore the moment capacity of the damaged section. The amount of CFRP was the same required for the AASHTO2 flexural test specimen.
2) The termination points of the longitudinal CFRP were staggered at a distance of 2 in (51 mm) to minimized plate-end debonding effects.

3) Two layers of 6 in (152 mm) wide transverse CFRP sheets were oriented perpendicular to the anticipated shear cracks to fully utilize their unidirectional strength. A 0.5 in (12.7 mm) space was left between each sheet to allow for moisture evaporation and allow for possible inspection. The transverse sheets started at the top flange of the girder, and made a 45 degree angle to the bottom of the girder. Once it reached the bottom, the sheet was smoothly transitioned and extended to the opposite side of the bottom flange before being terminated. This configuration created a crossing pattern on the bottom of the girder, as shown in Figure 3.25. This pattern of diagonal sheets began at the left support and ended below the loading point.
4) Two 10 in (254 mm) sheets were installed on the intersection of the top face of the bottom flange and bottom of web. These two sheets were placed over the diagonal struts to control cracking in the non-prestressed, damaged location, smear the distribution of stresses and prevent straightening of the sheets caused by tension in the struts at the location of the chamfer between the web and bottom flange. These sheets extended the same length as the longest longitudinal CFRP sheet.

The completed installation of the CFRP repair system for AASHTO2R is shown in Figure 3.26.

Figure 3.25 CFRP crossing pattern on bottom of AASHTO2R girder

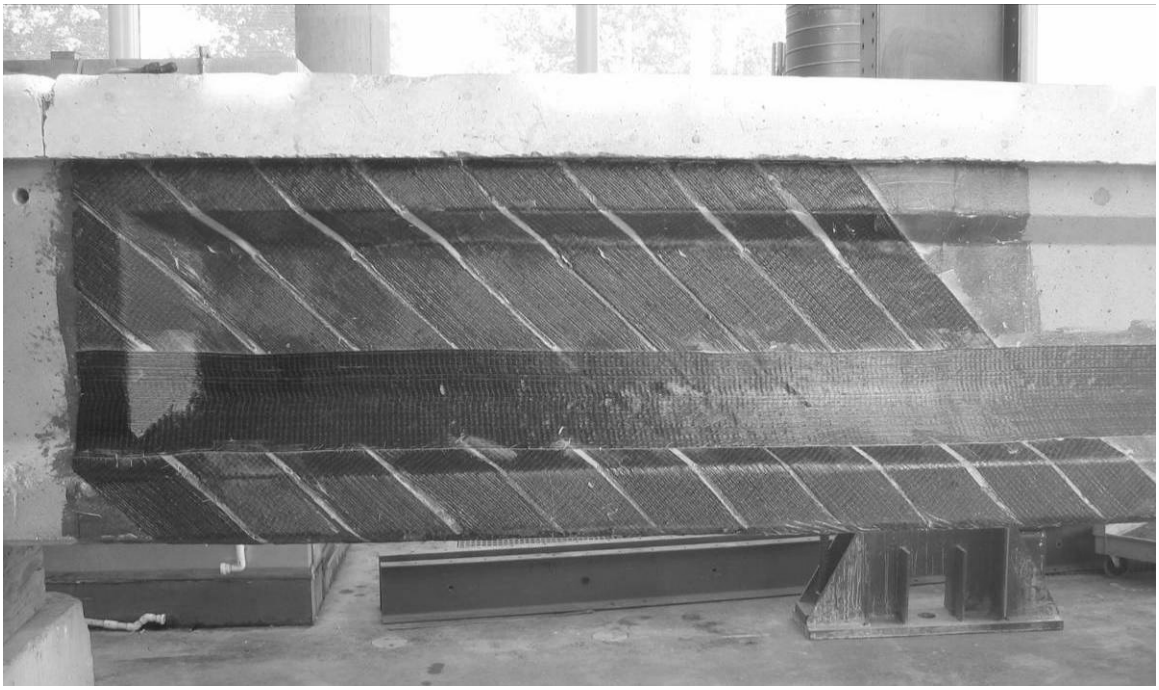

Figure 3.26 CFRP repaired AASHTO2R girder

3.5 Test Setup

This section discusses test setup for all five AASHTO Type II test specimens. AASHTO1 was first tested under fatigue loading conditions, which will be described later, before being tested to failure monotonically. AASHTO2 and AASHTO3 were tested in several cycles to failure. AASHTO2C and AASHTO2R were tested to failure under one loading cycle.

AASHTO1

The repaired AASHTO1 specimen was tested under fatigue loading conditions using a 110 k (490 kN) MTS hydraulic actuator. The 110 k (490 kN) actuator was chosen based on its high capacity servo-valve. This servo-valve allowed the girder to be tested at a higher frequency of cycles. The actuator was mounted to a steel frame which was located at midspan of the girder. As specified in AASHTO (2004), a 10 in by 20 in (254 mm by 508 mm) steel loading plate was placed in contact between the actuator and girder. A neoprene pad 11 x 21 x 0.5 in (279 x 533 x 12.7 mm) was placed below the load plate to evenly distribute the forces over any uneven surfaces on the girder. Figure 3.27 shows a drawing of the test setup for AASHTO1.

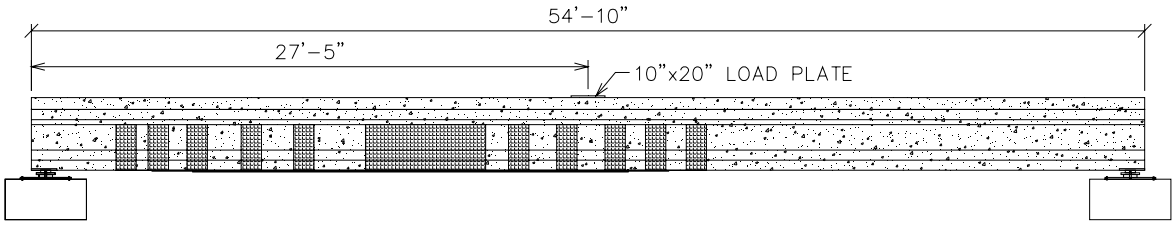

Figure 3.27 AASHTO1 test setup

For the end supports, 22 x 9 x 2.5 in (559 x 229 x 64 mm) neoprene pads were placed between two 1 in (25.4 mm) steel plates. The bottom plate measured 22 in by 30 in (559 mm

by 762 mm) and the top plate measured 11 in by 30 in (279 mm by 762 mm). The entire assembly was supported by a concrete block measuring 4 x 4 x 2 ft (1.23 x 1.23 x 0.61 m), as shown in Figure 3.28. The girder arrived at the testing facility with an 18 by 15 in (457 by 381 mm) flat steel plate built into each end, and an 18 by 6 in (457 by 152 mm) curved steel plate then welded onto it. This latter plate was centered over the top of the support system.

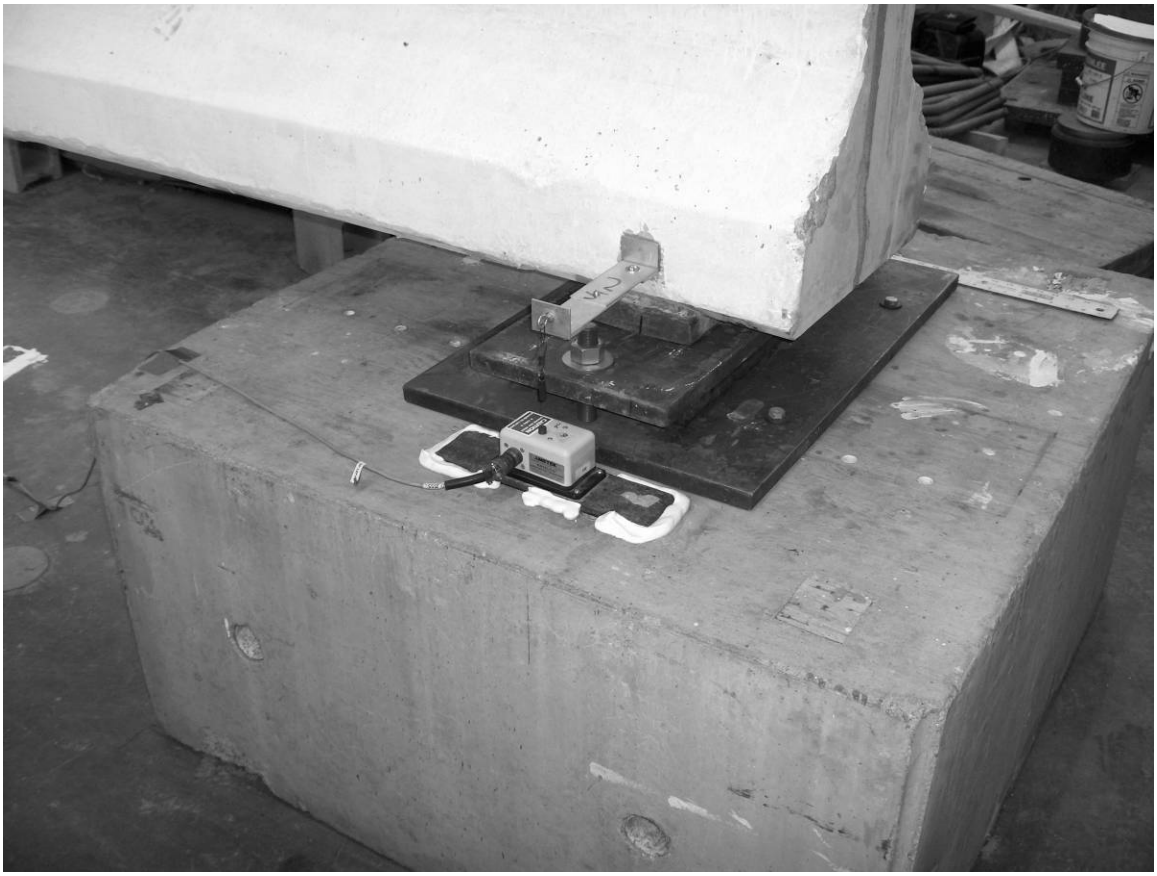

Figure 3.28 AASHTO1 girder support assembly

Fatigue Loading Range for AASHTO1

The fatigue loading scheme was designed to simulate the service loads that would be encountered during the life of the girder if it were to remain in the bridge superstructure. The loads were adjusted to simulate the same tensile stresses in the bottom layer of prestressing strands for in the test girder that would be experienced by the fully composite girder during

service loading. Two different fatigue loading schemes were considered for the repaired AASHTO1 girder: one which would simulate the original AASHTO HS-15 truck design loading, and another which would simulate tensile stress in the extreme bottom of the concrete flange equal to $3\sqrt{f'_c}$ psi ($0.25\sqrt{f'_c}$ MPa), which is specified by the AASHTO (2004) code for service loading in corrosive environments. Preliminary analysis of the girder indicated that the original girder was overdesigned; meaning that using HS-15 type loading would not simulate the worst case conditions. Therefore the design of the fatigue loading was based on determining a live load level which would simulate a tensile stress in the bottom flange of the concrete equal to $3\sqrt{f'_c}$ psi ($0.25\sqrt{f'_c}$ MPa).

The test girder had a composite deck slab approximately equal to the width of the top flange, 12 in (305 mm). In the actual bridge, the width of the deck slab working in composite action with the girder was 7 ft (2.13 m). In order to determine the live load required for testing of the test girder, the following analysis was conducted:

1) Determine the live load moment which induces a tensile stress in the bottom flange of the concrete equal to $3\sqrt{f'_c}$ psi ($0.25\sqrt{f'_c}$ MPa) for the actual bridge girder with a 7 ft (2.13 m) composite deck slab. The analysis includes the effects of the prestressing and the dead loads through sequencing of the different construction stages.
2) Determine the resulting stress profile through the cross-section of the actual girder with full composite deck based on the magnitude of live load determined in Step 1. Use the profile to calculate the stress at the level of the lower prestressing strands.

3) Determine the level of the applied load that should be used for the test girder to induce a stress in the lower prestressing strand equal to the value determined in Step 2.

Step 1: Magnitude of the Live Load

The section properties of the test girder AASHTO1 and the actual bridge girder with a 7 ft (2.13 mm) composite deck slab are shown in Figure 3.3. Properties of the transformed section of the actual bridge girder accounting for the weaker strength concrete of the cast-in-place deck slab can be determined using the modulus ratio, η, as follows:

$$\eta = \sqrt{\frac{f'_{cdeck}}{f'_{cgirder}}} \tag{3.3}$$

$$= \sqrt{\frac{3000}{5000}} = 0.7746$$

where f'_{cdeck} and $f'_{cgirder}$ are the concrete compressive strengths of the deck and AASHTO1 girder respectively.

The dead loads supported by the 53.34 ft (16.26 m) long bridge girder with and without the full 7 ft (2.13 mm) deck slab can be determined as follows:

Dead Loads Supported by Girder

Girder self weight		0.384 k/ft (5.60 kN/m)
Slab		0.531 k/ft (7.75 kN/m)
Diaphragms		0.036 k/ft (0.525 kN/m)
Total dead loads supported by girder	w_{dg} =	0.951 k/ft (13.88 kN/m)
Total dead load moment supported by girder	M_{dg} =	336.0 k-ft (455.5 kN-m)

Dead Loads Supported by Composite Section

Asphalt overlay		0.306 k/ft (4.46 kN/m)
Barrier walls		0.050 k/ft (0.73 kN/m)
Curb and gutter		0.289 k/ft (4.22 kN/m)
Total dead loads supported by composite section	w_{dc} =	0.246 k/ft (3.59 kN/m)
Total dead load moment supported by composite section	M_{dc} =	86.92 k-ft (117.8 kN-m)

The effective prestress force, P_f, was calculated assuming an effective stress of 165.1 ksi (1138 MPa) which corresponds to an assumed 12.6 percent prestress losses and a jacking force equal to 70 percent of the ultimate tensile strength of the strands. Therefore,

$$P_f = 16 \times 0.167 \times 165.12$$

=441.2 k (1962 kN).

Using the previously specified tensile stress in the concrete of $f_{bgc} = 3\sqrt{f'_c} = 0.212$ ksi (1.46 MPa), and the following stress condition at the extreme fiber of the bottom flange:

$$f_{bgc} = -\frac{P_f}{A_g} - \frac{P_f e_g}{S_{bg}} + \frac{M_{dg}}{S_{bg}} + \frac{M_{dc} + M_{lc}}{S_{bc}} \tag{3.4}$$

where A_g is the area of the girder, S_{bg} is the section modulus below the neutral axis for the girder, and S_{bc} is the section modulus below the neutral axis for the fully composite bridge girder with a 7 ft (2.13 mm) composite deck, the live load moment for the actual bridge girder with full composite deck, M_{lc}, was determined to be 458.6 k-ft (753 kN-m).

Step 2: Stress Level at the Lower Prestressing Strand

The top compressive stress in the concrete for the actual bridge girder with full composite deck, f_{tgc}, for the given live load moment, M_{lc}, can be determined using the following equation:

$$f_{tgc} = -\frac{P_f}{A_g} + \frac{P_f e_g}{S_{tg}} - \frac{M_{dg}}{S_{tg}} - \frac{M_{dc} + M_{lc}}{S_{ic}} \tag{3.5}$$

where S_{tg} is the section modulus above the neutral axis for the girder and S_{ic} is the section modulus at the interface of the girder and the 7 ft (2.13 m) composite section above the neutral axis. The compressive stress, f_{tgc}, was found to be 1.83 ksi (12.6 MPa). Given the stress profile of the actual bridge girder with full composite deck, the stress level in the concrete at the lower prestressing strand, f_{pslc}, can be determined from:

$$f_{pslc} = \frac{d_{lps}}{h}\left(f_{tgc} + f_{bgc}\right) - f_{tgc} \tag{3.6}$$

where d_{lps} is the distance from the extreme compression fiber in the concrete to the level of the lower prestressing strands and h is the depth of the section. f_{pslc} was found to be 0.0986 ksi (0.680 MPa).

Step 3: Applied Load to Test Girder

The live load moment that will induce the stress found in Equation 3.6 in the lower prestressing strand for the test girder, M_{ltg}, was determined by conducting the following analysis:

3.1) Determine the top and bottom stresses in the concrete, f_{tgt} and f_{bgt}, by assuming a value of M_{ltg} in the following equations:

$$f_{tgt} = -\frac{P_f}{A_g} + \frac{P_f e_g}{S_{tg}} - \frac{M_{dg}}{S_{tg}} - \frac{M_{dc} + M_{ltg}}{S_{it}} \tag{3.7}$$

$$f_{bgt} = -\frac{P_f}{A_g} - \frac{P_f e_g}{S_{bg}} + \frac{M_{dg}}{S_{bg}} + \frac{M_{dc} + M_{ltg}}{S_{bt}} \tag{3.8}$$

where S_{it} is the section modulus above the neutral axis at the interface of the girder and the composite section for the test girder and S_{bt} is the section modulus below the neutral axis for the test girder.

3.2) Determine the stress in the concrete at the level of the lower prestressing strands for the test girder, f_{psltg}, from the following equation:

$$f_{psltg} = \frac{34}{36}\left(f_{tgt} + f_{bgt}\right) - f_{tgt} \tag{3.9}$$

3.3) Perform iterations using different values of M_{ltg} until a value of f_{psltg} is determined which is equal to the value of f_{pslc} found in Step 2.

The live load moment applied to the test girder that will induce a stress in the concrete at the lower layer of prestressing strands of 0.0986 ksi (0.680 MPa) is $M_{ltg} = 351.9$ k-ft (477 kN-m). This moment corresponds to a concentrated load at midspan of 26.5 k (118 kN). The stress profiles of the girder with full 7 ft (2.13 m) composite deck slab, and the test girder are shown in Figure 3.29.

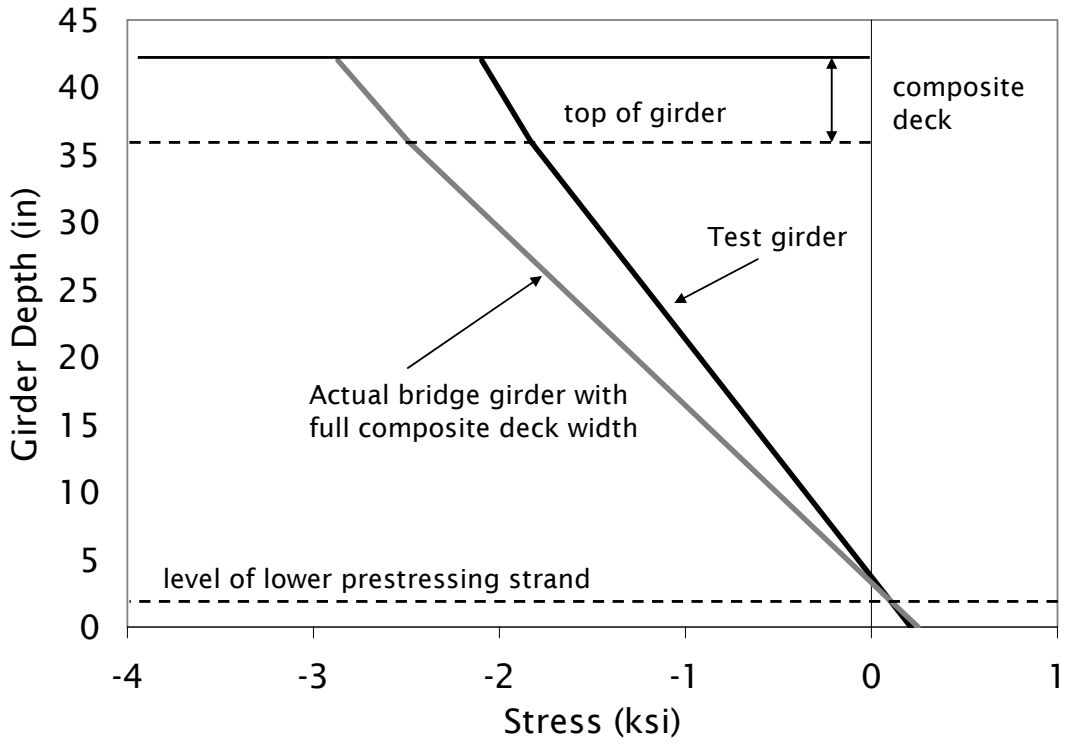

Figure 3.29 Stress profile used in AASHTO1 fatigue load determination

To determine the minimum load for the fatigue loading, the following total dead loads acting on the actual bridge girder with full composite deck, M_{DLc}, were calculated as follows:

$$M_{DLc} = M_{dg} + M_{dc} \tag{3.10}$$

$$= 425.6 \text{ k-ft } (577.1 \text{ kN-m})$$

The dead load of the test girder, M_{DLg}, includes the self weight of the girder and the weight of the 12 in (305 mm) of deck slab above the top flange of the girder. These loads correspond to a dead load moment of $M_{DLtg} = 177.0$ k-ft (240.1 kN-m). Therefore, the required applied load needed to simulate the dead loads acting on the bridge should be based on the difference between the above two moments and was found to be $M_{DLs} = 248.6$ k-ft (337.0 kN-m), which corresponds to a concentrated load at midspan of 18.7 k (83.2 kN).

Based on the above, the minimum load which should be used for the fatigue loading is 18.7 k (83.2 kN) and the maximum load, which is the summation of the dead load and the live load, is 45.2 k (201 kN). This range simulates a level of stress in the lower prestressing strand of the test girder equal to the stress in the lower prestressing strand for the actual bridge girder in composite action with the full width of the deck slab.

As mentioned previously, the design loading of HS-15 produced a bottom tensile stress in the concrete less than the $3\sqrt{f'_c}$ psi ($0.25\sqrt{f'_c}$ MPa) value specified by AASHTO (2004). Using the AASHTO 2004 code: for an exterior girder with bridge configuration "k", and with two design lanes loaded, the distribution factor, g_{ext}, is 0.6253. Using the distribution factor and an impact factor of 1.33, the axle loads of the HS-15 type loading were found to be: 4.99 k, 19.96 k and 19.96 k (22.2 kN, 88.8 kN and 88.8 kN). Using these loads will produce a maximum moment of 432.2 k-ft (586.1 kN-m) in the full composite bridge girder.

Using a procedure similar to the one described above, the live load which induces a stress in the prestressing strand for the test girder equal to the value found for the girder with full composite deck under HS-15 loading was found to be 24.9 k (110.8 kN). This is slightly lower than the value determined from the earlier analysis and therefore the girder was tested using the first conservative loading levels.

AASHTO2 and AASHTO3

The repaired AASHTO2 and AASHTO3 specimens were cycled monotonically to failure using a 440 k (1957 kN) MTS hydraulic actuator mounted to a steel frame located directly at midspan of the girder. The same load plate and neoprene pad described previously

for AASHTO1 were placed between the actuator and girder. Figure 3.30 and Figure 3.31 show a drawing of the test setup for AASHTO2 and AASHTO3.

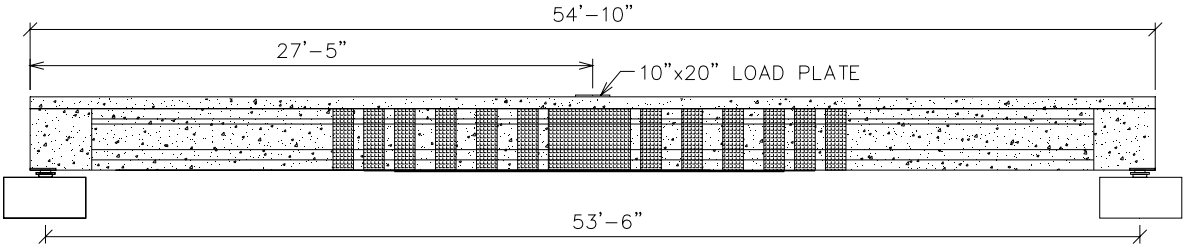

Figure 3.30 AASHTO2 test setup

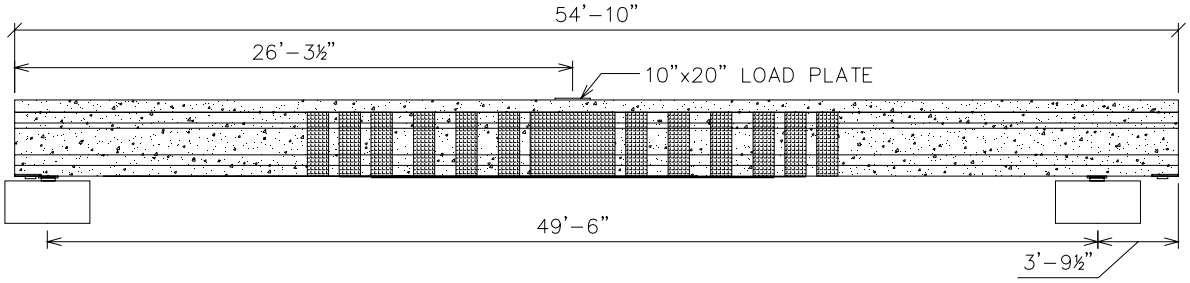

Figure 3.31 AASHTO3 test setup

The end supports for AASHTO2 and AASHTO3 were slightly different than the setup used for girder AASHTO1. The supports were comprised of the 4 x 4 x 2 ft (1.23 x 1.23 x 0.61 m) concrete support block, on which directly rested a 22 x 9 x 2.5 in (559 x 229 x 64 mm) neoprene bearing pad, and on which sat an 11 x 30 x 1 in (279 x 762 x 12.7 mm) steel plate. These were all placed beneath the 18 by 6 in (457 by 152 mm) curved steel plate already welded to the girder (Figure 3.32). The test setup for AASHTO3 was similar in that it used the previously mentioned concrete support block, neoprene bearing pad, and steel plate, however the difference is that since the supports were moved in to avoid the damaged end region, the 1 in (25.4 mm) steel plate was placed directly in contact with the concrete surface of the girder, as shown in Figure 3.33.

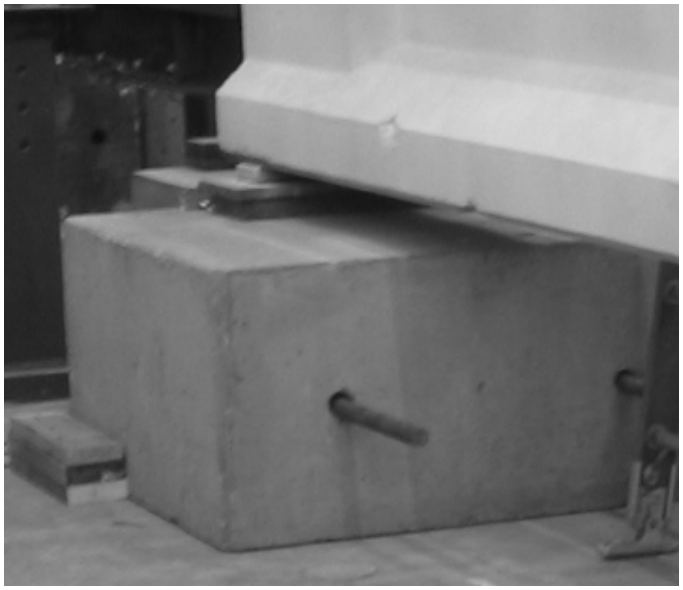

Figure 3.32 AASHTO2 girder support assembly

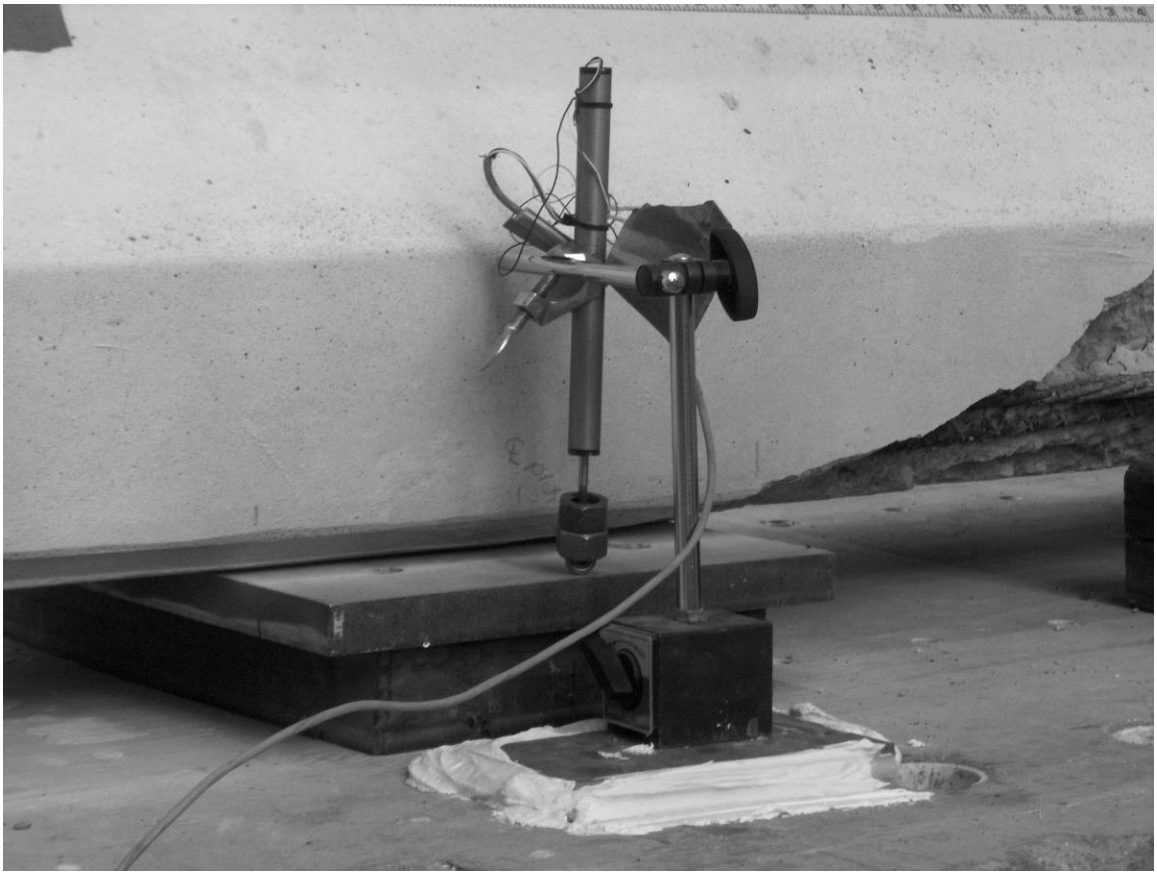

Figure 3.33 AASHTO3 girder support assembly

AASHTO2C and AASHTO2R

The test setup for both of the shear tests, AASHTO2C and AASHTO2R, were identical except for the loading mechanisms. AASHTO2C was tested to failure in one load cycle using a 440 k (1957 kN) MTS hydraulic actuator mounted to a steel frame, while AASHTO2R was tested to failure using a 600 k (2669 kN) hydraulic jack mounted to the same steel frame A drawing of the test setup is shown in Figure 3.34. The loading mechanism was placed at 5.5 ft (1.68 m) from the face of the left support of each girder, resulting in a shear span to depth ratio, a/d, of 1.57. The load was transferred to the girder through a 10 by 20 in (254 by 508 mm) and 11 x 21 x 0.5 in (279 x 533 x 12.7 mm) neoprene pad.

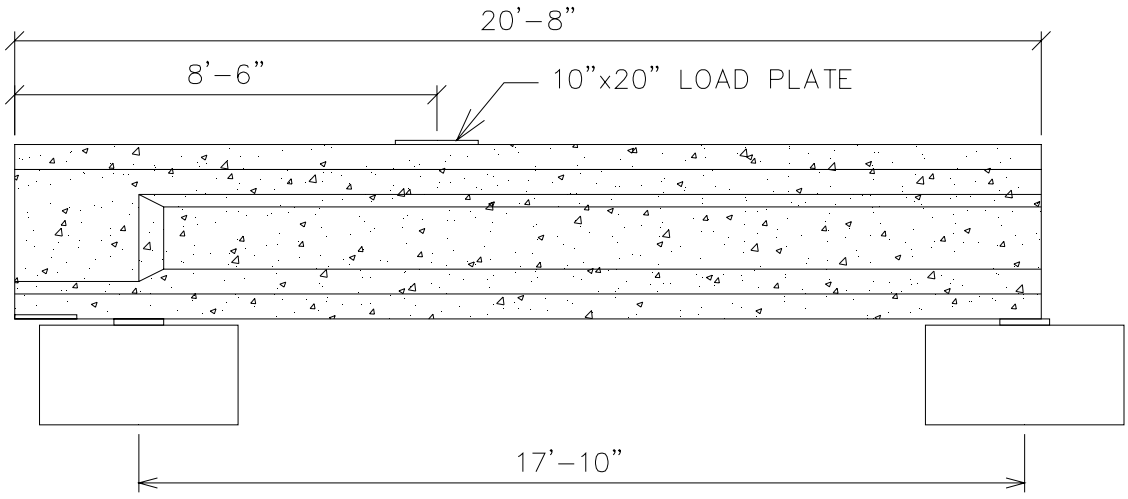

Figure 3.34 Test setup for shear study

The end supports for both AASHTO2C and AASHTO2R were the same as those previously described for AASHTO3 in Section 3.5. The right support was placed below the extreme right end of the girder, while the left support was placed beneath end block transition region in order to avoid any affects on the shear capacity that the end block would create.

3.6 Loading Scheme

AASHTO1

The loading of AASHTO1 consisted of three stages that all occurred after the installation of the CFRP repair system: 1) initial loading, 2) fatigue loading, and 3) final static loading to failure.

During the initial loading phase, the girder was loaded up to a level of 51 k (227 kN), applied using displacement control loading. This load was selected to simulate a bottom tensile stress in the girder of $3\sqrt{f'_c}$ ksi ($0.5\sqrt{f'_c}$ MPa), in order to evaluate the observed stress ratio in the lower prestressing strands and load-deflection behavior of the girder at this load level. The fatigue loading regime was performed by oscillating between 18.7 k and 45.2 k (83.2 kN and 201 kN) to simulate the dead load to the dead load plus live load, as determined in Section 3.5. The load was applied using a 110 k (490 kN) actuator, at a frequency of 2 Hz, for two million cycles. At regular intervals, the fatigue test was stopped to record data during intermediate static tests. The final static test of the girder consisted of several intermediate cycles of progressively increasing load up to a failure load of 136.1 k (605 kN).

AASHTO2 and AASHTO3

The loading of AASHTO2 and AASHTO3 consisted of four stages: 1) initial loading of undamaged specimen, 2) loading after removal of concrete section, 3) loading after cutting of prestressing strands, 4) final static loading to failure after CFRP repair.

During the initial loading of AASHTO2, the girder was first loaded to 75.6 k (336 kN) then unloaded to 5.0 k (22.4 kN). Immediately following the previous cycle, the girder

was loaded to 105.9 k (471 kN). Similarly, AASHTO3 was first loaded to 62.6 k (278 kN), unloaded to 2.0 k (8.9 kN), then reloaded to 89.0 k (396 kN). These loads were selected to evaluate the cracking and crack reopening loads of the girder, as well as the load-deflection behavior of undamaged specimen. Initially loading of both girders was also intended to ease the removal of the desired concrete section. After the desired amount of concrete was removed from each girder, AASHTO2 and AASHTO3 were loaded to examine any changes in the load-deflection behavior; 60.3 k (268 kN) and 50.3 k (224 kN), respectively. Following the cutting of prestressing strands, AASHTO2 and AASHTO3 were again loaded 50.3 k (224 kN) and 50.2 k (223 kN), respectively. The final static test of each girder consisted of two cycles up to a failure load of 135.1 k (601 kN) for AASHTO2 and 145.4 k (647 kN) for AASHTO3.

AASHTO2C and AASHTO2R

The loading of AASHTO2C and AASHTO2R was performed in one cycle up to failure. No initial tests were performed after the removal of the concrete or cutting of prestressing strands for fear that an unexpected brittle failure could ruin the test specimens. The ultimate failure load of AASHTO2C was 413.7 k (1840 kN). The ultimate failure load of AASHTO2R was 446.3 k (1985 kN).

3.7 Instrumentation

AASHTO1, AASHTO2, and AASHTO3

The displacement profile along the length of each girder was measured using string potentiometers. The tensile strain in the longitudinal CFRP was measured using 0.236 in (6

mm) TML FLA-6-11 120 Ω electrical resistance strain gauges. The compressive strain in the deck and girder were measured using both PI gauges (a strain gauge mounted to a spring plate) and 2.36 in (60 mm) TML FLA-60-11 120 Ω electrical resistance strain gauges. The location of the instrumentation was selected to determine: 1) the strain profile at the damaged region, 2) the behavioral differences between the damaged and undamaged section, if applicable, and 3) the tensile strain in the CFRP to determine the bond characteristics between the CFRP and concrete. Figure 3.35 shows a drawing of the instrumentation used during the testing of AASHTO1. Figure 3.36 shows a drawing of the instrumentation used during the final testing of AASHTO2 and AASHTO3.

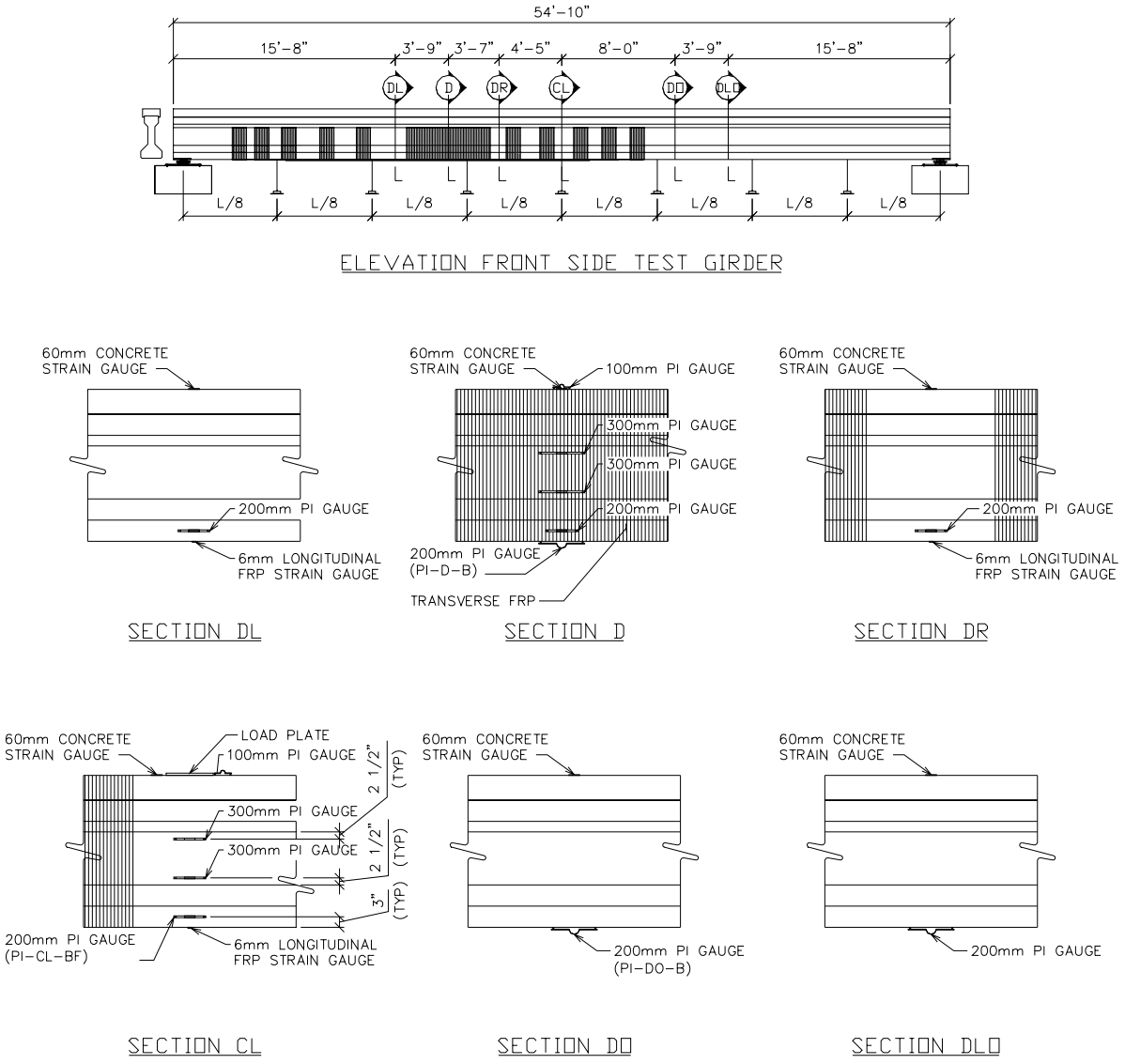

Figure 3.35 Repaired AASHTO1 instrumentation plan

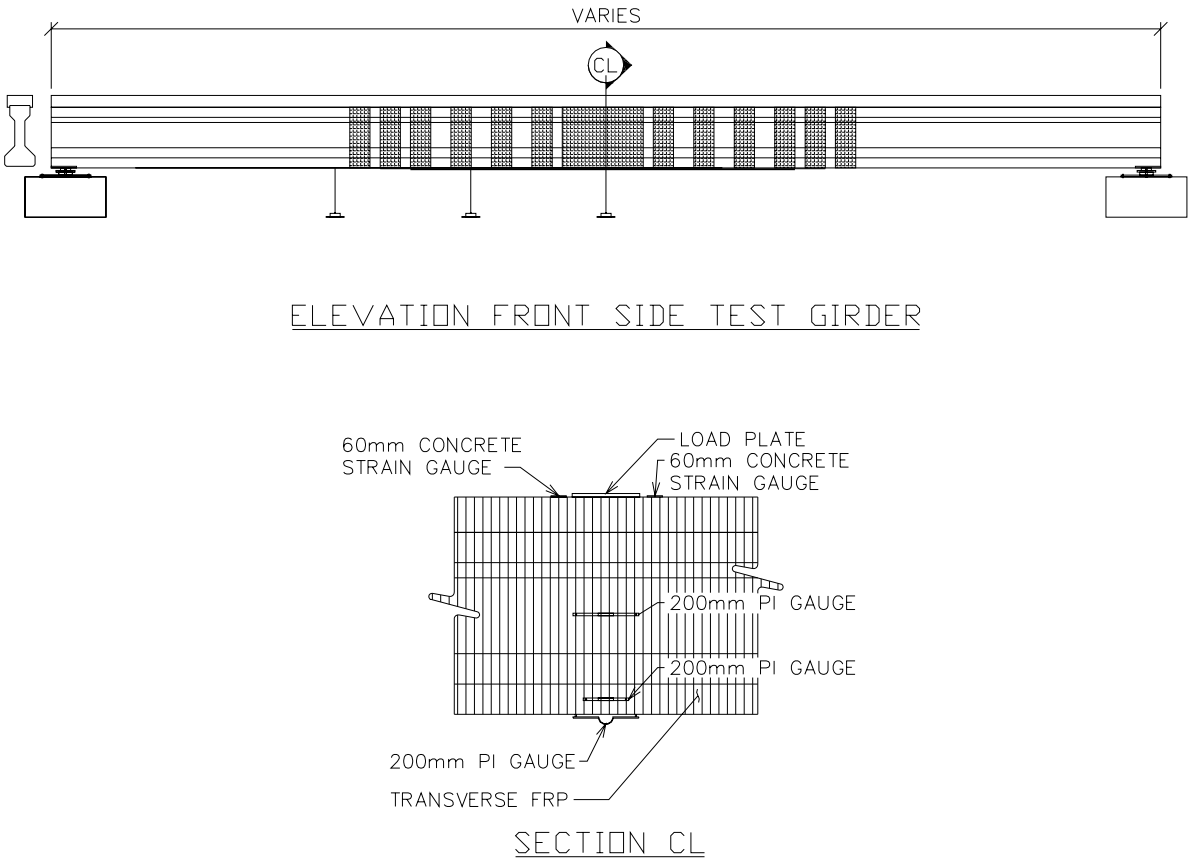

Figure 3.36 Instrumentation plan for AASHTO2 & AASHTO3 final static test

AASHTO2C and AASHTO2R

The displacement beneath the load point of each girder was measured using two string potentiometers. The compressive strain in the deck and girder were measured at midspan using both PI gauges (a strain gauge mounted to a spring plate) and 2.36 in (60 mm) TML FLA-60-11 120 Ω electrical resistance strain gauges. The shear crack widths were measured using three sets of two linear potentiometers oriented perpendicular to each other as shown in Figure 3.37. The location of the instrumentation for both girders was selected to determine: 1) the strain profile below the load point, and 2) to compare the crack widths of the control specimen with those of the repaired specimen. AAHTO2R was instrumented with 0.236 in

(6 mm) TML FLA-6-11 120 Ω electrical resistance strain gauges along the CFRP diagonal struts to determine the strain distribution along the length of the girder.

Figure 3.37 Typical layout of linear potentiometers for AASHTO2C and AASHTO2R

3.8 Test Descriptions

AASHTO1

Visual cracking was first observed just outside the transverse U-wraps enclosing the damaged region at 42.0 k (189 kN). The crack formed on the side of the girder with the ruptured prestressing strand. After the first three initial loading cycles, three additional visible cracks formed at the edge of the CFRP U-wraps in the damaged region. These cracks formed on the same side as the previous crack and extended from the edge of the CFRP

U-wrap to the top of the bottom flange. It should be noted that the three cracks that formed during the initial static test did not significantly propagate during the fatigue loading phase. After the completion of 2 million cycles of fatigue loading, the midspan deflection of the girder, at 45.2 k (201 kN), degraded from an initial value of 0.771 in to 0.922 in (19.6 mm to 23.4 mm). This resulted in a total midspan residual deflection of 0.12 in (3.0 mm) due to fatigue-creep of the concrete (ACI 215 1997). As well, very little degradation in stiffness was observed in the girder.

The final static test of AASHTO1 was performed in various deflection increments. The girder was first loaded up to a level of 76.2 k (339 kN) at a rate of 0.1 in/min (2.5 mm/min), resulting in a total deflection of 1.5 in (38.8 mm). Both the midspan and damaged region flexural cracks extended through the bottom flange of the section as a result of this loading. The girder was then unloaded and reloaded up to a level of 90.0 k (401 kN), resulting in a total deflection of 2.0 in (51.4 mm). Cracking within the area of the longitudinal CFRP did not extend during this cycle, but new flexural cracks formed just beyond the right termination point of the longitudinal CFRP. The test was stopped because the capacity of the girder unexpectedly exceeded the capacity of the actuator.

The final test to failure began after installation of a 220 k (977 kN) actuator was completed. At a load of 101 k (449 kN), the flexural cracks outside the longitudinal CFRP extended into the web. The presence of the longitudinal tension strut in the web prevented cracks in the damaged region from extending beyond the top of the bottom flange. Concrete crushing was observed in two locations at a load of 131.0 k (583 kN): 1) on both sides of the loading plate at midspan and, 2) above the damaged region at the location of a saw cut in the deck. The maximum measured load was 136.0 k (605 kN) at a midspan deflection of 5.78 in

(147 mm). After the maximum load was achieved, a sudden drop of 2.0 k (8.9 kN) occurred. The load rate was then increased to 0.2 in/min (5.1 mm/min) until at a displacement of 6.17 in (157 mm) a large flexural-shear crack suddenly extended from the right termination point of the longitudinal CFRP to the concrete crushing zone near the loading plate. This flexural-shear crack caused catastrophic failure, as shown in Figure 3.38. Complete test results are presented in Chapter 4.

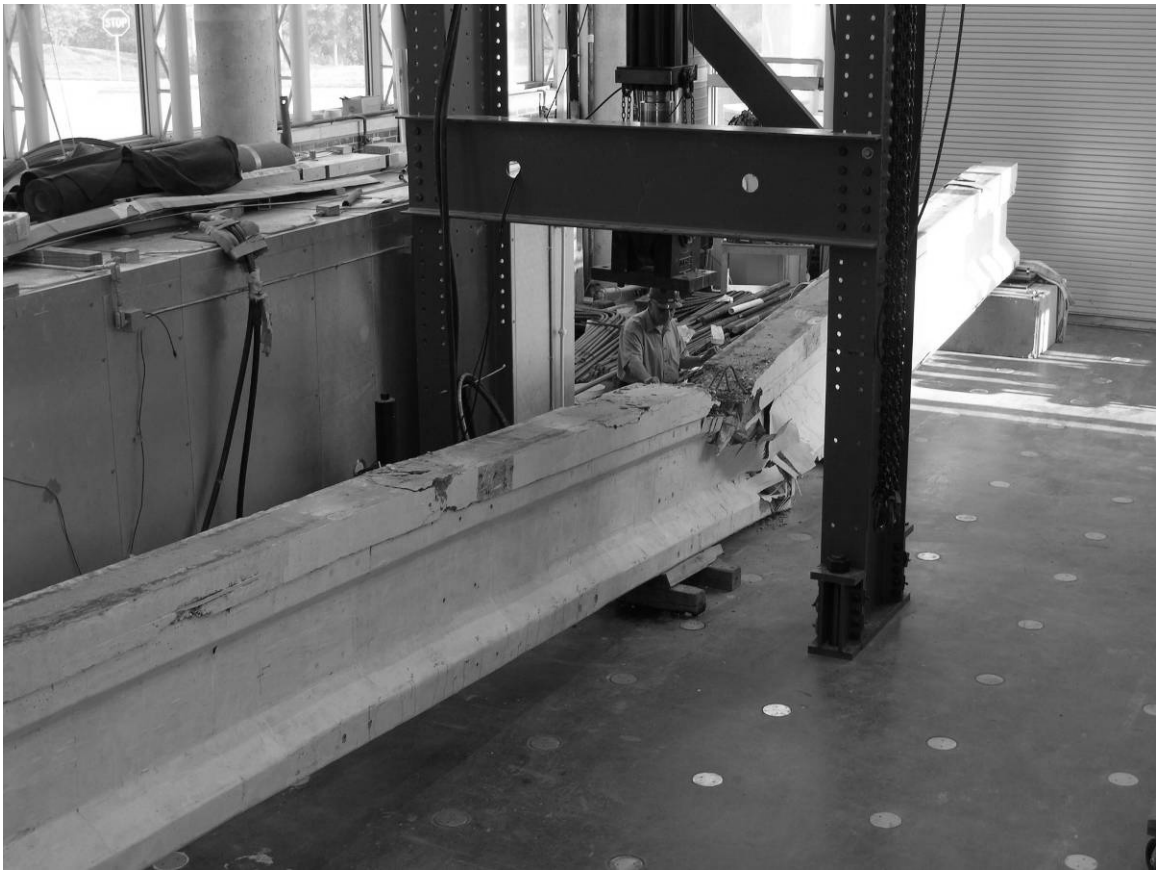

Figure 3.38 AASHTO1 girder after failure

AASHTO2

During the initial loading phase described in Section 3.6, visual flexural cracking of the undamaged specimen was first observed at 75.0 k (334 kN), occurring directly below the loading plate at midspan. All loading in the initial phase was performed at 0.1 in/min (2.5

mm/min) and was unloaded at a rate of 0.25 in/min (6.5 mm/min). The specimen was then reloaded again to 93.4 k (415 kN) to observe the crack reopening load, which was approximately 50.5 k (225 kN). The girder was then unloaded and reloaded one final time to 104.7 k (466 kN) at a displacement of 3.09 in (78.5 mm), which was estimated to be 90 percent of the girder's ultimate load capacity. The final initial load level caused a residual midspan deflection of 0.257 in (6.53 mm).

Following the removal of the concrete section previously described in Section 3.2, the girder was loaded up to 60.0 k (267 kN) at a rate of 0.15 in/min (3.8 mm/min) then unloaded at a rate of 0.25 in/min (6.5 mm/min) after the behavior of the girder became nonlinear. A residual deflection of 0.415 in (10.5 mm) formed between the first initial loading up to 60.0 k (267 kN) and the loading after the removal of the concrete section. After the cutting of prestressing strands, the girder was again loaded up to 49.3 k (219 kN) to examine the fully damaged behavior of the member, only resulting in an increase in girder deflection of 0.018 in (0.46 mm). However, a loss of stiffness occurred due to the cutting of the prestressing strands. The test was terminated because of the sudden non-linear behavior of the girder.

After repaired using CFRP sheets, the final static test of AASHTO2 was performed in one cycle, monotonically to failure, at a load rate of 0.1 in/min (2.5 mm/min). Cracking first occurred at midspan in the non-prestressed repair mortar at a load of 10.6 k (47.2 kN) and occurred at the undamaged side at 51.4 k (229 kN). These cracks were not visible but were detected by instrumentation. The loading was continued up to 90.0 k (400 kN) then held to look for cracks, but none were visible. The girder continued to be loaded up to 112.9 k (502 kN), but still no cracks were visible outside of the CFRP repaired region despite the load being significantly higher than the cracking load determined during the initial test. Localized

concrete crushing occurred at the left edge of the loading plate on the side with the simulated damaged at a load of 125 k (556 kN). Loading continued until the girder noticeably shifted approximately 1.0 in (25.4 mm) out-of-plane towards the damaged side. The maximum load achieved was 135 k (601 kN) with a midspan deflection of 4.77 in (121 mm). The concrete crushing failure is shown in Figure 3.39. Complete test results are presented in Chapter 4.

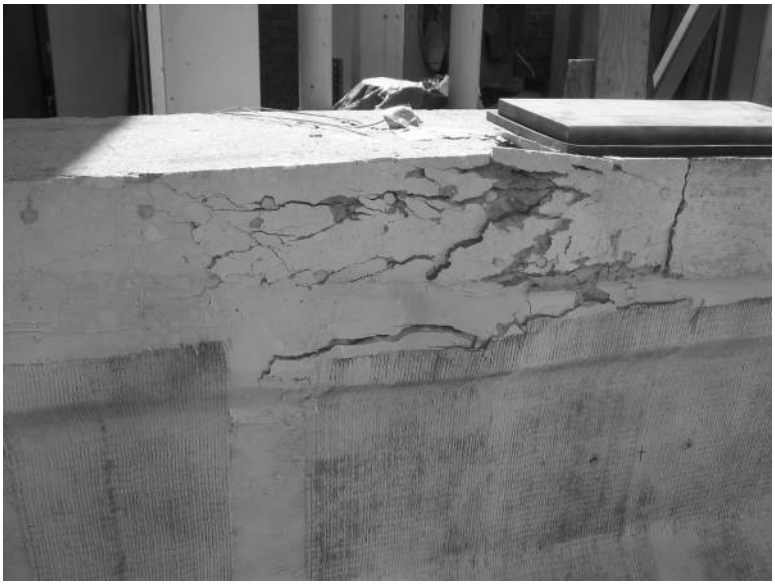

Figure 3.39 AASHTO2 girder localized concrete crushing

AASHTO3

During the initial loading phase described in Section 3.6, visual cracking of the undamaged specimen was first observed at a load of 59.0 k (262 kN), occurring directly below the loading plate at midspan. All loading in the initial and post damaging phases was performed at 0.1 in/min (2.5 mm/min) while unloading occurred at 0.25 in/min (6.5 mm/min). Additional flexural cracks formed as an additional three cycles were performed up to a load of 89.0 k (396 kN). It should be noted that several small cracks did not form during the loading regime, but one large crack and several medium width cracks formed instead. The large crack extended all the way up through to the interface between the girder and deck.

The final initial load was approximately 80 percent of the estimated ultimate capacity of the undamaged section. This load caused a residual midspan deflection of 0.240 in (6.1 mm).

Following the removal of the concrete section described in Section 3.2, the girder was loaded up to 50.3 k (224 kN) at the same rate as the initial tests. A residual deflection of 0.024 in (0.61 mm) resulted after this test. After cutting the three prestressing strands, the girder was again loaded up to 50.2 k (223 kN) to examine the fully damaged behavior of the member, resulting in a residual deflection of 0.021 in (0.53 mm). A loss of stiffness occurred in the girder after cutting of the prestressing strands.

The final static test of AASHTO3 was performed monotonically to failure in two cycles at a load rate of 0.1 in/min (2.5 mm/min). The first visible crack appeared between two CFRP U-wraps just to the right of the fully encapsulated area; at a load of 65.0 k (289 kN). The first cycle continued to load the specimen to 84.3 k (375 kN) where cracking was heard beneath the CFRP but was not visible. The girder was unloaded and reloaded to a maximum load of 145.5 k (647 kN) and a midspan deflection of 5.41 in (137 mm). Failure of the girder was caused by crushing of the concrete beneath the left side of the load plate at 144.7 k (644 kN), followed later by catastrophic failure as a flexural crack extended into the deck, splitting the member in two. Figure 3.40 shows the progressive failure of the AASHTO3 girder, and Figure 3.41 shows catastrophic failure of AASHTO3.

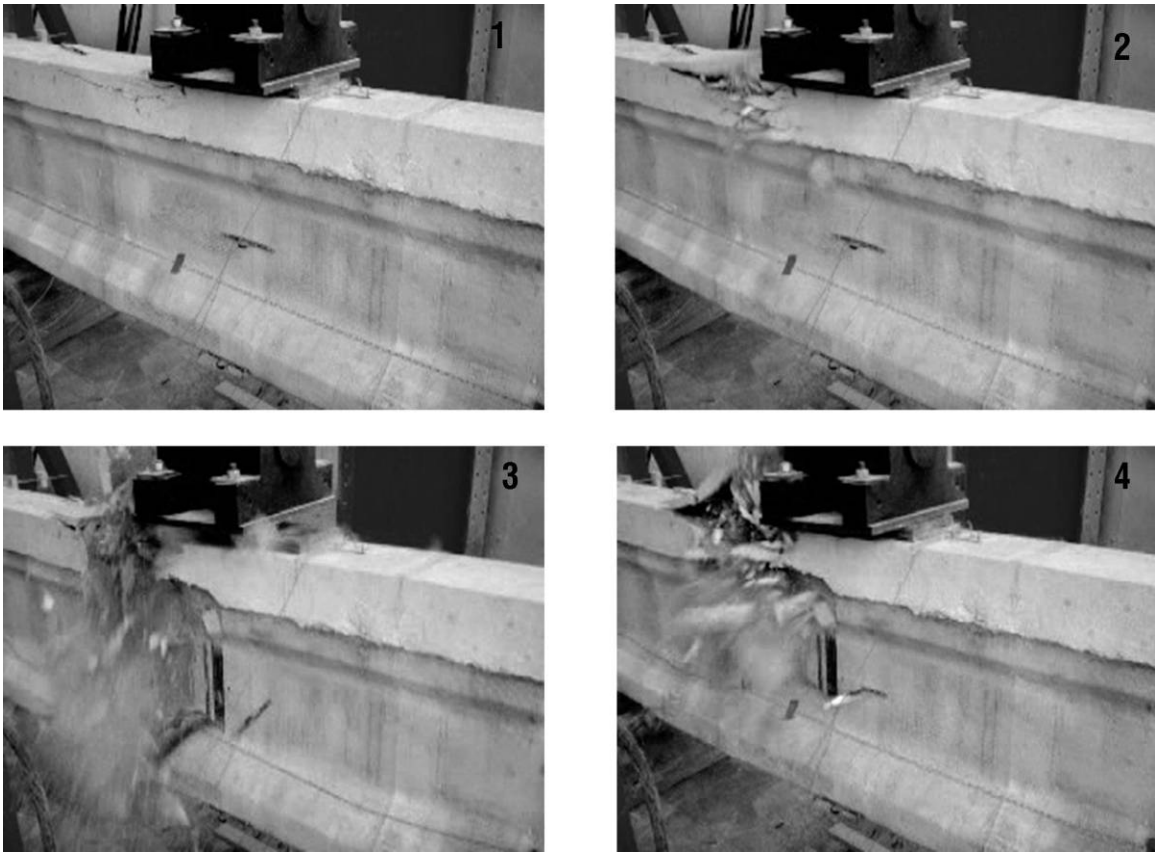

Figure 3.40 Progressive failure of AASHTO3 girder

Figure 3.41 AASHTO3girder after failure

AASHTO2C

AASHTO2C was loaded at a constant rate of 0.05 in/min (1.3 mm/min) up to a load of 275 k (1223 kN), then loaded at a rate of 0.02 in/min (0.5 mm/min) up to failure. The first visual crack formed in the web at 45 degrees from the left support on the back side of the girder at a load of 225 k (1001 kN). Additional shear cracks formed in the web as the girder continued to be loaded up to its ultimate capacity of 413.7 k (1840 kN) before failing in web shear. At ultimate, a shear crack on the shear critical span, left side, of the girder in the web propagated toward both the left support and left edge of the loading plate, causing the section to split along this line. The initial web shear cracks on the back side of the girder are shown

in Figure 3.42, while the catastrophic web shear failure is shown in Figure 3.43. Complete test results are presented in Chapter 4.

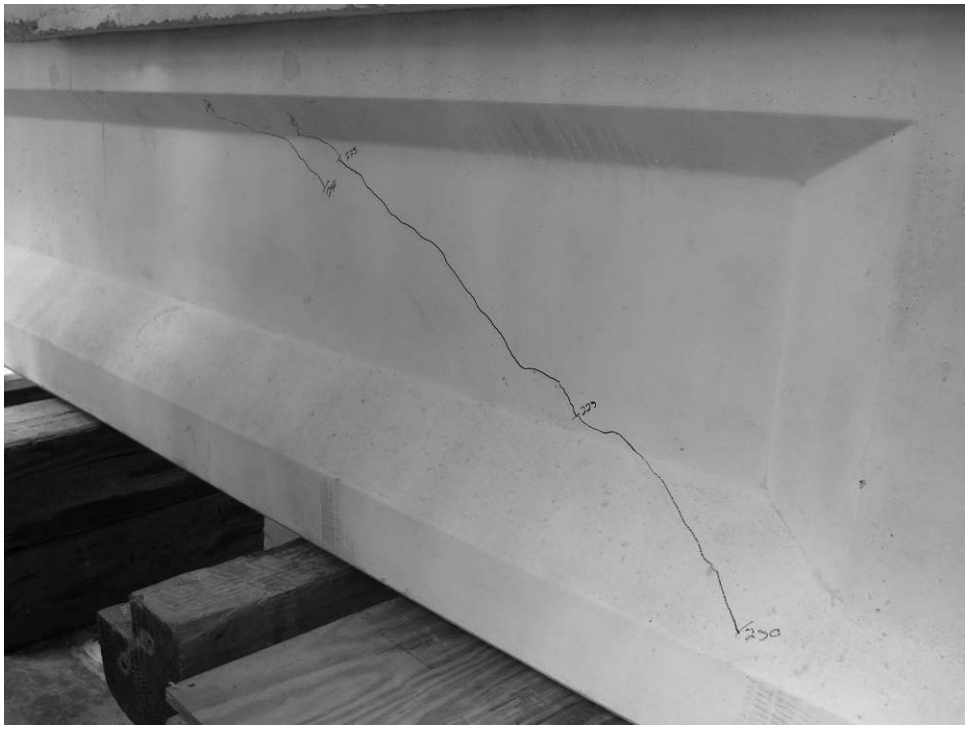

Figure 3.42 Initial shear cracks in AASHTO2C girder (back side)

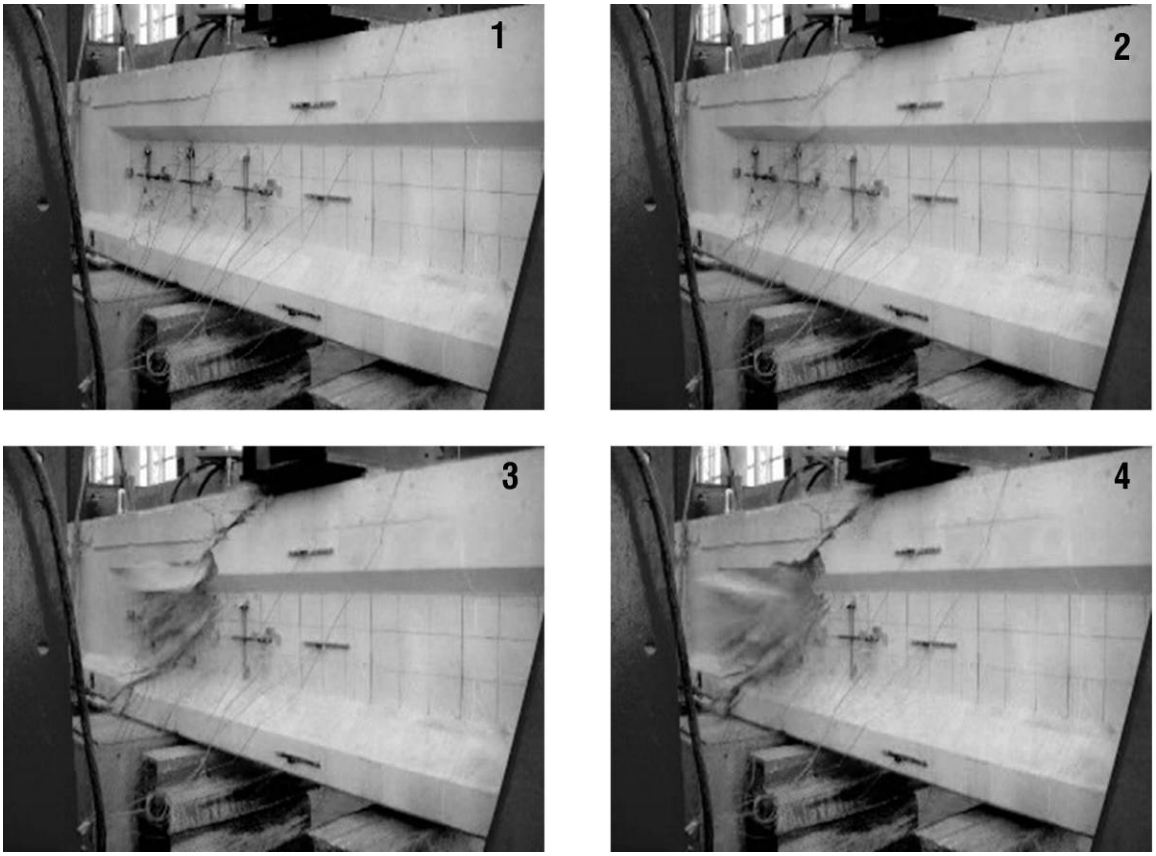

Figure 3.43 Progressive failure of AASHTO2C girder (front side)

AASHTO2R

AASHTO2R was loaded using a 600 k (2670 kN) hand-controlled jack. The girder was loaded as evenly as was possible with the hand-controlled hydraulic unit. The first visible crack formed on the test specimen at a load of 344 k (1530 kN) just beyond the right termination point of the CFRP on the front side of the girder. The crack that formed was a flexural crack, however other cracks were heard prior to this, but they were located beneath the diagonal CFRP struts and thus not visible. The girder was then loaded to an ultimate load of 446.3 k (1985 kN) before shear forces in the right transfer region began debonding the prestressing strands, as shown in Figure 3.44. This debonding led to decreased flexural capacity on the right side of the girder, which ultimately resulted in a flexural-shear crack

propagating through the right, undamaged, side of the specimen from the load point to the support. Plate end debonding at the right termination point of the bottom longitudinal CFRP also occurred in this same region. The flexural-shear failure is shown in Figure 3.45. It should be noted that the transverse CFRP sheets that are visibly debonded were not part of the shear study, but were left over from the flexural repair of the specimen. Complete test results are presented in Chapter 4.

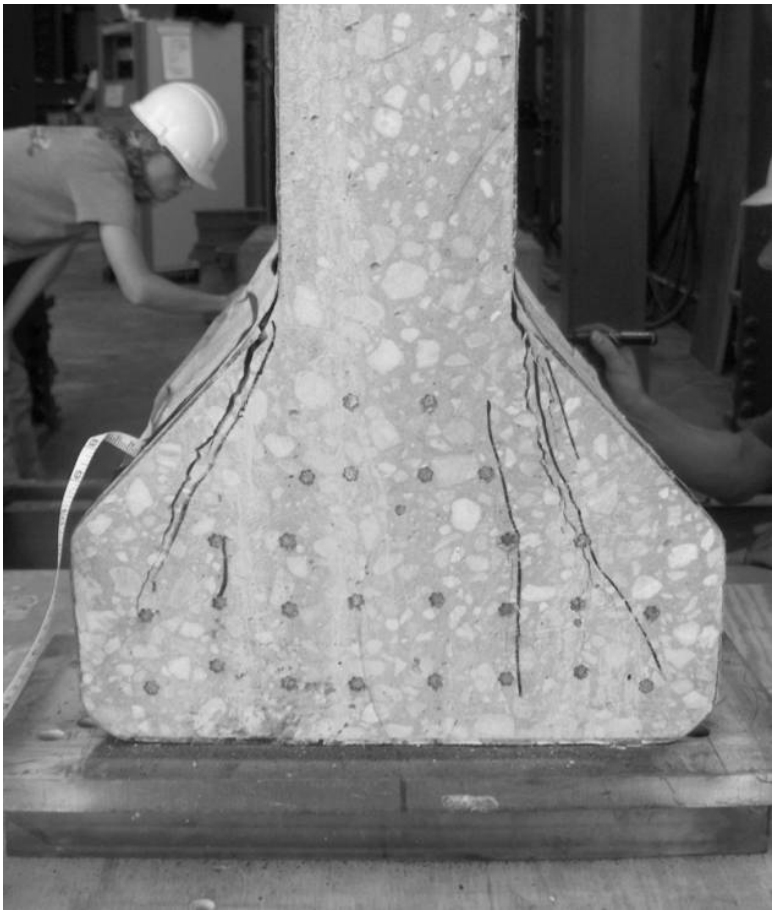

Figure 3.44 Failure in transfer zone of girder AASHTO2R

Figure 3.45 Failure of AASHTO2R girder (front side)

4. Test Results and Discussion

4.1 Introduction

Five AASHTO Type II girders were tested in this research project. Three were damaged (either by impact of simulated impact) at or near midspan, and repaired using CFRP sheets (AASHTO1, AASHTO2, AASHTO3). Two additional AASHTO Type II short span girders were tested under induced shear critical loading, one as a control specimen (AASHTO2C), and one intentionally damaged near the support and repaired with CFRP sheets (AASHTO2R). Summarized test results for the AASHTO girders are provided Table 4.1 for the flexural tests and Table 4.2 for the shear tests.

4.2 Modeling

The following modeling procedures were used in the design of the repair systems for each of the test specimens. It should be noted that the first step of any repair system is to determine if the shear capacity or the flexural capacity of the section will be the critical failure mode of the member. Once the critical failure mode is determined, the proper repair model, presented below, can be chosen.

Introduction

A combination of various design and analysis procedures were used throughout the research project. A cracked section analysis was performed to predict the undamaged, damaged and repaired flexural capacity of girders AASHTO1, AASHTO2, and AASHTO3. The analysis of the undamaged shear strength of AASHTO2C and AASHTO2R was determined using Prestressed/Precast Concrete Institute (PCI (2006)) guidelines. The same

PCI guidelines were combined with ACI Committee 440 (2002) design guidelines to determine the repaired capacity of AASHTO2R. The cracked section analysis procedure, PCI guidelines, and ACI Committee 440 guidelines will be presented in this section. A complete design example using RESPONSE 2000© for repairing a flexurally critical specimen with CFRP is presented in Appendix A. Likewise, a complete design example for shear repair of a member using CFRP is presented in Appendix B.

Flexural Modeling

RESPONSE 2000© Cracked Section Analysis

A cracked section analysis was performed on all five of the AASHTO Type II girder test specimens using RESPONSE 2000© software to analyze their flexural capacities. Verification of this program can be found in Bentz (2000). The default cross section of the AASHTO Type II girder was used without any modification. The width of the composite deck was modified using the modular ratio of concrete strengths (Equation 3.3). The strength of the concrete for the girder and the deck was based on material testing of concrete core samples previously described in Section 3.3. The behavior of the concrete was modeled using Popovics curve; tension stiffening was also included in the analysis. The prestressing steel for each girder was modeled using the Ramberg-Osgood function (Equation 3.1), using constants derived from the tension tests taken from each girder. The CFRP was modeled as a linear-elastic material up to failure with the modulus of elasticity, rupture strain, and ultimate tensile strength values determined from coupon tension tests.

The results of the cracked section analyses for both the undamaged and repaired specimens showed very good agreement with the experimental results presented in Section

4.3. Finite element simulation was not included in this research based on the good agreement of the predicted versus experimental results.

Shear Modeling

An analysis technique combining two different design approaches was used in the modeling of the girder repaired with CFRP in shear. The method combined guidelines from the Precast/Prestressed Concrete Institute (PCI) (2006) design manual with the CFRP shear analysis approach from ACI Committee 440 (2002). Below are the steps used in the model for the prediction of the shear capacity of an impact damaged and CFRP repaired AASHTO girder:

1) The first step is to determine the shear capacity along the undamaged girder using the PCI (2006) guidelines. The nominal shear capacity envelope was then plotted to determine the maximum applied load.
2) The second step is to determine the flexural capacity of the undamaged section using cracked section analysis to ensure that the expected ultimate load determined in step one will not produce flexural failure of the girder.
3) The third step is to restore the shear capacity along the member using PCI (2006) and ACI Committee 440 (2002) design guidelines. The difference in shear capacity between the damaged and undamaged girder is restored using CFRP sheets modeled using ACI Committee 440 (2002) recommendations.
4) The last step is to check the flexural capacity of the damaged section and restore with CFRP sheets if needed.

Step 1: Calculation of Shear Strength of Undamaged Section

Using the PCI Design Handbook (2006), the nominal shear strength along the length of the girder (V_n) was determined by finding the shear strength contribution from the concrete section (V_c) and steel stirrups (V_s). The detailed analysis method was used in the determination of V_c; the web shear capacity (V_{cw}) and the flexure-shear capacity (V_{ci}) were both examined at each section:

$$V_{ci} = 0.6\sqrt{f_c'}b_w d + V_d + \frac{V_i M_{cr}}{M_{\max}} \tag{4.1}$$

$$V_{cw} = \left(3.5\sqrt{f_c'} + 0.3f_{pc}\right)b_w d + V_p \tag{4.2}$$

where V_d is the shear force caused by the unfactored dead load, V_i is the factored shear force at a section due to externally applied loads, M_{cr} is the cracking moment of the section, $M_{\max}$ is the maximum factored moment at a section due to externally applied loads, f_{pc} is the compressive stress in concrete at the centroid due to effective prestressing forces, and V_p is the vertical component of the effective prestress force at the section centroid. M_{cr} can be calculated as:

$$M_{cr} = \left(\frac{I}{y_t}\right)\left(6\sqrt{f_c' + f_{pe} - f_d}\right) \tag{4.3}$$

where I is the moment of inertia, y_t is the distance from the top of the girder to the center of gravity, f_{pe} is the compressive stress in the concrete at the extreme tension fiber due to the effective prestressing force, and f_d is the stress due to service dead load. The shear strength contribution of the steel stirrups (V_s) can be calculated as:

$$V_s = \frac{A_v f_y d}{s} \tag{4.4}$$

where A_v is the area of the shear reinforcement, f_y is the yield stress of the shear reinforcement, and s is the spacing between stirrups. The total nominal shear strength (V_n) is then determined by $V_n = V_c + V_s$ for every section along the length of the girder.

Step 2: Calculation of Flexural Strength of Undamaged Section

The moment capacity of the undamaged section is determined using cracked section analysis approach similar to the one described in the previous section.

Step 3: Restore the Shear Capacity Using CFRP

Step three of the shear model is to restore the shear capacity of the damaged girder using CFRP sheets. This task was performed using the same procedure described in step one, with the application of ACI Committee 440 (2002) guidelines for the usage of CFRP materials. First the shear capacity of the damaged section should be calculated with an appropriate reduction in prestressing force, and a reduced value for the concrete contribution (V_c) corresponding to the level of damage in the section. The shear strength contribution of CFRP materials was included in the nominal shear strength equation (V_n) with an additional term (V_f) used to account for the presence of CFRP materials:

$$V_n = \left(V_c + V_s + \Psi_f V_f\right) \tag{4.5}$$

where (ψ_f) is a reduction factor of 0.85 for members using U-wraps. The shear contribution from the FRP material can be calculated using:

$$V_f = \frac{A_{fv} f_{fe} (\sin\alpha + \cos\alpha) d_{fv}}{s_f} \tag{4.6}$$

where A_{fv} is the area of CFRP shear reinforcement, f_{fe} is the tensile stress in the CFRP shear reinforcement at ultimate, α is the angle of the CFRP, d_{fv} is the depth of CFRP shear reinforcement, and s_f is the spacing of the CFRP shear reinforcement. The area of CFRP shear reinforcement was calculated using the following:

$$A_{fv} = nt_f \mathrm{w}_f \tag{4.7}$$

where n is the number of layers of transverse CFRP sheets, t_f is the thickness of each transverse CFRP sheet, and $\mathrm{w_f}$ is width of the transverse CFRP plies. The tensile stress in the CFRP shear reinforcement at ultimate was calculated as follows:

$$f_{fe} = \varepsilon_{fe} E_f \tag{4.8}$$

where ε_{fe} is the effective strain, or maximum strain that can be achieved in the CFRP system, and E_f is the tensile modulus of elasticity of the CFRP. The type of CFRP system used for shear strengthening determines the effective tensile strain permitted. The effective tensile strain for U-wrap systems is calculated using:

$$\varepsilon_{fe} = \kappa_v \varepsilon_{fu} \le 0.004 \tag{4.9}$$

where κ_v is the bond-reduction coefficient, and ε_{fu} is the design rupture strain of the CFRP. The bond reduction coefficient is a function of the concrete strength, type of wrapping scheme, and laminate stiffness, computed as follows:

$$\kappa_v = \frac{k_1 k_2 L_e}{468\varepsilon_{fu}} \le 0.75 \tag{4.10}$$

where k_1 and k_2 are modification factors that account for the concrete strength and type of wrapping system, and L_e is the active bond length over which the majority of the bond stress is maintained. The active bond length is calculated as follows:

$$L_e = \frac{2500}{\left(nt_f E_f\right)^{0.58}} \tag{4.11}$$

The modification factors are calculated as follows:

$$k_1 = \left(\frac{f_c'}{4000}\right)^{2/3} \tag{4.12}$$

$$k_2 = \frac{d_{fv} - L_e}{d_{fv}} \tag{4.13}$$

Step 4: Restoration of the Flexural Strength of the Section

The last step in the modeling process of a shear-critical specimen is to check the flexural capacity of the damaged section. If it is found to be deficient, the flexural repair procedures described in Section 4.2 are to be used.

4.3 Flexural Study

Three AASHTO Type II girders were damaged (either by impact or simulated impact) at or near midspan, and repaired using CFRP sheets (AASHTO1, AASHTO2, AASHTO3). The girders were damaged and repaired as previously described in Chapter 3. Summarized test results for the flexural tests are provided in Table 4.1.

Table 4.1 Summarized test results for AASHTO girders tested in flexure

Specimen Designation	**AASHTO1**	**AASHTO2**	**AASHTO3**
Repair system	CFRP sheets	CFRP sheets	CFRP sheets
Initial cracking load*, k	---	59.5	63.2
Cracking load**, k	42.0	58.9	65.0
Prestress losses*, %	12.6	18.2	12.9
Effective prestress*, k	27.6	15.5	27.5
Predicted ultimate load of undamaged girder, k	115.7	119.1	126.5
Predicted ultimate load of repaired girder, k	145.1	140.5	143.0
Measured ultimate load, k	135.9	134.1	145.3
Maximum compressive strain in concrete, με	2600	2630	3090
Maximum tensile strain in CFRP, με	4680	4620	5760
Failure mode	Crushing of concrete	Crushing of concrete	Crushing of concrete

* For the girders which were tested prior to simulated impact damage
** The cracking load of the repaired material

AASHTO1

Girder AASHTO1 was damaged due to an overheight vehicle, extracted from a bridge, repaired using CFRP sheets, and tested under fatigue loading conditions. The damage included one ruptured prestressing strand, corresponding to a loss of prestressing force of 6.25 percent. A test description can be found in Chapter 3.

Load versus Displacement Hysteric Response

The applied load versus midspan displacement relationship for the fatigue loading ranging between the load values 18.7 k to 45.2 k (83.2 kN to 201.1 kN) for the repaired AASHTO1 girder is shown in Figure 4.1. The girder survived 2 million cycles with very

little degradation or crack propagation in the repaired region after the initial cycles. Fatigue creep of concrete (El-Tawil et al. 2001) caused small amounts of displacement degradation totaling 0.11 in (2.8 mm) after 2 million cycles of loading. No stiffness degradation in the girder was observed after 2 million cycles of fatigue loading.

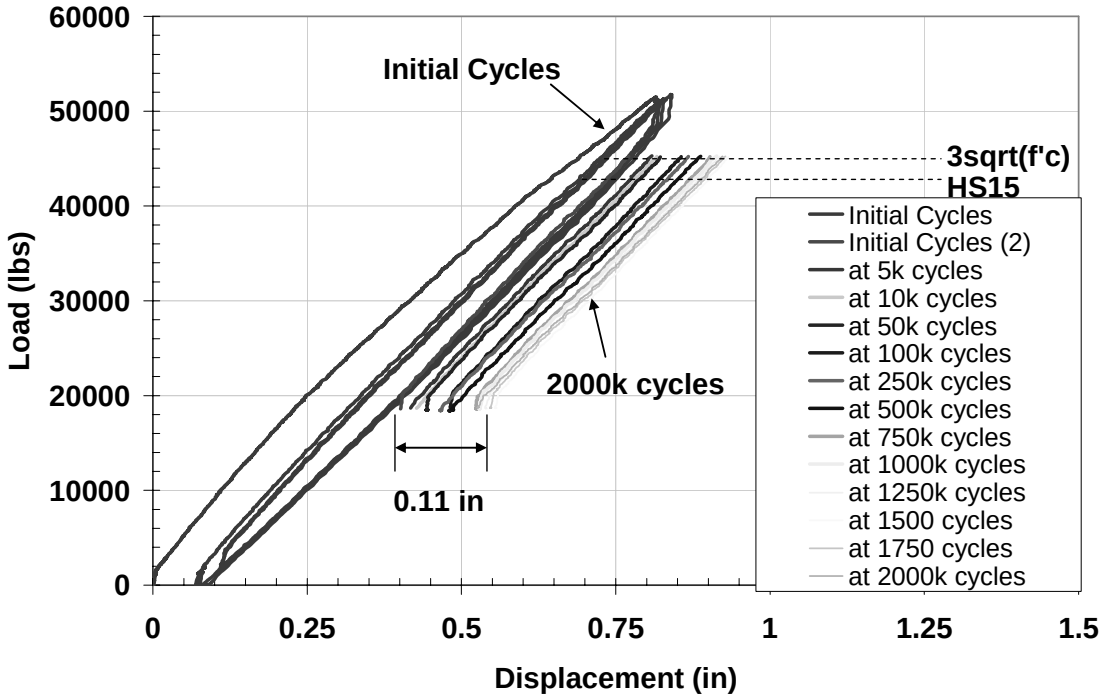

Figure 4.1 Load versus displacement for girder AASHTO1

Stress Ratio in Prestressing Strands

Due to the impact damage imparted on the AASHTO girder and the concrete restoration process, a good estimate of the effective prestress force in the prestressing strands was difficult to obtain. Using a prestress loss of 12.6 percent, the measured stress ratio in the lower prestressing strands at midspan during the initial cycles was found to be 1.7 percent. The stress ratio in the lower prestressing strands was also determined using a Response 2000© analysis and was determined to be 2.6 percent, slightly higher than the measured value. It should be noted that all of the prestressing strands were straight in girder AASHTO1. Previous work demonstrates that fatigue rupture of prestressing strands is rare at

such low stress ratio values in straight prestressing strands (Naaman 1991, Collins & Mitchell 1991) therefore no degradation was observed after completion of 2 million cycles, as shown in Figure 4.2.

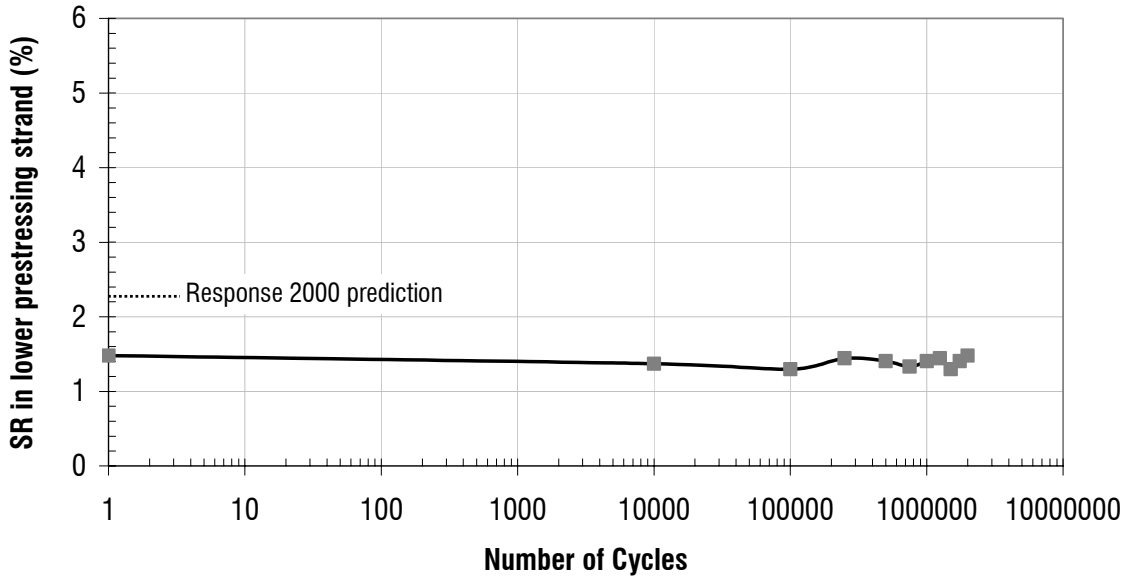

Figure 4.2 Stress ratios in prestressing strands versus number of cycles for AASHTO1

Residual Strength

A full description of the final static test on girder AASHTO1 is provided in Section 3.8. Flexure-shear cracks, which initiated outside the termination point of the longitudinal CFRP in the undamaged region, propagated in an inclined fashion towards the compression zone and eventually caused failure of the girder near midspan. Test results indicated that the presence of the main longitudinal CFRP significantly increased the flexural capacity of the damaged zone of the girder causing the failure outside this region. The presence of the tension-strut CFRP reinforcement and transverse U-wraps controlled crack propagation within the damaged zone as well as enhancing the shear capacity of the strengthened section. The overall behavior of the repaired girder far exceeded the predicted strength of the undamaged girder in both strength and ultimate displacement, as shown in Figure 4.3.

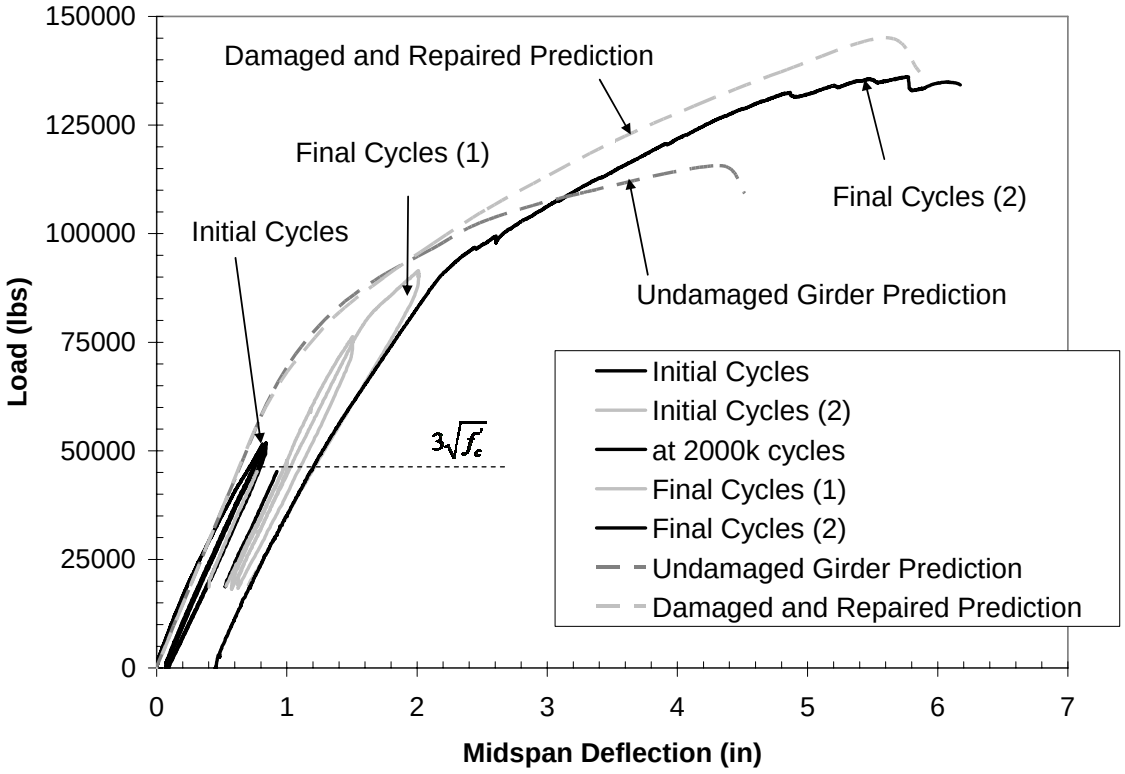

Figure 4.3 Final static test to failure of girder AASHTO1

The tensile strains in the repaired AASHTO girder during the final static test measured from various PI gauges is shown in Figure 4.4. Several items that should be noted in the figure include: 1) residual tensile strains in the CFRP of 0.07 percent can be seen in the repaired region after the fatigue cycling due to crack opening and aggregate interlock in the restored concrete, 2) flexural cracks first formed at the undamaged section at an applied load of 94.4 k (420 kN), 3) the stiffness of the damaged region and the undamaged region were almost the same after flexural cracking occurred in the undamaged region.

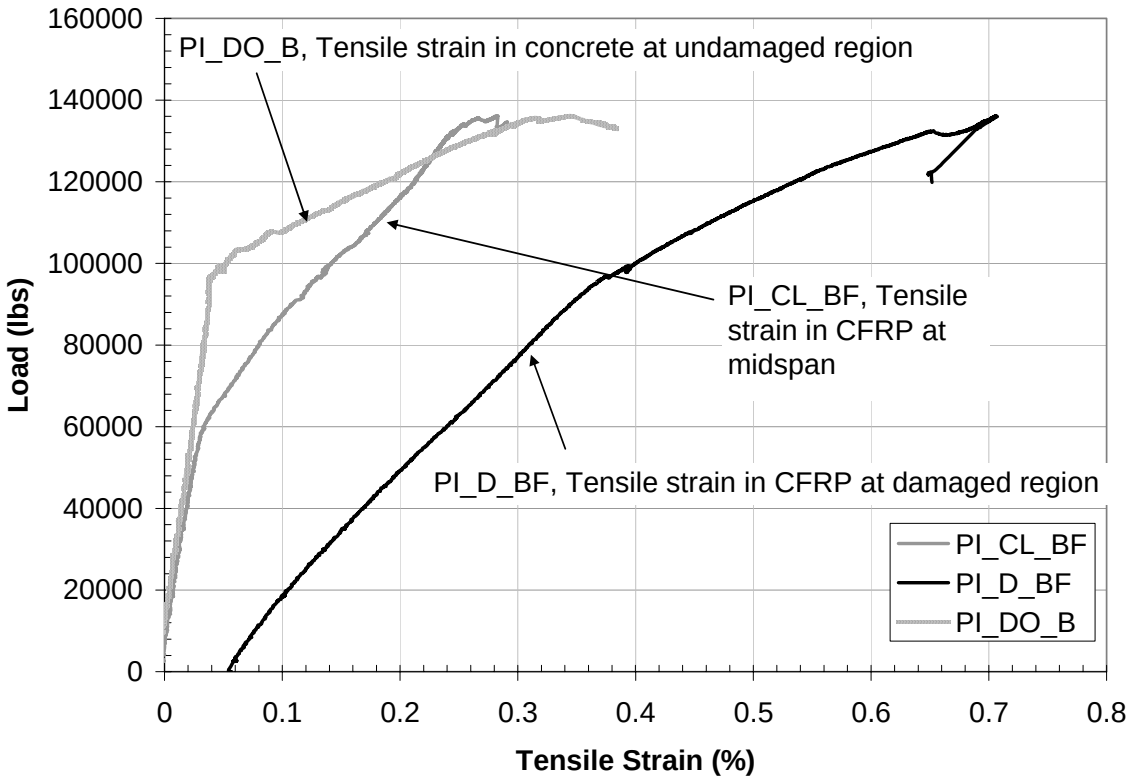

Figure 4.4 Load versus tensile strain during final static test of girder AASHTO1

Predicted versus Experimental

A prediction using Response 2000© was performed on the undamaged girder as well as the repaired girder, and is shown with the experimental results in Figure 4.3. Due to the difficulties in assessing the cracking load of the girder, the value for effective prestress used was determined from calculations (AASHTO 2004). In the analysis, the following scenarios were included: 1) all the longitudinal CFRP was modeled (including tension strut CFRP reinforcing), 2) a prestressing strand on the bottom layer was removed and considered to be ineffective throughout the length of the girder, and 3) one average value for the width of the composite deck (14.9 in (379 mm)) was used in the analysis in spite of the fact that the width varied slightly throughout the length of the girder. Response 2000© predicted concrete crushing failure for the damaged and repaired girder at an applied load of 145.1 k (645 kN)

which corresponds well to the measured load at failure of 136.1 k (605 kN). The measured ultimate load was 17.6 percent higher than the ultimate load predicted for the undamaged girder. The measured ultimate displacement of the repaired girder was 37 percent greater than the undamaged prediction and 5.2 percent greater than the repaired prediction.

AASHTO2

Girder AASHTO2 was intentionally damaged at midspan with four out of twenty-eight prestressing strands ruptured, corresponding to a 14.3 percent loss of prestressing force. The girder was then repaired with CFRP sheets and tested in several stages to failure. A description of the test and other set-up details can be found in Chapter 3.

Behavior of Girder during Initial Loadings

Girder AASHTO2 was subjected to four cycles of initial loading. Two of those cycles were performed on the undamaged girder, with only minor repair of the composite deck performed prior to testing. One of these initial cycles loaded the girder up to 90 percent of the predicted ultimate load value. The resulting flexural cracks during this loading stage were well spaced, a result of the numerous and well distributed prestressing strands. The third and fourth cycles of loading that the girder was subjected to occurred after the simulated impact damage was applied to the girder, as described in detail in Chapter 3. The third loading cycle followed the concrete removal around midspan, and the fourth cycle was after four prestressing strands, representing a 14.3 loss of prestress force, were ruptured in the damaged zone. A comparison of the stiffness of girder AASHTO2 in each of these cycles is provided in Table 4.2. The largest drop in stiffness was a result of the severe initial loading combined with the concrete damage, for a reduction of approximately 17 percent. A

further reduction was observed after the cutting of the prestressing strands. The load versus deflection curve for girder AASHTO2 due to the initial loading scheme is shown in Figure 4.5.

Table 4.2 Stiffness comparison of AASHTO girders tested in flexure (lb/in)

Specimen Designation		**AASHTO1**	**AASHTO2**	**AASHTO3**
Prior to CFRP repair	Initial cycle 1*	---	78.8	77.7
	Initial cycle 2*	---	81.1	77.7
	Post concrete damage*	---	68.0	65.7
	Post cutting of prestressing strands*	---	62.8	60.5
After CFRP repair	Final cycle 1	65.7	69.1	68.0
	Final cycle 2	60.0	67.4	70.2

* For the girders which were tested prior to simulated impact damage

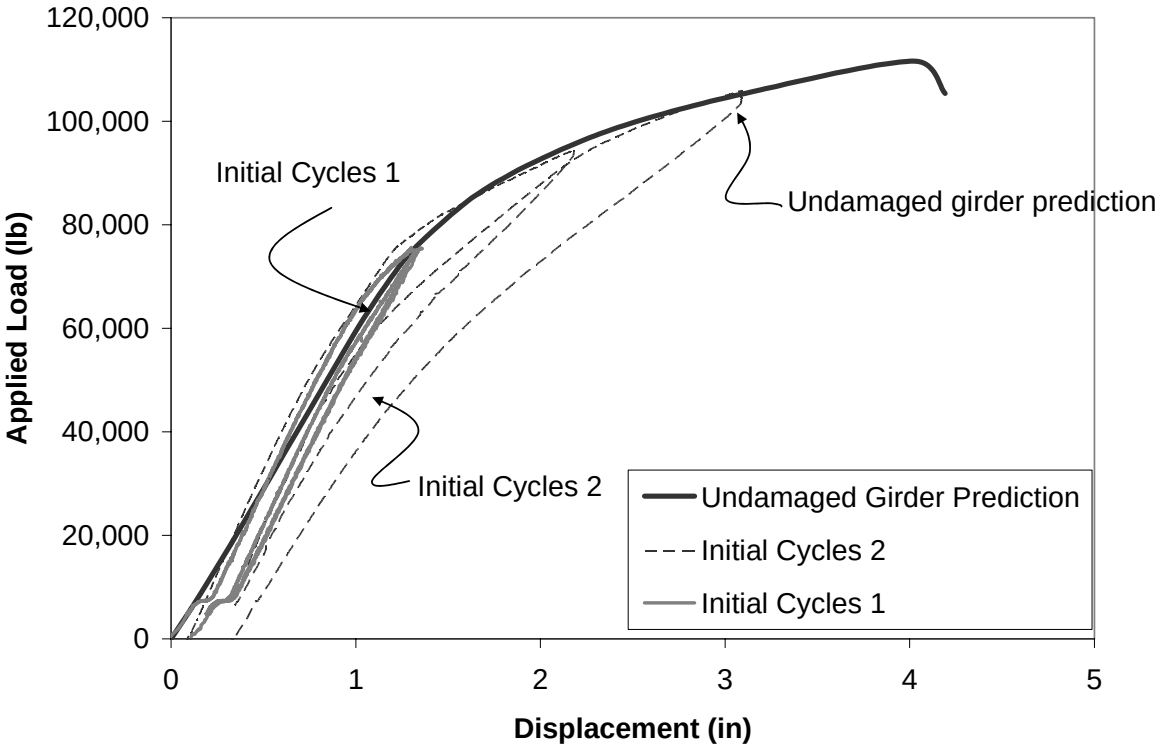

Figure 4.5 Initial load versus deflection of girder AASHTO2

In addition to stiffness loss, there was also increasing residual deflections following each of the loading cycles. The largest residual deflection came as a result of the initial

cycles on the undamaged girder, where a residual deflection of 0.25 in (6.5 mm) was observed. The residual deflection after the concrete damage, prestressing strand cutting, and subsequent cycles was 0.36 in (9.2 mm). The stiffness change and the residual deflections in the girder through the various cycles can be seen in Figure 4.6, which plots a detail of the load versus deflection behavior of all loading cycles.

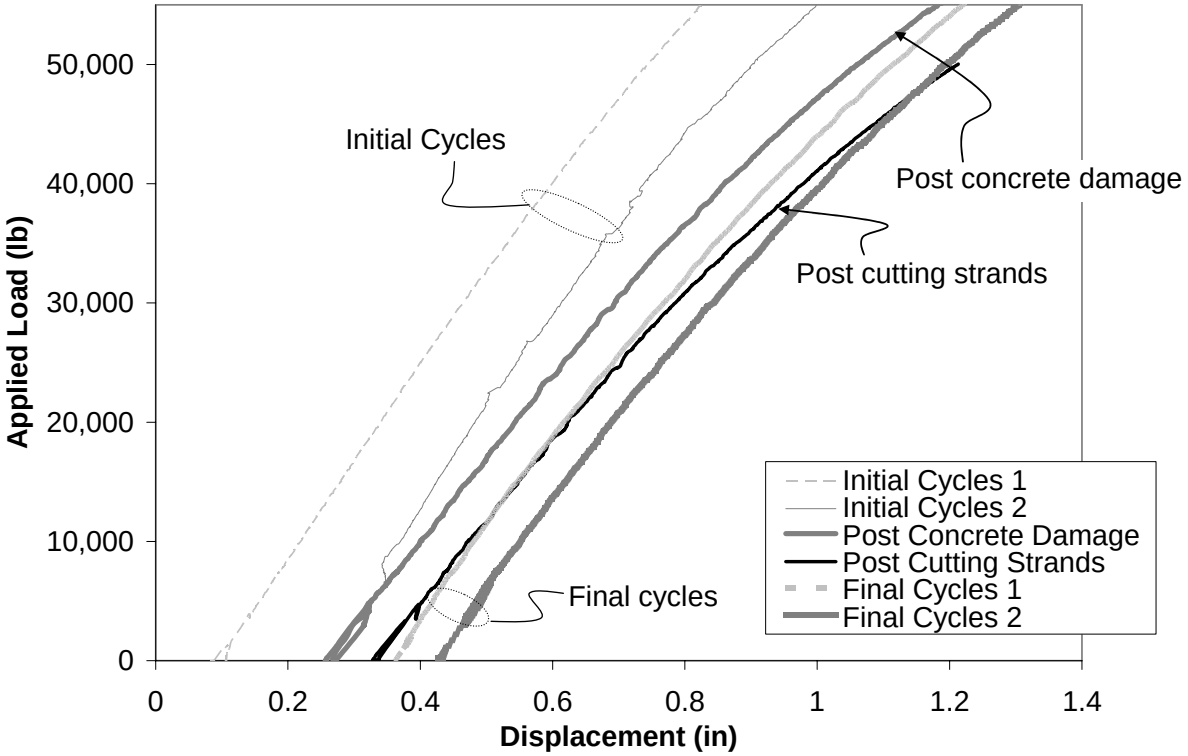

Figure 4.6 Close-up of load versus deflection of girder AASHTO2

Behavior at Ultimate

After the section was restored with repair mortar and CFRP sheets were installed, girder AASHTO2 was subjected to two loading cycles up to failure. A full description of the final static test is provided in Chapter 3. Failure initiated in the concrete material around the loading plate, where localized crushing led to out-of-plane behavior rapidly causing failure. The maximum measured value of concrete compressive strain was 2630 με. The relatively low value at crushing of concrete was likely a result of the poor condition of the concrete at

midspan due to extant transverse cuts. The damaged and repaired girder far exceeded the strength and ultimate displacement of the original undamaged girder, as shown in Figure 4.7. The longitudinal CFRP system was able to adequately carry the tensile forces, and showed very little debonding or damage even after the failure event. The transverse CFRP sheets were also virtually unaffected during the loading, with only the U-wraps positioned directly below the loading area becoming damaged at failure.

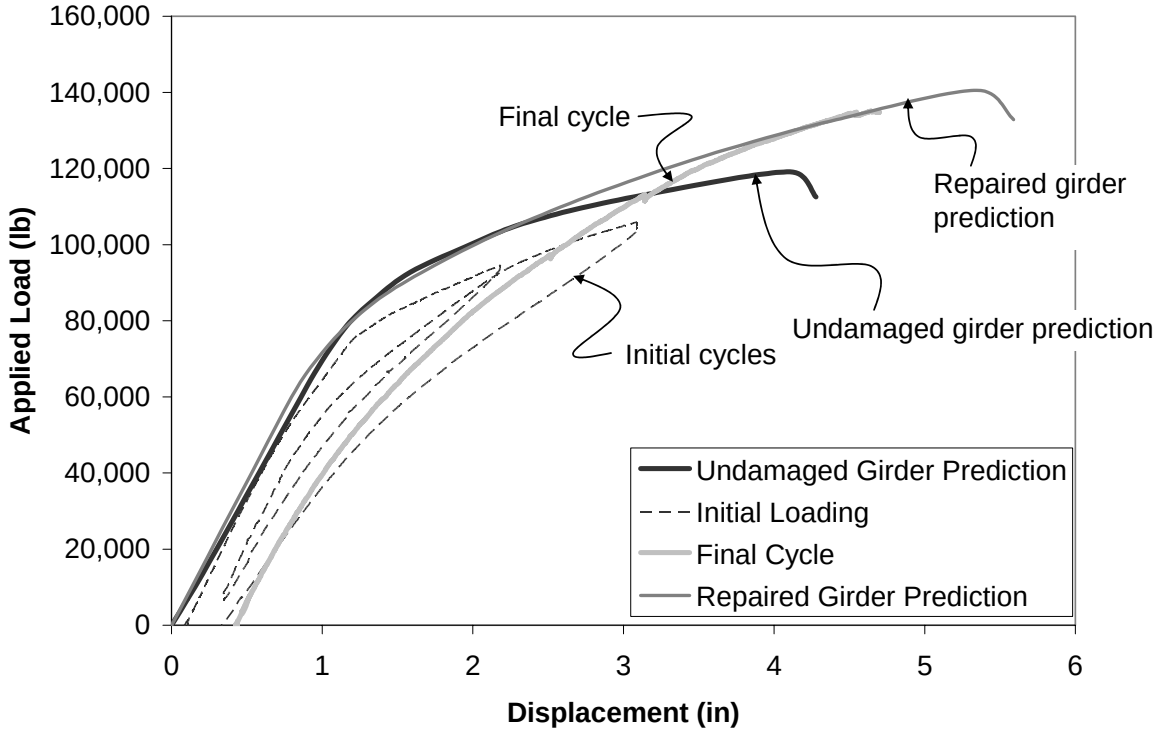

Figure 4.7 Load versus deflection of girder AASHTO2

The maximum tensile strain in the CFRP system at failure was 4620 με, very close to the maximum tensile strain observed during the test of girder AASHTO1. Due to the location of several wide transverse U-wraps used to encapsulate the damaged region, tensile strain gauges could only be located at a distance approximately 3.94 ft (1.2 m) from midspan. Therefore, the maximum strain in the longitudinal CFRP was likely larger than the maximum measured value. Multiple strain gauges were affixed to the longitudinal CFRP throughout

the repaired area, and the measured tensile strain profile is shown in Figure 4.8. Due to the thickness of the longitudinal CFRP, the presence of the transverse U-wraps, and the large distance between the gauges, the effect of stress concentrations at the toes of the flexural cracks is not manifested in the plot. At failure the large increase in tensile strain which can be seen around 78.7 in (2000 mm) from the end of the CFRP repair is likely due to the yielding of the prestressing strands at that location along the length of the girder.

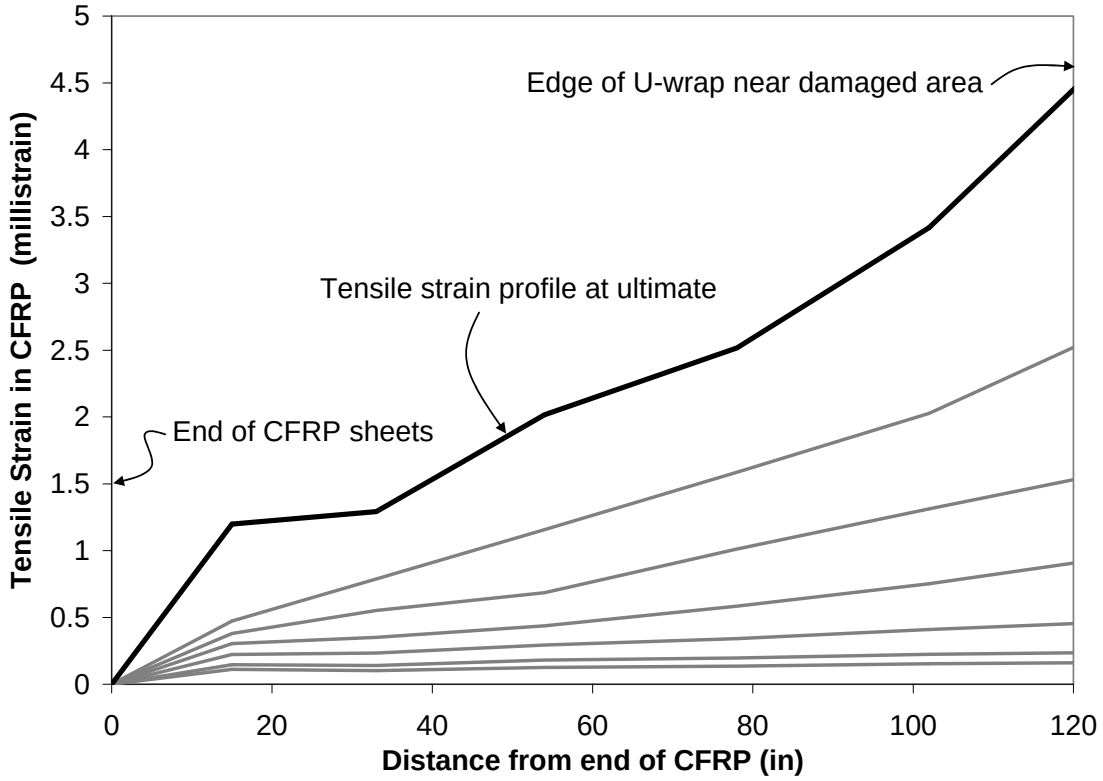

Figure 4.8 CFRP tensile strain profile during final static test of girder AASHTO2

Predicted versus Experimental

In Figure 4.7, the load versus deflection predictions are shown for two scenarios: 1) the undamaged girder, and 2) for a repaired girder modeled with a similar amount of CFRP as the actual repaired girder. Both of the predictions were made using cracked section analysis described earlier in this chapter and constituent properties taken from material testing. The prediction of the undamaged girder matches closely the measured values from

the initial static test, in both load and deflection, until the static test was terminated at around 90 percent of ultimate. Based on experience gained from the testing of other girders and their predictions using cracked section analysis, it is possible that the ultimate deflection of the undamaged AASHTO2 girder could have been greater than that of the prediction (Rosenboom 2006). If four prestressing strands are taken out of the cracked section analysis and the total amount of CFRP used in the repair of girder AASHTO2 is included, counting all CFRP tension struts on the girder flange and web, a prediction can be made which closely matches the observed behavior. The ultimate load of the repaired girder is 13.4 percent greater than the undamaged girder prediction, and is similar to the repaired girder prediction.

AASHTO3

Girder AASHTO3 was intentionally damaged at midspan with three prestressing strands ruptured, corresponding to an 18.8 percent loss of prestressing force. The girder was repaired with CFRP sheets and tested in several stages to failure. A description of the test and other set-up details can be found in Chapter 3.

Behavior of Girder during Initial Loadings

Similar to girder AASHTO2, AASHTO3 was subject to four cycles of initial loading: two on the undamaged girder up to 80 percent of the predicted ultimate load value, one cycle after concrete damage, and one cycle after three prestressing strands were cut. As mentioned in Chapter 3, the original girder was delivered to the laboratory in poor condition, with numerous impact events and subsequent repairs evident on one side and significant permanent out of plane deflection. A comparison of the stiffness of girder AASHTO3 in each of these four cycles is provided in Table 4.2. Due to the simulated impact damage, the

stiffness of the girder was reduced by 22.1 percent. The load versus deflection curve for girder AASHTO3 due to the initial loading scheme is shown in Figure 4.9.

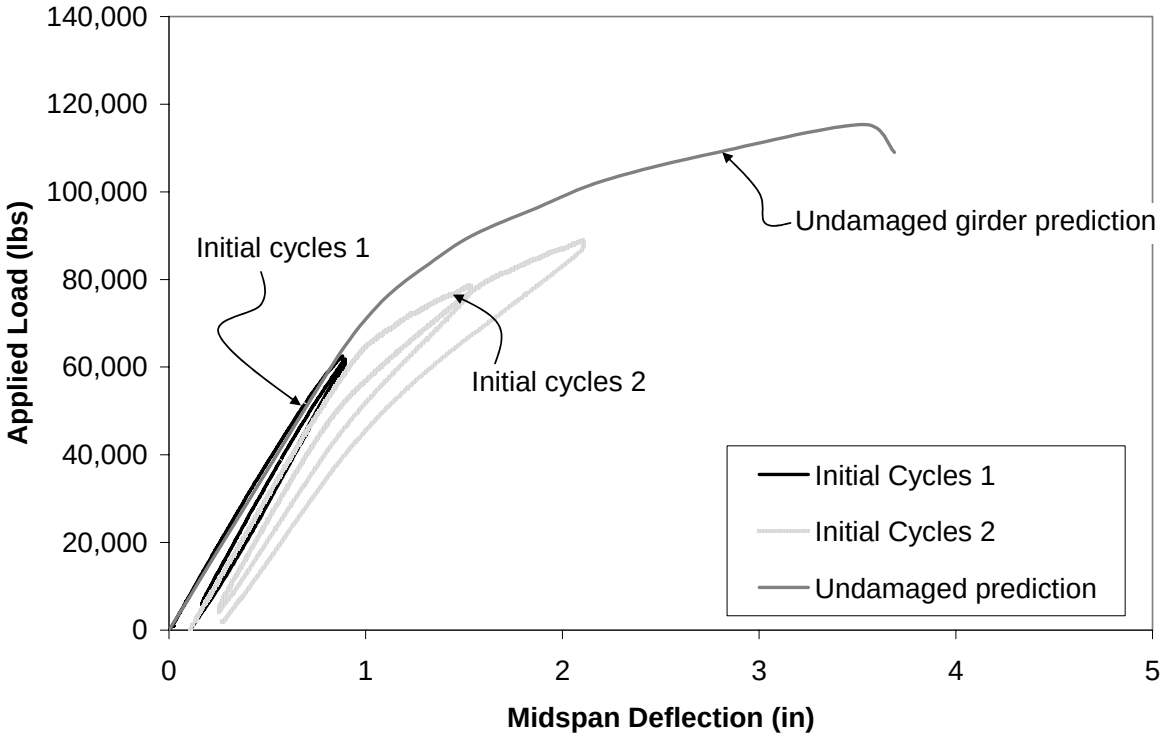

Figure 4.9 Initial load versus deflection of girder AASHTO3

Similar to girder AASHTO2, AASHTO3 also experienced residual deflections as a result of the simulated impact damage and initial cycling. The largest residual deflection came as a result of the initial cycles on the undamaged girder, where a residual deflection of 0.24 in (6.0 mm) was measured. The residual deflection after the concrete damage, prestressing strand cutting, and subsequent cycles was 0.36 in (9.1 mm). The stiffness change and the residual deflections in the girder through the various cycles can be seen in Figure 4.10, which plots a detail of the load versus deflection behavior of all loading cycles.

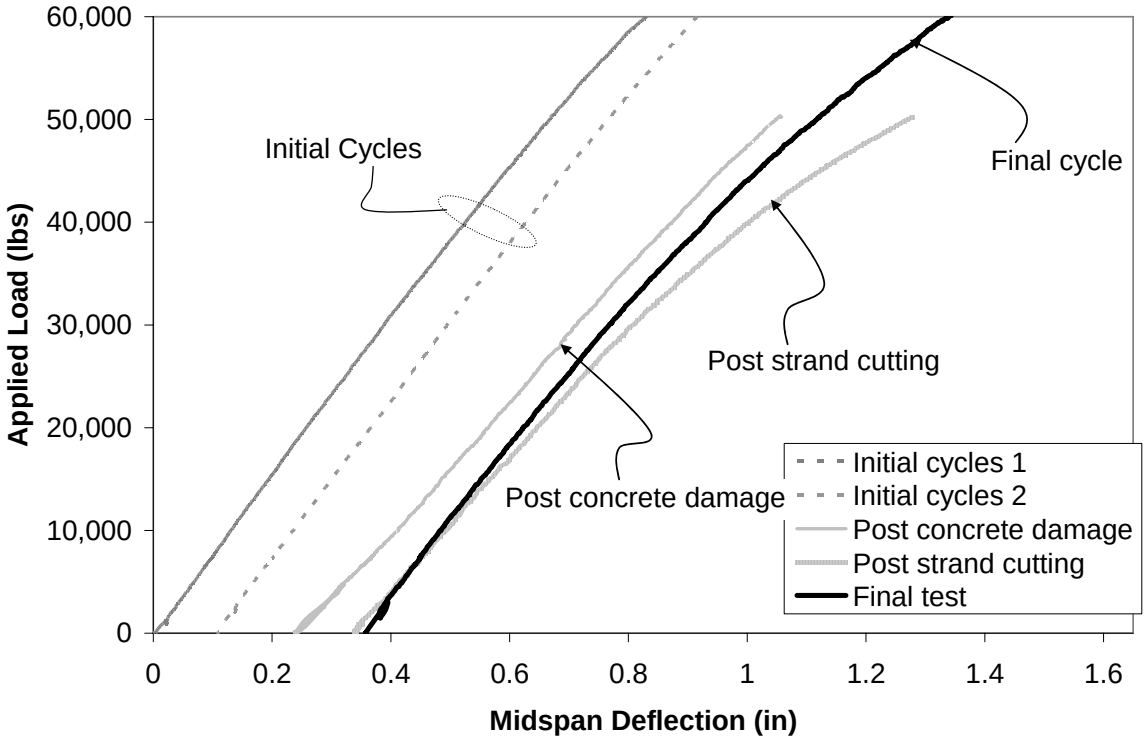

Figure 4.10 Close-up load versus deflection of girder AASHTO3

Behavior at Ultimate

After the section was restored with repair mortar and CFRP sheets were installed, girder AASHTO3 was subjected to two loading cycles up to failure. A full description of the final static test is provided in Chapter 3. Failure was due to concrete crushing in the compression region around the loading plate. The maximum measured value of concrete compressive strain at failure was 3090 με, significantly larger than the measured value for the previous AASHTO flexural tests. There was no evidence of debonding in the longitudinal CFRP at failure. The transverse U-wraps buckled at failure but contained most of the concrete damage. The load versus deflection behavior of girder AASHTO3 is shown in Figure 4.11.

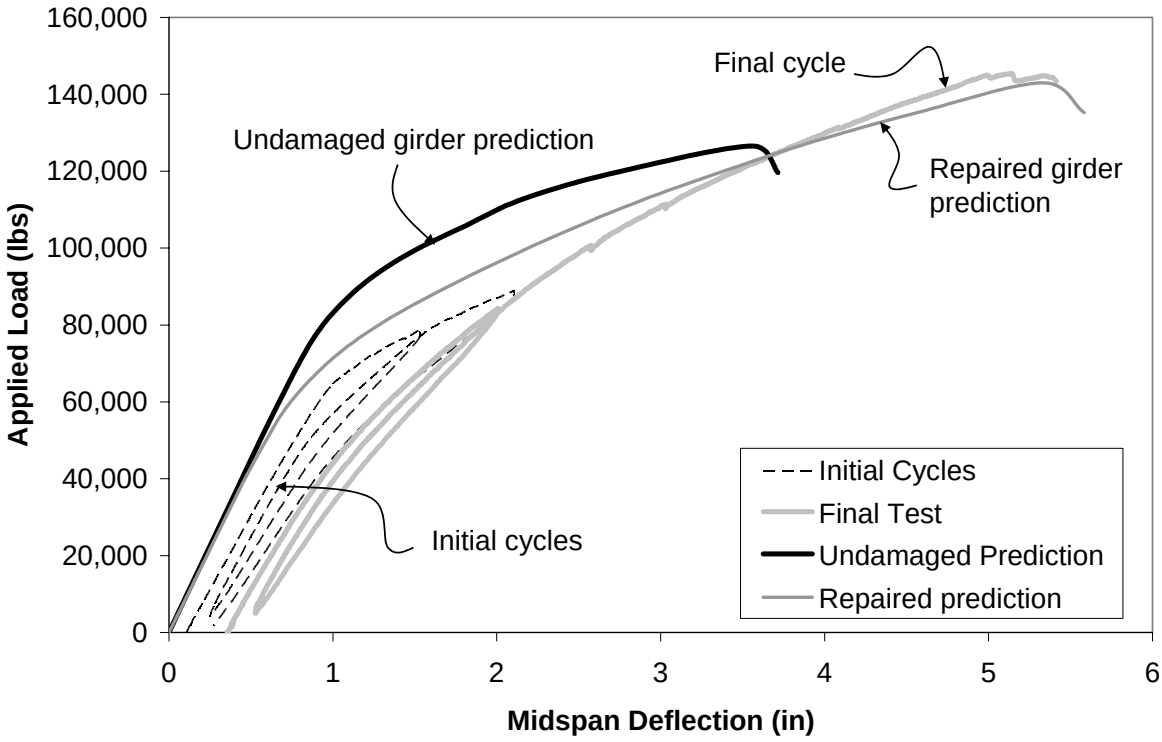

Figure 4.11 Load versus deflection of girder AASHTO3

The maximum measured tensile strain in the longitudinal CFRP at failure was 5760 με, significantly larger than the tensile strain measured in previous AASHTO flexural tests. The higher compressive strain capacity in the concrete led to a greater demand placed on the CFRP system which in turn led to a large increase in ultimate load compared to the undamaged girder. In this girder, tensile strain gauges were installed in the CFRP throughout the repaired area, and the measured tensile strain profile is shown in Figure 4.12. Also shown in the figure is the location of the 4.0 ft (1.22 m) wide transverse U-wrap which encapsulated the area of simulated impact damage. At a distance of 216.5 in (5500 mm) from the end of the CFRP the profile shows a strain peak, most likely the result of the strain gauge location near the toe of a flexural crack. The distance around midspan where the prestressing strands are yielding is also obvious in the figure, from approximately 98.4 to 236.2 in (2500 to 6000 mm) from end of the longitudinal CFRP.

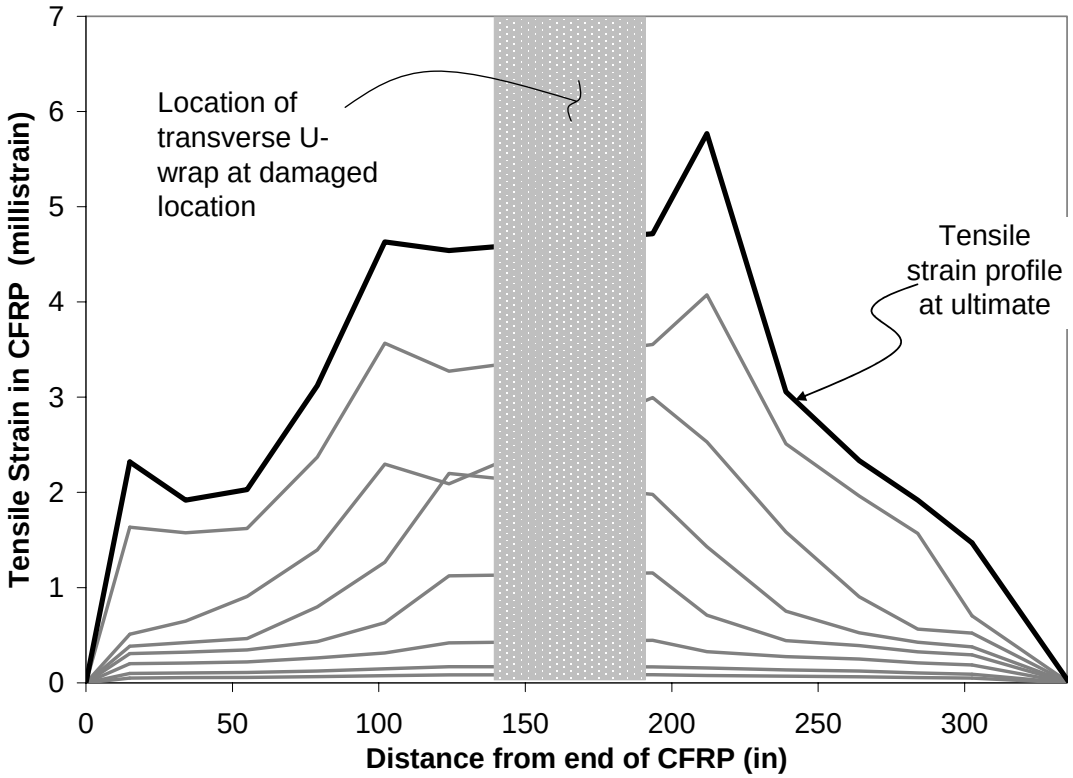

Figure 4.12 CFRP tensile strain profile during final static test of girder AASHTO3

Predicted versus Experimental

Similar to girder AASHTO2, in Figure 4.11 the load versus deflection predictions from cracked section analysis are shown for two scenarios: 1) the undamaged girder, and 2) the repaired girder with all CFRP. The undamaged girder prediction with the measured effective prestress force does not adequately reflect the measured load versus deflection behavior. This is likely the result of the poor condition of this girder upon delivery to the laboratory, with numerous impact events evident on one side. This internal damage and cracked nature of the beam could have resulted in the lower cracking load and stiffness compared to the prediction. The load versus deflection prediction for the repaired girder corresponds extremely well to the measured response of the girder. The predicted ultimate load of the repaired girder is 1.7 percent lower than the measured value. It should be noted

that both the predicted scenarios show crushing of concrete as the failure mode, the same as the observed mode.

4.4 Shear Study

Two short span AASHTO Type II girders were tested under shear critical loading schemes. One girder was tested as a control specimen (AASHTO2C); the other girder was damaged and repaired using CFRP sheets and tested to failure (AASHTO2R). Summarized test results for the shear tests are provided in Table 4.3.

Table 4.3 Summarized test results for AASHTO girders tested in shear

Specimen Designation	**AASHTO2C**	**AASHTO2R**
Repair system	None	CFRP sheets
Cracking load, k	226.4	256.3
Average crack width at failure, in	0.148	0.019
Failure load, k	413.7	446.3
Predicted failure load, k	373	486
Failure mode	Web shear failure	Shear in right transfer zone followed by flexure-shear
Max tensile strain in longitudinal CFRP, με	---	810
Max tensile strain in diagonal CFRP strut, με	---	1920
Max compressive strain, με	680	1400

AASHTO2C and AASHTO2R

The cracking behavior, tensile strain in the longitudinal and diagonal CFRP, ultimate behavior, and predicted versus experiment results and discussion will be presented for AASHTO2C and AASHTO2R in this section.

Cracking Behavior

Girder AASHTO2C and AASHTO2R were loaded in one cycle up to failure. During the loading process, several inclined cracks formed at 45 degrees from the support at various load levels. The number of cracks in the control specimen was visually obtained, however the cracks were not visible in the repaired girder as a result of the diagonal CFRP struts. In order to compare the average crack widths of the two specimens, it was assumed that the same number of cracks formed in the repair specimen that was visible in the control specimen. Figure 4.13 shows the average crack widths for both specimens at each of the three instrumented locations. It should be noted that the maximum crack widths formed closest to the loading point. The maximum crack width in AASHTO2C was 0.15 in (3.8 mm) and 0.02 in (0.5 mm) for AASHTO2R.

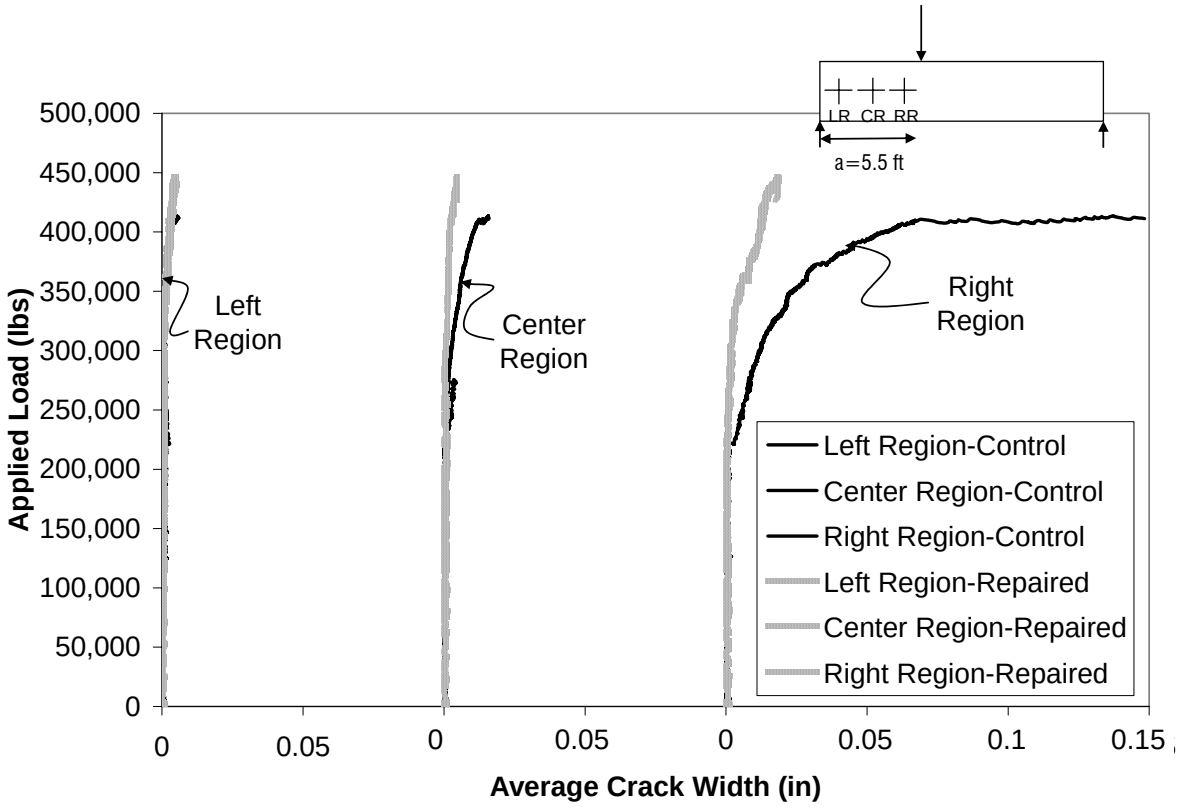

Figure 4.13 Average crack widths of AASHTO2C and AASHTO2R girders

Tensile Strain in CFRP

The tensile strain in the CFRP was measured at the right end of the longitudinal CFRP sheets. Figure 4.14 shows the load versus tensile strain plot for AASHTO2R. Several points that should be noticed were the presence of interfacial cracking, followed by plate-end debonding of the CFRP. The strain value near the termination point of the longitudinal CFRP was low (810 με) when plate-end debonding occurred. The presence of a U-wrap at this location would have minimized the plate-end debonding effects.

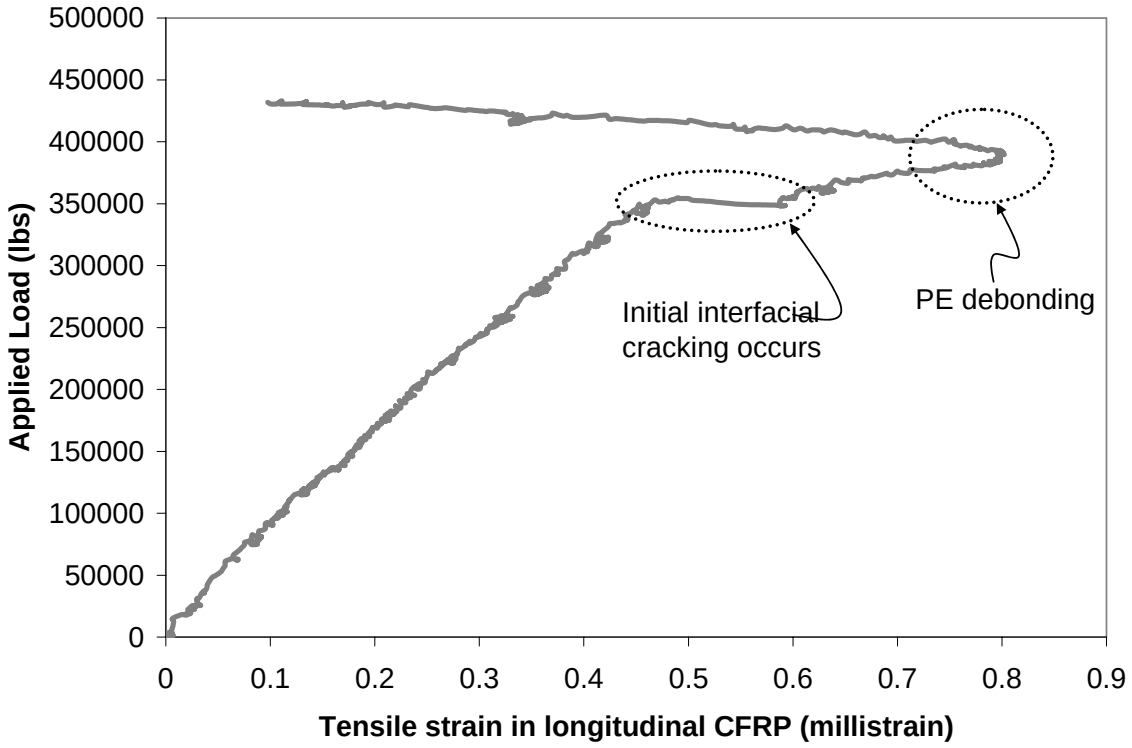

Figure 4.14 Tensile strain in longitudinal CFRP of girder AASHTO2R

The tensile strain at the center of each diagonal CFRP strut was also measured during the loading of AASHTO2R, as shown in Figure 4.15. This figure indicates that the largest inclined crack openings were located approximately half way between the left support and load plate, as expected. Also, the strain induced in the diagonal CFRP struts was much lower

than the ACI Committee 440 (2002) rupture design value of 0.004 in/in, therefore not causing debonding or rupturing of the sheets.

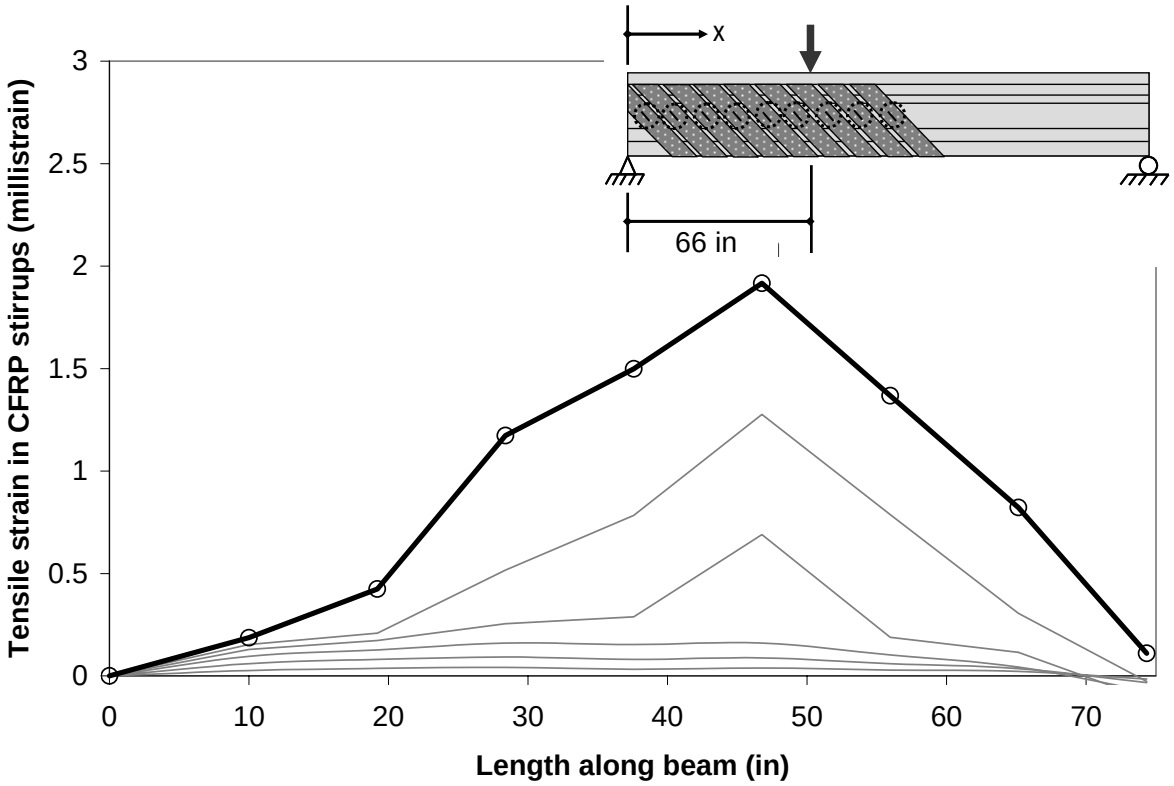

Figure 4.15 Distribution of tensile strain in diagonal CFRP struts

Behavior at Ultimate

The ultimate load versus deflection behavior of girders AASHTO2C and AASHTO2R are shown in Figure 4.16. Full descriptions of the static tests to failure are provided in Chapter 3. Failure of AASHTO2C initiated in the inclined cracks that formed on the shear-critical side of the test specimen. The failure of AASHTO2R initiated beyond the longitudinal CFRP sheets after shear failure in the right transfer region had occurred. As flexural shear cracks began propagating through the web, caused by the debonding of prestressing strands resulting from the failure in the transfer region, plate-end debonding occurred. The diagonal CFRP struts remained intact after the failure of AASHTO2R.

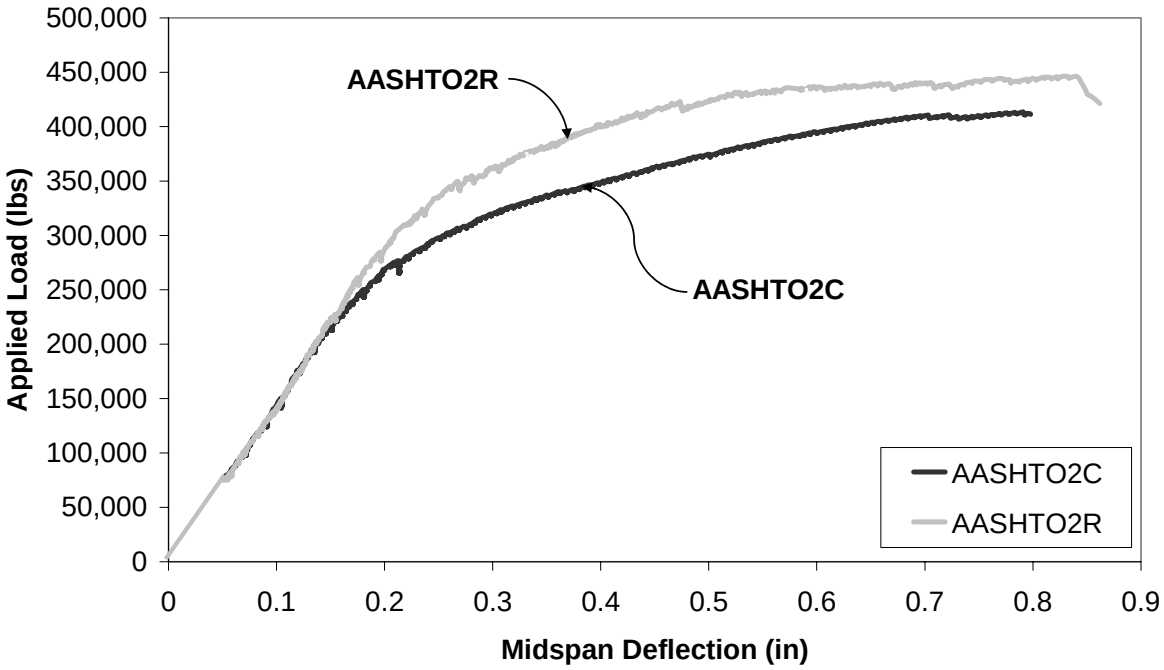

Figure 4.16 Load versus deflection of girders AASHTO2C and AASHTO2R

The initial stiffness of both AASHTO2C and AASHTO2R was roughly identical. The cracking load of the repaired specimen was greater than the control specimen and is shown in Figure 4.16. The ultimate load capacity of AASHTO2R was 7 percent higher than that of AASHTO2C, and the ultimate displacement was slightly enhanced. The maximum compressive strain reached in each of the tests was 680 με and 1400 με for girders AASHTO2C and AASHTO2R, respectively.

Predicted versus Experimental

The initial predicted shear capacity of AASHTO2C was 373 k (1659 kN), made using the PCI guidelines previously described in Section 4.2. The predicted shear capacity was less than the experimental ultimate load of 413.7 k (1840 kN). The test results clearly demonstrated that shear failure was the mode of failure in girder AASHTO2C, as previously shown in Figure 3.43. Therefore, an alternative method of examining the shear capacity of

the girder was devised in hopes of more accurately predicting the shear failure load of girder AASHTO2C.

After thoroughly examining the PCI (2006) equations for calculating shear capacity, and in comparison with AASHTO2C test results, it was discovered that replacing PCI's maximum effective depth of the prestressing strands (d) of 0.8 times the height (h) of the member with the true effective depth a far more accurate comparison to the test results could be obtained, as shown in Figure 4.17. It should be noted that the 0.8 times the height of the girder is intended for use as a conservative design value, however because this was an analysis of the girder and not the design, it was ignored. This method of examining the shear capacity will be referenced as the modified PCI method for here on out. The modified PCI method predicted an ultimate shear capacity of 414 k (1842 kN), similar to the experimental result of 413.7 k (1841 kN). It should be noted that the FRP U-wraps shown on the bottom of Figure 4.17 were left over from the flexural repair of girder AASHTO2.

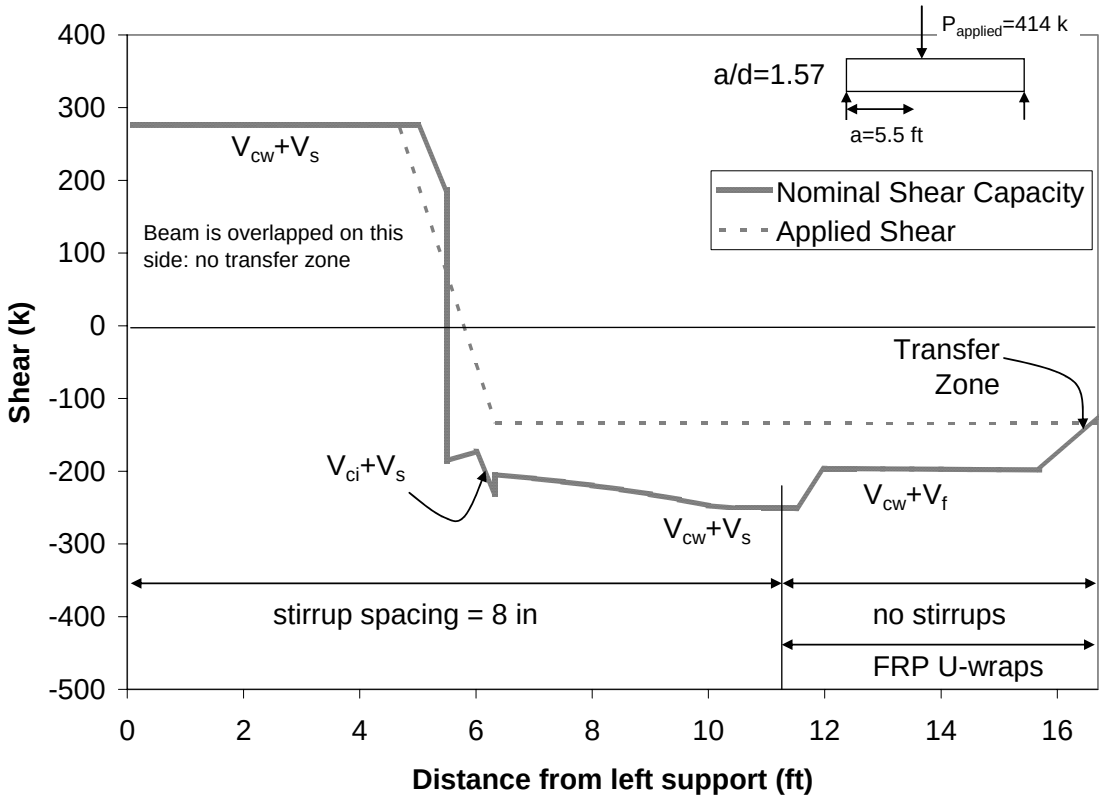

Figure 4.17 Modified AASHTO2C girder predicted and applied shear

The predicted shear capacity of the CFRP repaired AASHTO2R girder, shown in Figure 4.18, was determined using the modified PCI design guidelines previously presented in conjunction with ACI Committee 440 (2002) shear FRP design guidelines. The predicted shear failure load was 519 k (2309 kN), but the test specimen failed at 446 k (1985 kN), as shown in Figure 4.18. Shear failure to the left of the applied load, the shear-critical span, was not the failure mode of the test specimen, which led to further inspection of possible failure modes. In Figure 4.18, it is evident that the applied shear at the right end exceeded the allowable shear in the transfer region. Shear failure in the transfer region allowed the prestressing strands to debond, in turn lowering the moment capacity of the section on the right end. The moment capacity of the girder prior to debonding of the strands is shown in

Figure 4.19, but became much less after the contribution of the prestressing strands is progressively lowered due to debonding.

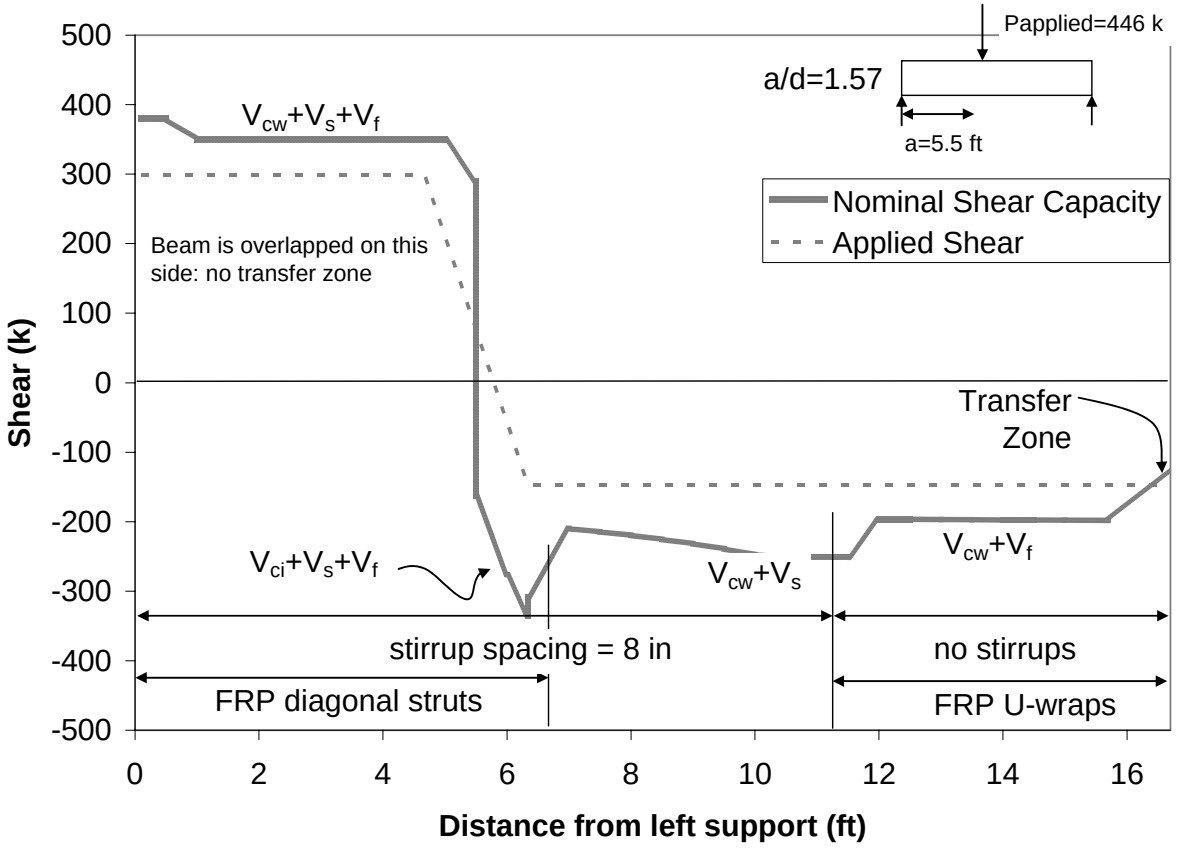

Figure 4.18 Predicted shear capacity versus the applied shear load of girder AASHTO2R

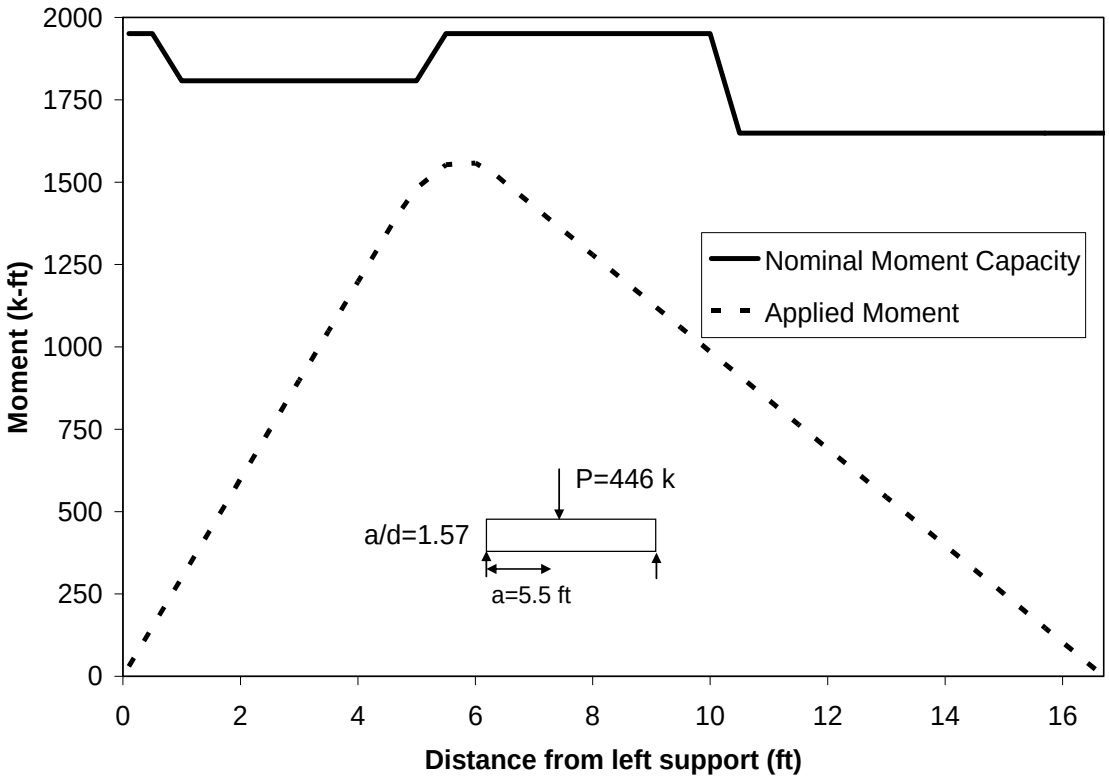

Figure 4.19 Repaired moment capacity of girder AASHTO2R

5. Summary and Conclusions

Due to the increasing frequency of overheight vehicular impact and rising costs of complete girder replacement, the structural behavior of CFRP repaired prestressed concrete beams were studied to determine the effectiveness of the repair system. Damage in flexure and shear critical zones, including loss of concrete and rupturing of prestressing strands was examined. Every specimen's original undamaged flexure/shear capacity was successfully restored using externally bonded CFRP sheets. An analytical model for restoring the ultimate load capacity of all four repaired girders was created by combining existing design guidelines.

Flexural CFRP Repair

Three AASHTO Type II girders were damaged at or near midspan, repaired with longitudinal and transverse CFRP sheets, and tested under flexurally critical loading. The findings from this research include:

1) Based on the testing regime, it was possible to repair an impact-damaged girder with up to an 18 percent loss of prestressing force using CFRP sheets.
2) Test results showed that the ultimate deflection of repaired girders can meet or exceed that of the same undamaged girder.
3) Based on test results, it was found that a loss of initial stiffness equal to 20 percent occurred between the undamaged girders and cutting of the prestressing strands. Following the restoration of the concrete section and application of the CFRP, a difference of approximately 10 percent initial stiffness was exhibited between the undamaged girder and repaired girder.

4) Results from the fatigue test of AASHTO1 demonstrated that a CFRP repaired AASHTO Type II prestressed girder can withstand 2 million cycles of cyclic loading with very little loss of stiffness or residual deflection.

Shear CFRP Repair

Two AASHTO Type II girders were tested as short-span shear critical sections; one as a control specimen and the other damaged near the support and repaired using longitudinal and diagonal U-wraps of CFRP sheets. The findings from this research include:

1) Shear failure occurred in an undamaged prestressed concrete girder when loaded at an a/d ratio equal to 1.57 during this study.
2) Test results showed that a damaged AASHTO Type II girder with up to 14 percent loss of prestressing force and 1 in (25 mm) loss of web concrete can be repaired using CFRP sheets.
3) When repairing a girder in shear, all possible failure modes must be examined.
4) The use of CFRP sheets reduced the shear crack widths of the repaired girder in comparison to the control specimen.
5) Comparison of test results and predictions showed that PCI and ACI Committee 440 guidelines accurately predict the behavior of a prestressed girder repaired in shear.

Flexure and Shear Modeling Using CFRP

Several analytical models were examined and used to predict both the flexural response and shear response of a repaired prestressed concrete girder. Several conclusions can be drawn from these two models:

1) Assuming a perfect bond, test results showed that the flexural behavior of a n undamaged as well as CFRP repaired prestressed member can be predicted using cracked section analysis.
2) Comparison of test results and predictions showed that PCI and ACI Committee 440 guidelines accurately predict the behavior of a prestressed girder tested in shear both with and without the presence of CFRP.

REFERENCES

Aboutaha, Riyad S. "Rehabilitation of Reinforced Concrete Beams by the Use of Bonded Steel Plates." ACI Special Publication SP-174 p.225-244, April 1, 1998.

ACI 440.2R-02 "Guide for the Design and Construction of Externally Bonded FRP Systems for Strengthening Concrete Structures." Published by the American Concrete Institute, Farmington Hills, MI, pp 13, 2002.

ACI Committee 215. "Considerations for Design of Concrete Structures Subjected to Fatigue Loading (ACI 215R-74 revised 1997)", ACI Manual of Concrete Practice, American Concrete Institute, 1997.

Adhikary, B.B. and Mutsuyoshi, H. "Behavior of Concrete Beams Strengthened in Shear with Carbon-Fiber Sheets." Journal of Composites for Construction. 8.3 (2004): 258-264.

American Association of State Highway and Transportation Officials. AASHTO LRFD Bridge Design Specifications. AASHTO, 2004.

Arduini, M., Nanni, A., and Romagnolo, M. "Performance of Decommissioned RC Girders Strengthened with FRP Laminates." ACI Structural Journal. 99.5 (2002): 652-659.

Bentz, E. C. "Section Analysis of Reinforced Concrete Members", Ph.D. Thesis, University of Toronto, 2000.

Ceroni, F., Pecce, M., Prota, A., and Manfredi, G. "Flexural Strengthening of RC Beams using Emerging Materials: Cracking Behavior." Proceedings of the International Conference FRP Composites in Civil Engineering – CICE 2004 – Seracino (2004): 171-178.

ChemRex. EMACO® T430 2002. 9 August 2006 <http://www.cadeco.com/productfiles/MasterBuilders-EmacoT430.pdf>.

Collins, M.P. and Mitchell, D. “Prestressed Concrete Structures.” Prentice Hill, New Jersey, 1991.

De Lorenzis, L. and Nanni, A. "Shear Strengthening of Reinforced Concrete Beams with Near-Surface Mounted Fiber-Reinforced Polymer Rods.” ACI Structural Journal. 98.1 (2001): 60-68.

El-Tawil, S. and Okeil, A.M. "LRFD Flexural Provisions for PSC Bridge Girders Strengthened with CFRP Laminates." ACI Structural Journal. 99.2 (2002): 300-310.

Feldman, Lisa R., Jirsa, James O., and Kowal, Edward S.. "Repair of Bridge Impact Damage." Concrete International. 20.2 (1998): 61-66.

Fyfe Co. LLC. Tyfo SCH-41 Composite Using Tyfo S Epoxy. 2006. 7 July 2006 <http://www.fyfeco.com/products/compositesystems/sch-41.html>.

Fyfe Co. LLC. Tyfo P® Polymer Cement Modified Mortar. 2002. 9 August 2006 <http://www.fyfeco.com/products/concreterepair/pdf/p.pdf l>.

Green, P.S., Boyd, A.J., and Lammert, K. “CFRP Repair of Impact-Damaged Bridge Girders Volume 1 – Structural Evaluation of Impact Damaged Prestressed Concrete I Girders Repaired with FRP Materials.” Florida DOT Project BC354 RPWO #55, Gainesville, Florida, June 2004.

Hutchinson, R. and Rizkalla, S. “Shear Strengthening of AASHTO Bridge Girders Using CFRP Sheets.” ACI Special Publication SP-188, November 1999, pp 945-958.

Khaloo, A.R. “Shear Repair of Reinforced Concrete Beams Using Post-Tensioning.” ACI Special Publication SP-193 p. 519-550, 1 August 2000.

Klaiber, F.W., Wipf, T.J., Russo, F.M., Paradis, R.R., and Mateega, R.E. "Field/Laboratory Testing of Damaged Prestressed Concrete Girder Bridges." Iowa DOT Project HR-397, Final Report, Ames, Iowa, December 1999.

Li, A., Assih, J, and Delmas, Y. "Shear Strengthening of RC Beams with Externally Bonded CFRP Sheets." Journal of Structural Engineering. 127.4 (2001): 374-380.

Ludovico, Marco Di. "Experimental Behavior of Prestressed Concrete Beams Strengthened with FRP." Report CIES 03-42, University of Missouri-Rolla, Rolla, MO, 2003.

Ludovico, Marco Di, Nanni, A., Prota, A., and Cosenza, E. "Repair of Bridge Girders with Composites: Experimental and Analytical Validation." ACI Structural Journal. 102.5 (2005): 639-648

MacGregor, James G. and Wight, James K. Reinforced Concrete: Mechanics and Design. Upper Saddle River, New Jersey: Pearson Education, Inc., 2005.

Micelli, F., Annaiah, R., and Nanni, A. "Strengthening of Short Span RC-T Joists With FRP Composites." ASCE Journal for Composites in Construction. 6.4 (2002): 264-271.

Naaman, A.E. "Fatigue in Partially Prestressed Concrete Beams: Summary of Ten Years of Research", International Symposium on Fatigue and Fracture in Steel and Concrete Structures, 1991.

Oehlers, D.J., Seracino, R. Design of FRP and Steel Plated RC Structures. London: Elsevier Press, 2004.

PCI Design Handbook. 6th ed. Chicago, IL: Precast/Prestressed Concrete Institute, 2006.

Prota, A., Manfredi, G., Nanni, A., Cosenza, E., and Pecce, M. "Flexural Strengthening of RC Beams using Emerging Materials: Ultimate Behavior." Proceedings of the

International Conference FRP Composites in Civil Engineering – CICE 2004 – Seracino (2004).

Reed, Calvin E, and Peterman, Robert J. "Evaluation of Prestressed Concrete Girders Strengthened with Carbon Fiber Reinforced Polymer Sheets." ASCE Journal of Bridge Engineering. 9.2 (2004): 185-192.

Rizkalla, S., Rosenboom, O.A., and Miller, A.D. "Value Engineering and Cost Effectiveness of Various Fiber Reinforced Polymer (FRP) Repair Systems." Final Report Research Project 2005-10, July 2005, North Carolina DOT, Raleigh, NC.

Rosenboom, O.A. "Behavior of FRP Repair/Strengthening Systems for Prestressed Concrete." Ph.D Dissertation, North Carolina State University, Raleigh, NC, 2006.

Rosenboom, O.A. and Rizkalla, S. "Flexural Behavior of Aged Prestressed Concrete Girders Strengthened with Various FRP Systems." Accepted for publication in Construction and Building Materials, 2006.

Schiebel, S., Parretti, R., and Nanni, A. "Repair and Strengthening of Impacted PC Girders on Bridge A4845." Final Report RDT01-017/RI01-016, Nov. 2001, Missouri DOT, Jefferson City, MO, 21 pp.

Shanafelt, G.O. and Horn, W.B. "Damage Evaluation and Repair Methods for Prestressed Concrete Bridge Members." National Cooperative Highway Research Program Report 226, Transportation Research Board, 1980.

Sika Corporation. SikaTop®123 PLUS 2003. 9 August 2006 <http://www.sikaconstruction.com/tds-cpd-SikaTop123PLUS-us.pdfl>.

Stallings, J.M., Tedesco, J.W., El-Mihilmy, M., and McCauley, M. "Field Performance of FRP Bridge Repairs." Journal of Bridge Engineering. 5.5 (2000): 107-113.

Teng, J. G., Chen, J.F., Smith, S.T., and Lam, L. FRP Strengthened RC Structures. England: Wiley and Sons, Ltd, 2002.

Tumialan, J.G., Huang, P.C, and Nanni, A. "Strengthening of an Impacted PC Girder on Bridge A10062." Final Report RDT01-013/RI99-041, Nov. 2001, Missouri DOT, St. Louis County, MO, 41 pp.

Watson Bowman Acme Corporation. Wabo®MBrace Saturant, 2002. 9 August 2006. <http://www. degussa-cc-la.com/paises/caribbean/productos/mbracesaturant-eng.pdf>.

Zobel, R.S., Jirsa, J.O., Fowler, D.W., and Carrasuqillo, R.L. "Evaluation and Repair of Impact-Damaged Prestressed Concrete Bridge Girders." Report CTR 1370-3F, University of Texas, Austin, TX.

APPENDICES

APPENDIX A – CFRP FLEXURAL DESIGN EXAMPLE

A.1 Introduction

This appendix provides a design example to illustrate the various steps involved in the design of a CFRP flexural repair system for a prestressed concrete bridge girder. The analysis is based on a cracked section analysis, which is performed using the RESPONSE 2000© analysis program. The program is available to download free of cost, along with the instruction manual, at http://www.ecf.utoronto.ca/~bentz/home.shtml.

A.2 Problem Statement

A simply supported 50 ft (15.24 m) AASHTO Type II concrete bridge girder prestressed with sixteen 0.5 in (12.7 mm) diameter 270 ksi (1862 MPa) straight strands, as shown in Figure A.1, was impacted by an overheight vehicle 3 ft (0.91 m) from midspan. The impact caused significant loss of the concrete section as well as the rupture of three prestressing strands, or 18.8 percent loss of prestressing force. The objective is to restore the original flexural capacity of the member.

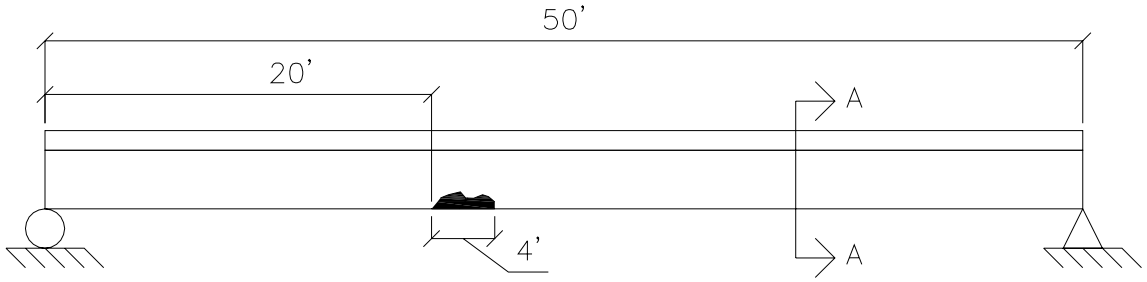

ELEVATION

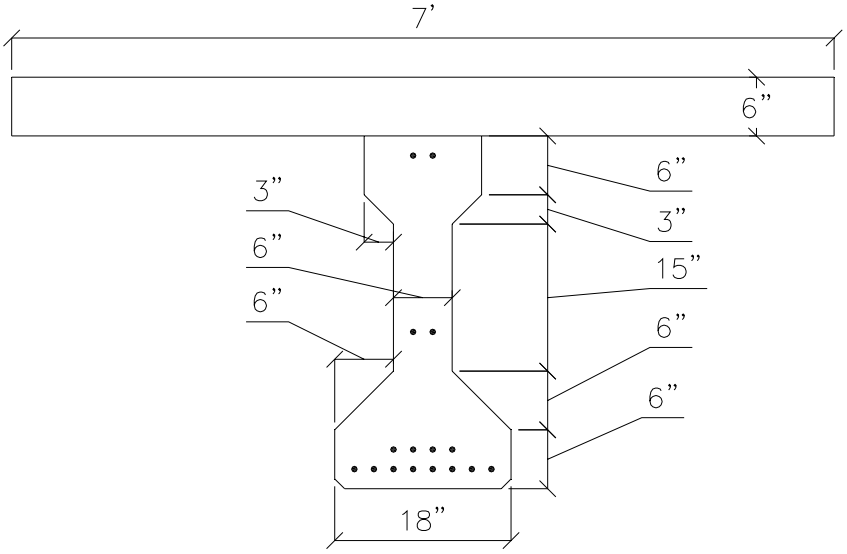

SECTION A-A

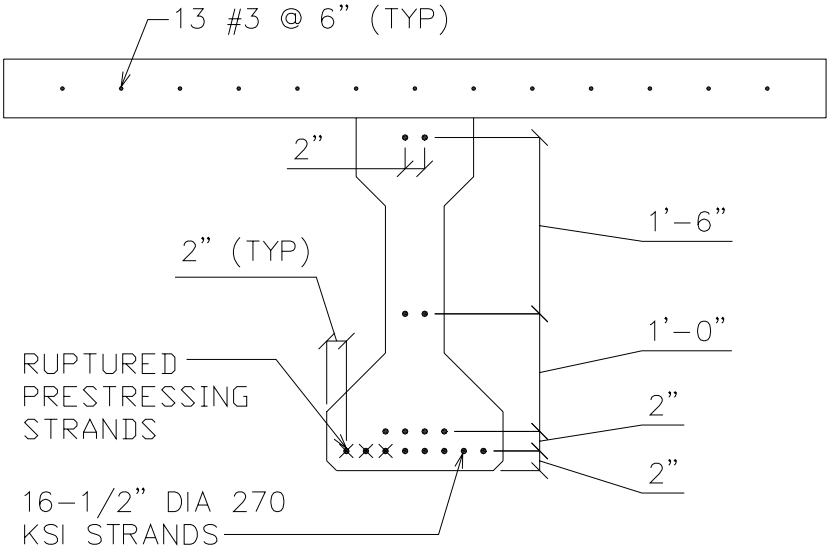

SECTION A-A

Figure A.1 Elevation and cross section of AASHTO Type II girder to repaired with CFRP

Testing of core samples taken from the girder indicates a concrete compressive strength in the girder of 6000 psi (41.4 MPa) and A 3000 psi (21.7 MPa) deck strength. The composite deck is 7 ft (2.14 m) wide by 6 in (152 mm) thick. The cross sectional area of each strand is A_{ps} = 0.167 in^2 (108 mm^2). Assume an initial prestress level of 0.7 f_{pu} and a total prestress loss of 20 percent. Use the Ramberg-Osgood equation for the stress-strain relationship of the strand:

$$f_p = E_p \varepsilon_{ps} \left[A + \frac{1 - A}{\left[1 + \left(B\varepsilon_{ps}\right)^C\right]^{1/C}} \right] \qquad \text{(A.1)}$$

where A = 0.015, B = 108, and C = 10, and E_p = 29000 ksi (200 GPa). Assume a rupture strain of 0.06 in/in. Non-prestressed reinforcement in the composite deck consists of thirteen #3 (D10) longitudinal bars spaced at 6 in (152 mm) and #4 (D13) closed-loops stirrups spaced at 9 in (229 mm) throughout the length of the girder.

It is proposed to use externally bonded CFRP wet lay-up sheets as the repair system. The material properties provided by the manufacturer are:

Ultimate tensile strength for design laminate:	143,000 psi (986 MPa)
Laminate thickness:	0.04 in (1 mm)
Tensile Modulus:	13.9 x 10^6 psi (95.8 GPa)
Ultimate elongation:	1.0%

A.3 Analysis of the Undamaged Section

The first step in the design is to conduct a flexural analysis of the undamaged section in order to predict the ultimate flexural strength of the girder.

Input of the Material and Geometric Properties

It is assumed that the reader is familiar with the RESPONSE 2000© Instruction Manual. Additional recommendations for input are described below:

1) The cross section of the AASHTO Type II girder can be chosen from the set of predefined shapes.
2) The material properties of the concrete can be automatically calculated by RESPONSE 2000© for the given value of $f_c^{'}$.
3) The effective width of the composite deck, 59.4 in (1509 mm) for this example, should be used to account for the difference in concrete strengths.
4) The material constants of the Ramber-Osgood equation are required to define the characteristics of the type of prestressing steel used.
5) The prestrain in the prestressing strands can be calculated using the Ramberg-Osgood equation by first calculating the stress in one of the prestressing strands after losses, then dividing the effective prestressing force by the modulus of elasticity and multiplying by 100 to determine the prestrain value in units of millistrain:

$$\text{prestrain} = \frac{f_{pe}}{E_{ps}} * 100 \qquad \text{(A.2)}$$

$$\text{where } f_{pe} = 0.7 f_{pu} \left(1 - 0.2\right) \qquad \text{(A.3)}$$

Moment-Curvature Response of the Section

Using RESPONSE 2000©, the moment versus curvature behavior of the prestressed section is easily obtained by clicking SOLVE >> SECTIONAL RESPONSE. The section response is shown in Figure A.2. Note that the mode of failure indicated is crushing of the concrete in the compression region of the girder. The undamaged section capacity was found to be 1960.9 k-ft (2585 kN-m).

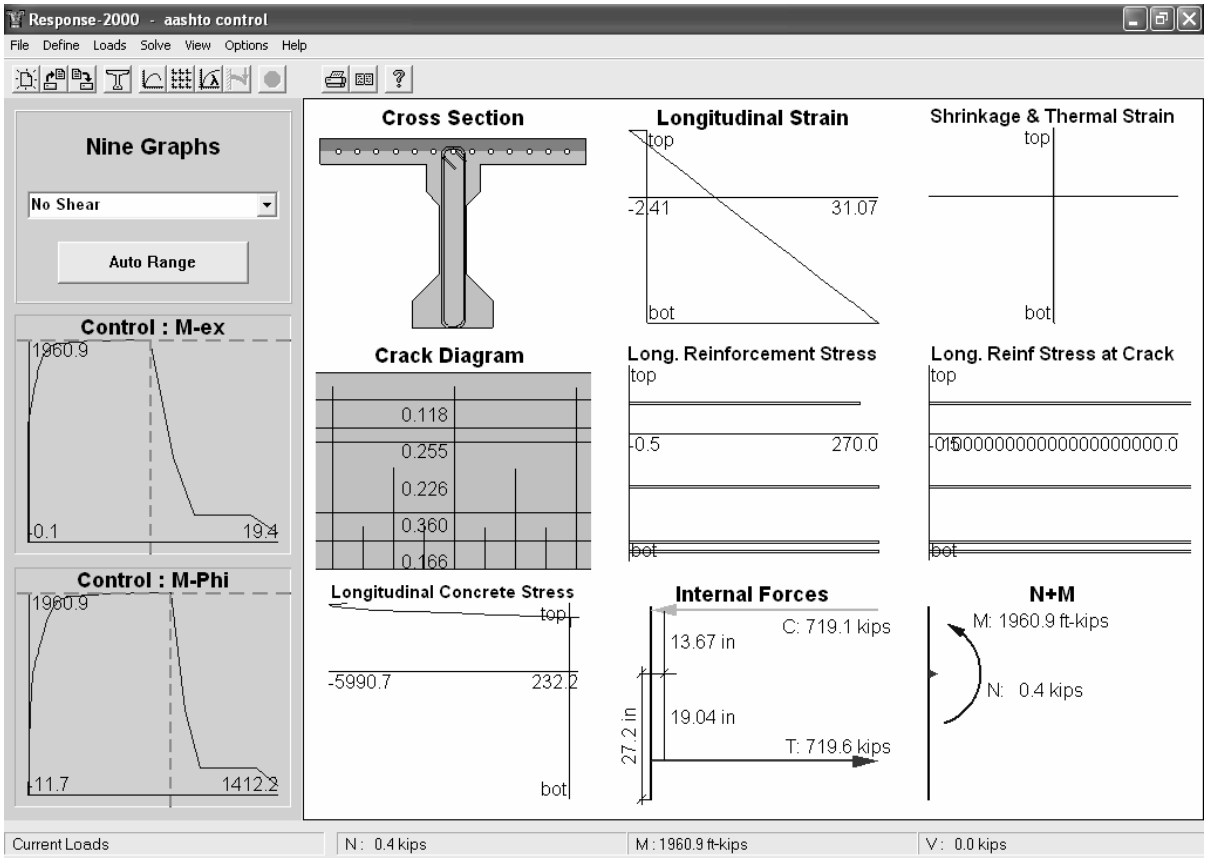

Figure A.2 Section analysis from RESPONSE 2000© of undamaged section

A.4 Analysis of the Damaged Section

After determining the undamaged flexural capacity of the section, the next step is to determine the damaged flexural capacity of the section. This is done by removing the proper number of prestressing strands from the cross section. It is important to not change the cross

section to account for removal of damaged concrete, in that this will incorrectly redistribute the initial prestressing forces. The damaged section capacity was found to be 1535.8 k-ft (2082 kN-m).

A.5 Design of the Longitudinal CFRP

After analyzing the undamaged and damaged sections, the next step is to choose the required amount of longitudinal CFRP to restore the original flexural capacity of the section.

Design Material Properties

The material properties provided by the manufacturer should be considered initial properties and should be appropriately reduced to account for environmental degradation. ACI Committee 440 (2002) recommends an environmental reduction factor (C_E) of 0.85 to be applied to the ultimate tensile strength (f_{fu}^*) and rupture strain (ε_{fu}^*) provided by the manufacturer for Carbon Fiber Reinforced Polymer materials subjected to exterior exposure. Therefore, the design ultimate strength (f_{fu}) and rupture strain (ε_{fu}) can be calculated as:

$$f_{fu} = C_E f_{fu}^* \tag{A.4}$$

$$= 0.85 \cdot (143)$$

$$= 121.5 \text{ ksi (838 MPa)}$$

$$e_{fu} = C_E \varepsilon_{fu}^* \tag{A.5}$$

$$= 0.85 \cdot (0.01)$$

$$= 0.0085 \text{ in/in}$$

using the reduced properties, the elastic modulus of the CFRP (E_f) can be calculated:

$$E_f = \frac{f_{fu}}{\varepsilon_{fu}} \tag{A.6}$$

$$= \frac{121.5}{0.0085}$$

= 14,300 ksi (98.6 GPa)

Input Material and Geometric Properties of CFRP

In consultation with the developer of the RESPONSE 2000© program, the procedure below should be followed for input of the material characteristics of CFRP:

1) The CFRP material properties should be input as "Longitudinal Reinforcement".
2) The "Elastic Modulus" should be input as E_{frp}. The "e-Strain Hardening" can be entered as $1000 \times \varepsilon_{fu}$. The "Rupture Strain" should be entered as $2 \times 1000 \times \varepsilon_{fu}$, a value recommended by the developer of the program.
3) When defining the FRP as "Longitudinal Reinforcement", the appropriate area and location of the FRP should be specified, even if it is located outside the concrete cross-section.
4) RESPONSE 2000© will unrealistically predict a large horizontal shear in the cover concrete below the lower prestressing strand if the transverse non-prestressed reinforcement is terminated at the bottom of the web. The transverse steel should extend to the centroid of the FRP to eliminate this problem; even though it will be located outside of the concrete cross-section.

Design of the Longitudinal CFRP

The task of this step is to determine the amount of CFRP required to restore the ultimate flexural capacity of the damaged section. Based on section analysis of the

unstrengthened section, the ultimate flexural capacity was found to be 1960.9 k-ft (2585 kN-m). Similarly, the ultimate flexural capacity of the damaged section was found to be 1535.8 k-ft (2082 kN-m). We need to add sufficient CFRP to gain an internal moment capacity of 425.1 k-ft (576.4 kN-m). After several trials, it was found that two layers of CFRP 16 in (406 mm) wide gives an area of CFRP, $A_{FRP} = (2)(0.04)(16) = 1.28$ in^2 (826 mm^2), which exceeds our required moment capacity with a value of 1979.1 k-ft (2683 kN-m), as shown in Figure A.3. It should be noted that the mode of failure predicted by RESPONSE 2000[2] for the repaired section was rupturing of the longitudinal CFRP.

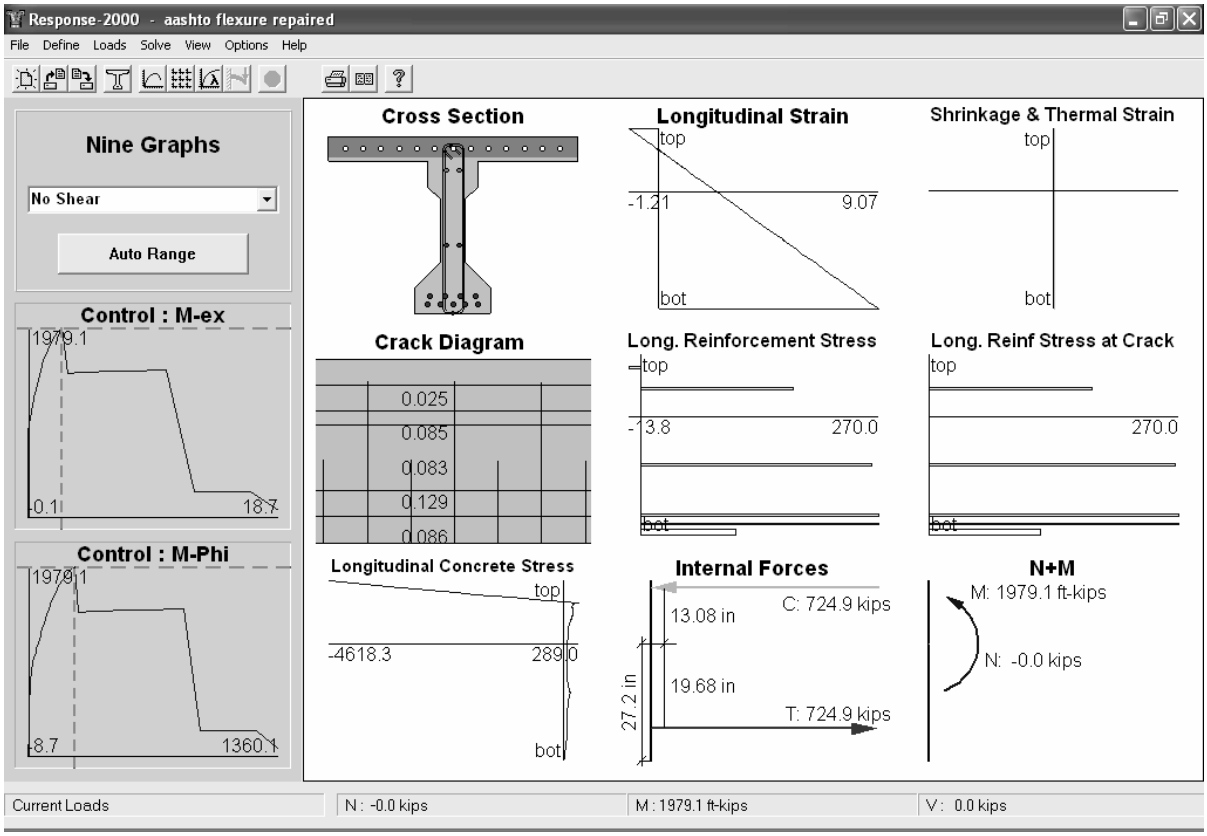

Figure A.3 Section analysis from RESPONSE 2000© of CFRP repaired section

Stress Ratio in Prestressing Strands

According to design guidelines presented in Rizkalla (2005), the stress ratio in straight prestressing strands should not exceed 5 percent under service loading. This must be

confirmed in order to prevent the rupture of prestressing strands under cyclic service loading. The dead load moment due to the self weight of the girder and the composite deck can be determined assuming that the unit weight of concrete is 150 lbs/ft^3 (23.56 kN/m^3) as follows:

$w_{DLg} = 0.384$ k/ft (5.61 kN/m)

$w_{DLd} = 0.525$ k/ft (7.66 kN/m)

$$M_{DL} = \frac{(0.384 + .525) \cdot (50)^2}{8}$$

$= 284.1$ k-ft (385.2 kN-m)

The maximum allowable live load was determined as the load that induced a maximum tensile stress in the extreme bottom of the concrete flange equal to $3\sqrt{f'_c}$ psi ($0.25\sqrt{f'_c}$ MPa), which is specified by the AASHTO (2004) code for service loading in corrosive environments. The corresponding allowable live load moment is equal to 556.1 k-ft (754.0 kN-m), therefore the service loading conditions will vary between a minimum value of:

$M_{DL} = 284.1$ k-ft (385.2 kN-m)

and a maximum value of:

$M_{DL+LL} = 840.2$ k-ft (1139 kN-m)

From the "Section Response" screen in the lower left corner is the "Control: M-Phi" plot. The cursor on this plot can be moved to show the corresponding strains, stresses and forces acting on the section at any given value of moment. At values of moments equal to the DL and the DL+LL shown above, the stress in the reinforcing can be determined using Response 2000© and is given in Table A.1. Using the following equation, the stress ratio can be calculated for the 270 ksi (1862 MPa) prestressing strands:

$$SR_{ps} = \frac{f_{ps2} - f_{ps1}}{f_{pu}} \times 100 \quad \text{(A.7)}$$

Table A.1 Stress ratios in the prestressing strands of repaired AASHTO girder

Prestressing strand location	**Bottom**
Type of strand	Straight
Stress at DL, ksi	145.5
Stress at DL+LL, ksi	153.3
SR_{ps}, %	2.89
SR_{ps} limit from guidelines, %	5

The analysis indicated that the stress ratios in prestressing strands of the repaired girder at the service loading levels are below the specified values recommended in the design guidelines.

Check Deflections

AASHTO (2004) specifies in Article 2.5.2.6.2 a maximum deflection (Δ_{max}) due to dead load and vehicular live load of:

$$\Delta_{max} = \frac{l_g}{800} \quad \text{(A.8)}$$

where l_g is the girder span length (in inches). For our girder span, this limit corresponds to 0.75 in (19.1 mm). The dead and live load moments previously found can be resulted into concentrated loads at midspan from:

$$P_{DL} = \frac{(284.1)\cdot(4)}{50}$$

$$= 22.7 \text{ k } (101 \text{ kN})$$

$$P_{LL} = \frac{(556.1)\cdot(4)}{50}$$

$$= 44.5 \text{ k } (198 \text{ kN})$$

The service load level, P_s, at which the deflection should be calculated should include the dead load, P_{DL}, and the live load, P_{LL}, multiplied by the impact factor, IM, as follows:

$$P_s = 22.7 + 44.5$$

$$= 67.2 \text{ k } (299 \text{ kN})$$

In RESPONSE 2000©, the full member response can be calculated by entering various properties under LOAD >> FULL MEMBER PROPERTIES. The values given below correspond to a simply supported girder, 50 ft (15.2 m) clear span, loaded with a concentrated load at midspan.

1) "Length subjected to shear" equal to half of the girder span, 300 in (7620 mm).
2) "Constant Moment zone on right" equal to zero.
3) Use "Constant shear analysis", "support on bottom", and "Load on continuous beam, load on top", to create a simply supported girder.

The full member response of the girder can be calculated by clicking on SOLVE >> MEMBER RESPONSE. Due to symmetry, RESPONSE 2000© only calculates the response of half of the member, so the load versus deflection plot shown in the lower left hand corner is half of the actual member response. The deflection at half the service load, $P_s/2$, is 0.20 in (5.1 mm), therefore the AASHTO deflection criteria is satisfied. The member response is shown in Figure A.4.

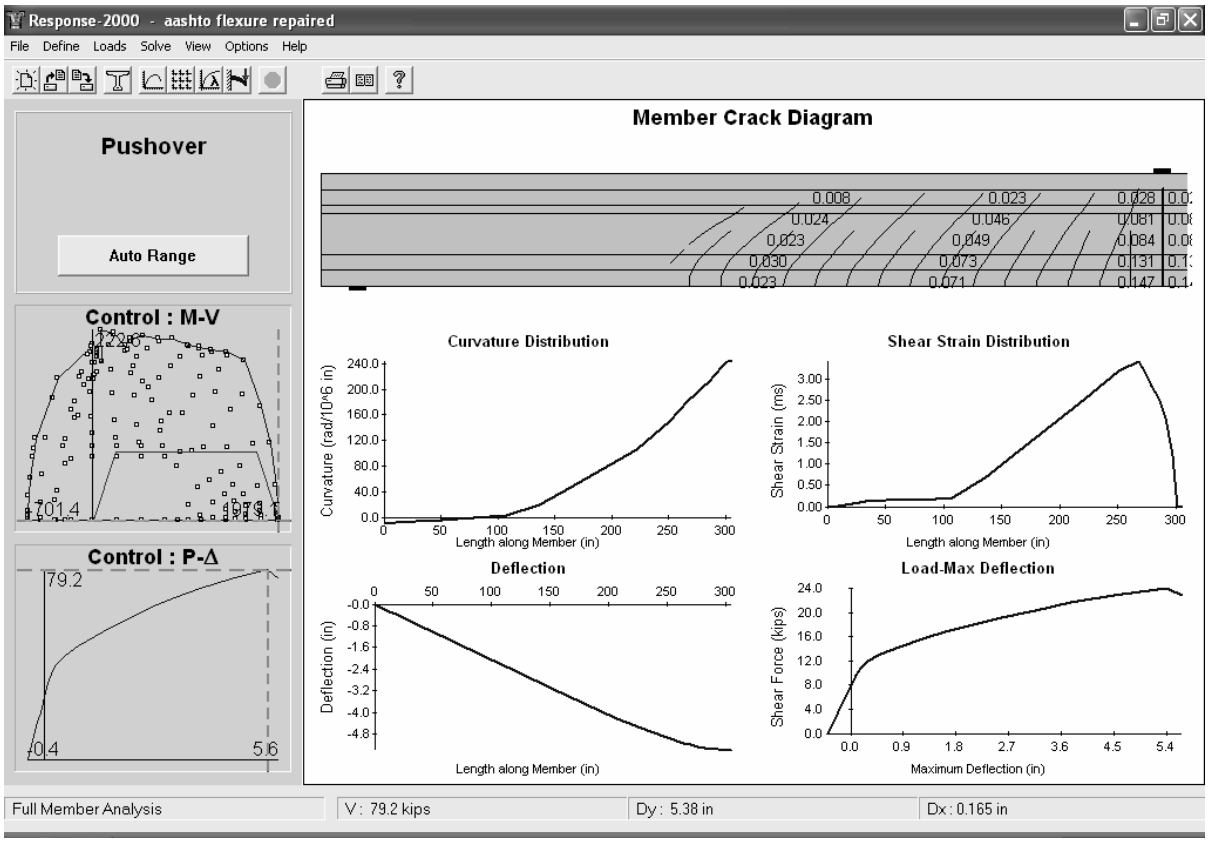

Figure A.4 Member response of CFRP repaired girder

A.6 CFRP Detailing

To ensure full usage of material capacities and to control premature failures due to debonding, the following detailing should be included in the design:

1) Each layer of longitudinal CFRP must extend past the damage a length equal to or greater than the development length of the prestressing strands.
2) The termination of the longitudinal CFRP sheets should be staggered to minimize plate-end debonding effects.
3) To further control plate-end type debonding, 12 in (305 mm) wide transverse CFRP U-wraps should be provided at the termination point of each layer of the

longitudinal CFRP. The U-shape should extend to the top flange on both sides of the girder.

4) Additional transverse U-wraps, identical to the ones described above, should be provided at intervals of 3 ft (914 mm) or less along the length of the longitudinal CFRP to control possible intermediate crack debonding.
5) Continuous 2 ft (610 mm) wide transverse U-wraps should be provided, with minimum spacing in between, at the location of the repair mortar to minimize cracking in the non-prestressed region.

APPENDIX B – CFRP SHEAR DESIGN EXAMPLE

B.1 Introduction

This appendix provides a design example to illustrate the various steps involved in the design of a CFRP system to repair lateral impact damage of a prestressed concrete bridge girder near a support. The analysis is based on guidelines proposed by the Precast/Prestressed Concrete Institute (PCI) Design Handbook (2006) for the shear strength of prestressed concrete members and ACI Committee 440 (2002) proposed guidelines for the contribution of CFRP used in shear applications.

B.2 Problem Statement

A simply supported 50.0 ft (15.24 m) AASHTO Type II concrete bridge girder prestressed with sixteen 0.5 in (12.7 mm) diameter 270 ksi (1862 MPa) straight strands, as shown in Figure B.1, was impacted by an overheight vehicle 3 ft (0.91 m) from the face of the left support. The impact caused a loss of the concrete section along a 4 ft (1.22 m) length of the girder, including the loss of 3 in (76.2 mm) of the web cross section, as well as rupturing three prestressing strands. The primary objective is to restore the original shear capacity of the member.

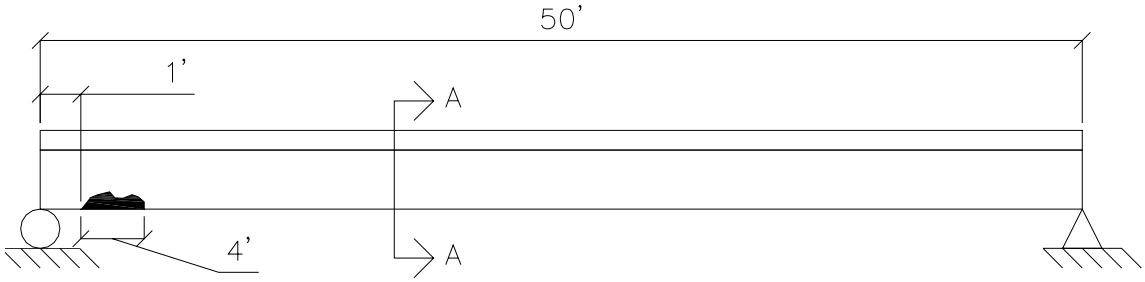

ELEVATION

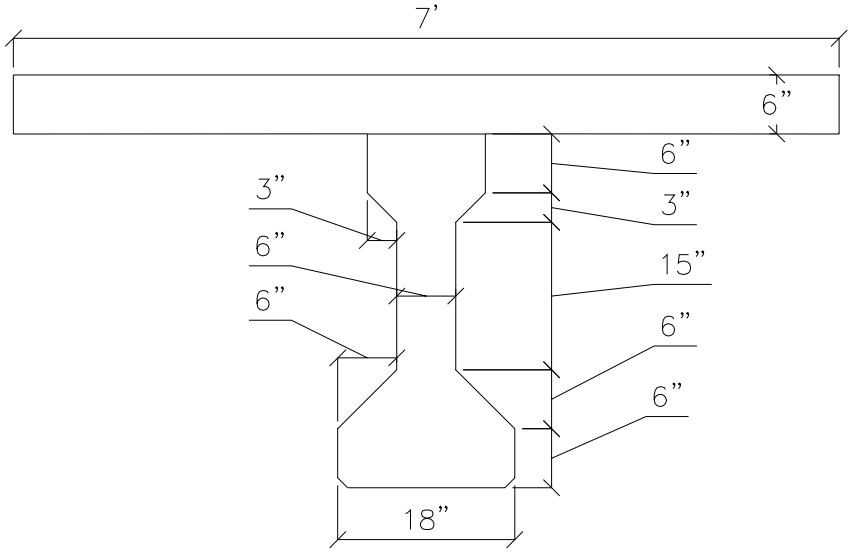

SECTION A-A

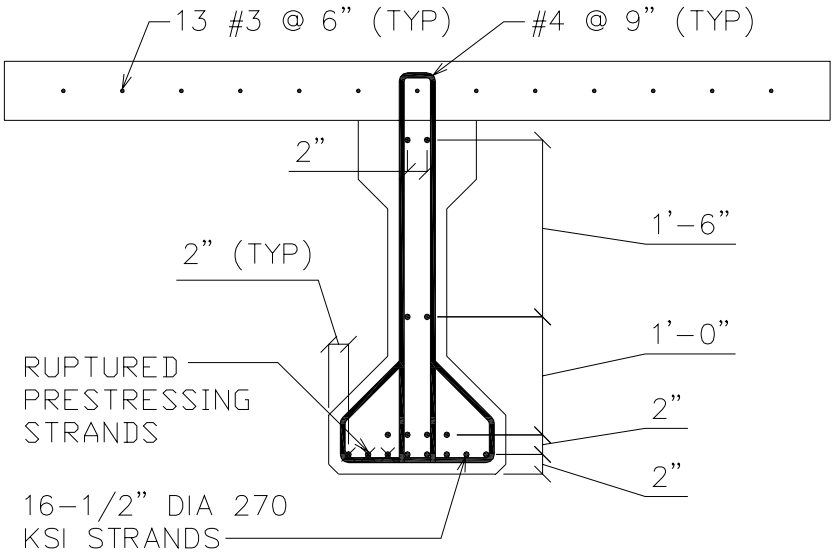

SECTION A-A

Figure B.1 Elevation and cross section of AASHTO Type II girder repaired with CFRP

The composite deck is 7 ft (2.14 m) wide by 6 in (152 mm) thick. Testing of core samples taken from the girder indicates a concrete compressive strength in the girder of 6000 psi (41.4 MPa) and a 3000 psi (21.7 MPa) deck strength. The cross sectional area of each strand is A_{ps} = 0.167 in^2 (108 mm^2). Assume an initial prestress level of 0.7 f_{pu} and a total prestress loss of 20 percent. Use the Ramberg-Osgood equation for the stress-strain relationship of the strand:

$$f_p = E_p \varepsilon_{ps} \left[A + \frac{1 - A}{\left[1 + \left(B\varepsilon_{ps}\right)^C\right]^{1/C}} \right] \qquad \text{(B.1)}$$

with A = 0.015, B = 108, and C = 10, and E_p = 29000 ksi (200 GPa). Assume a rupture strain of 0.06 in/in. Non-prestressed reinforcement in the composite deck consists of thirteen #3 (D10) longitudinal bars spaced at 6 in (152 mm) and #4 (D13) closed-loops stirrups spaced at 9 in (229 mm) throughout the length of the girder. It is proposed to use externally bonded CFRP wet lay-up sheets as the repair system. The material properties provided by the manufacturer are:

Ultimate tensile strength for design laminate:	143,000 psi (986 MPa)
Laminate thickness:	0.04 in (1 mm)
Tensile Modulus:	13.9 x 10^6 psi (95.8 GPa)
Ultimate elongation:	1.0%

B.3 Analysis of the Undamaged Section

The first step in the design is to conduct a shear analysis of the undamaged girder at various intervals to predict the nominal shear strength at each section. The nominal shear strength, $V_n = V_c + V_s$ is found by adding up the contribution of the concrete and the steel

stirrups at each section. Since the nominal shear capacity changes at each section, this example shows a sample calculation of the shear capacity of the section at the centerline of the damage, or 3 ft (0.91 m) from the left support.

In order to calculate the shear capacity of a prestressed member, the applied loads first need to be determined. Finding the critical shear loading scheme for the girder was performed using AASHTO (2004) moving truck load design guidelines. After several iterations, the critical loading scheme was determined and is shown in Figure B.2. Due to the location of the damage, it was decided that the critical loading scheme would induce the largest constant shear force throughout the damaged region.

From the PCI Design Handbook (2006), the contribution of the concrete (V_c) to the shear capacity of the section is the lesser value of V_{cw} and V_{ci}, calculated as follows:

$$V_{ci} = 0.6\sqrt{f_c'}\,b_w d + V_d + \frac{V_i M_{cr}}{M_{\max}} \tag{B.2}$$

$$= 0.6\sqrt{6000}\,(6)(33.75)/1000 + 20.01 + \frac{(51.36)(23,467)}{1,849}$$

= 681 k (3030 kN)

and

$$V_{cw} = \left(3.5\sqrt{f_c'} + 0.3 f_{pc}\right) b_w d + V_p \tag{B.3}$$

$$= \left(\left(\frac{3.5\sqrt{6000}}{1000}\right) + 0.3(404/369)\right)(6)(33.75) + 7.4$$

= 128 k (569 kN)

where V_d is the shear force caused by the unfactored dead load, V_i is the factored shear force at a section due to externally applied loads, M_{cr} is the cracking moment of the section, $M_{\max}$

is the maximum factored moment at a section due to externally applied loads, f_{pc} is the compressive stress in concrete at the centroid due to effective prestressing forces, and V_p is the vertical component of the effective prestress force at the section centroid. M_{cr} is the cracking moment and can be calculated as:

$$M_{cr} = \left(\frac{I}{y_t}\right)\left(6\sqrt{f_c^{'} + f_{pe} - f_d}\right) \tag{B.4}$$

where I is the moment of inertia, y_t is the distance from the top of the girder to the center of gravity, f_{pe} is the compressive stress in the concrete at the extreme tension fiber due to the effective prestressing force, and f_d is the stress due to service dead load. Since $V_{cw} < V_{ci}$, then the contribution of concrete to the nominal shear strength of the girder is 128 k (569 kN).

The contribution of the steel stirrups (V_s) to the shear capacity of the section is primarily dependent on the size of the reinforcing bar used and the spacing between bars. The stirrup contribution is calculated as follows:

$$V_s = \frac{A_v f_y d}{s} \tag{B.5}$$

$$= \frac{(0.44)(60)(33.75)}{9}$$

= 99 k (440 kN)

where A_v is the area of the shear reinforcement, f_y is the yield stress of the shear reinforcement, and s is the spacing between stirrups. The shear contribution of the stirrups is 99 k (440 kN).

The total nominal shear strength (V_n) is 128 + 99 = 227 k (1010 kN). The nominal shear capacity of the entire girder was calculated at different sections in the same manner as above, except in the transfer region of the prestressing strands. The transfer region is defined as $50d_b = 50 * 0.5 = 25$ in (635 mm), where d_b is the diameter of the prestressing strand. In order to account for this lesser bond strength in the transfer region, PCI (2006) guidelines specify that the shear capacity at the end of the girder be governed by $3.5\sqrt{f_c'}\,(b_w)(d) = 3.5\sqrt{6000}\,(6)(33.75) = 54.9$ k (244 kN). A linear interpolation is then performed between this value and the shear capacity 25 in (635 mm) from the end of the girder. The nominal shear capacity and the factored applied shear load along the entire length of the girder are shown in Figure B.2. The factored applied loading diagram shown in Figure B.2 was calculated using a dead load factor of 1.2, a live load factor of 1.7, and an impact factor of 1.33, all per AASHTO (2004).

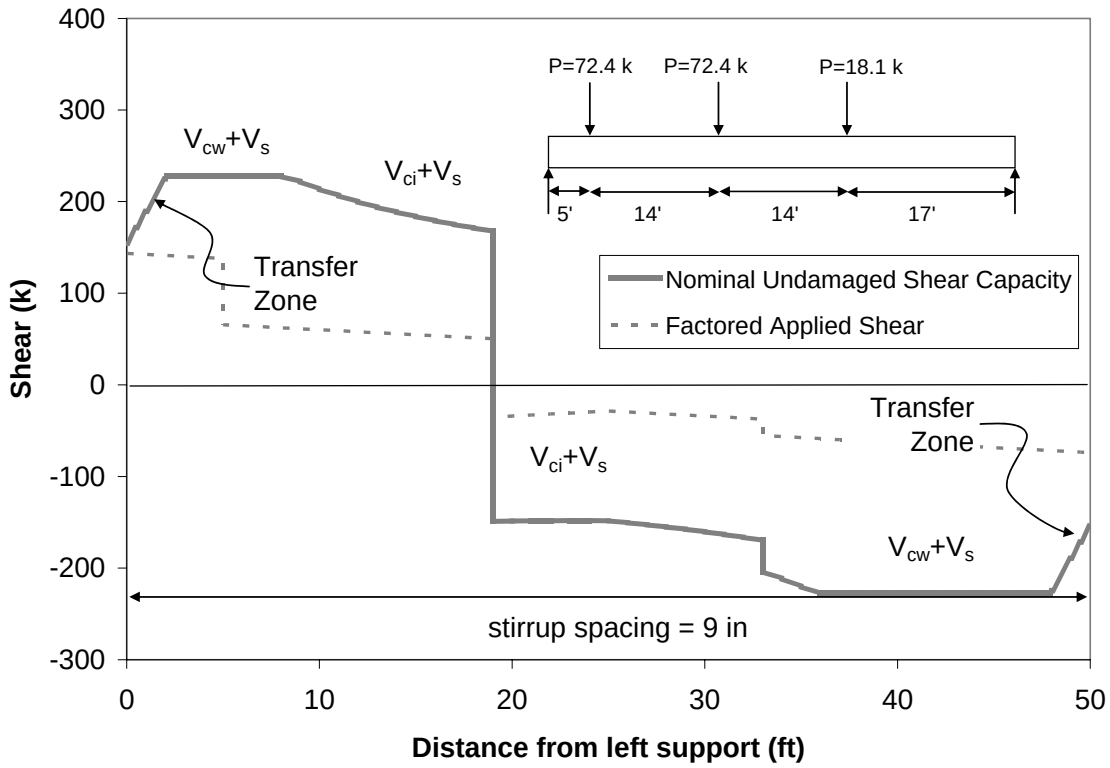

Figure B.2 Nominal undamaged shear capacity of AASHTO Type II girder

B.4 Analysis of the Damaged Section

The next step in the design of a CFRP shear repair system is to analyze the nominal shear strength of the damaged girder. This is performed in the same manner as previously described for the undamaged section, except several changes are made to correspond with the lateral impact damage. Unlike the flexural design example shown in Appendix A, the shear design model requires that the loss of concrete section be included as well as the loss of prestressing strands. The most critical variable in a shear-critical specimen is the width of the web (b_w). The girder is evaluated at various sections along the entire length to determine the nominal shear capacity envelope. A sample calculation of the damaged section 3 ft (0.91 m) from the left support, the same location examined in detail above, is presented below. V_c is calculated in the same manner as before using equation B.2 and B.3, as shown:

$$V_{ci} = 0.6\sqrt{6000}\,(3)(33.75)/1000 + 20.01 + \frac{(51.36)(25,605)}{1,849} \qquad \text{(B.2)}$$

= 736 k (3270 kN)

and $$V_{cw} = \left(\left(\frac{3.5\sqrt{6000}}{1000}\right) + 0.3(328/291)\right)(3)(33.75) + 7.4 \qquad \text{(B.3)}$$

= 69.1 k (307 kN)

Since $V_{cw} < V_{ci}$, then the contribution of concrete to the nominal shear strength of the girder is 69.1 k (307 kN), which is 58.9 k (262 kN) less than the undamaged concrete section shear capacity contribution.

The contribution of the steel stirrups changes throughout the length as a result of the width of the web changing through the damaged section. Per PCI (2006), the maximum allowed contribution of the steel stirrups, $V_s = 8\sqrt{f_c'}\,b_w d$, exceeds the direct calculation of the stirrups contribution.

$$V_s = 8\sqrt{f_c'}\,b_w d \qquad \text{(B.6)}$$

$$= 8\sqrt{6000}\,(3)(33.75)$$

= 62.7 k (279 kN)

Therefore, the contribution of the steel stirrups at this location is 62.7 k (279 kN), which is 36.3 k (161 kN) less than the undamaged section stirrup shear capacity contribution. As previously described, the transfer zone at each end of the girder was taken into account, but in addition to the transfer zones at the ends of the girder, a third transfer zone is created beyond the ruptured prestressing strands that must be taken into account. To be conservative, it is assumed that all prestressing strands are effected in this other transfer zone, not just the

ruptured ones. The nominal shear capacity of the entire girder was calculated at different sections in the same manner as above and plotted with factored applied loads in Figure B.3.

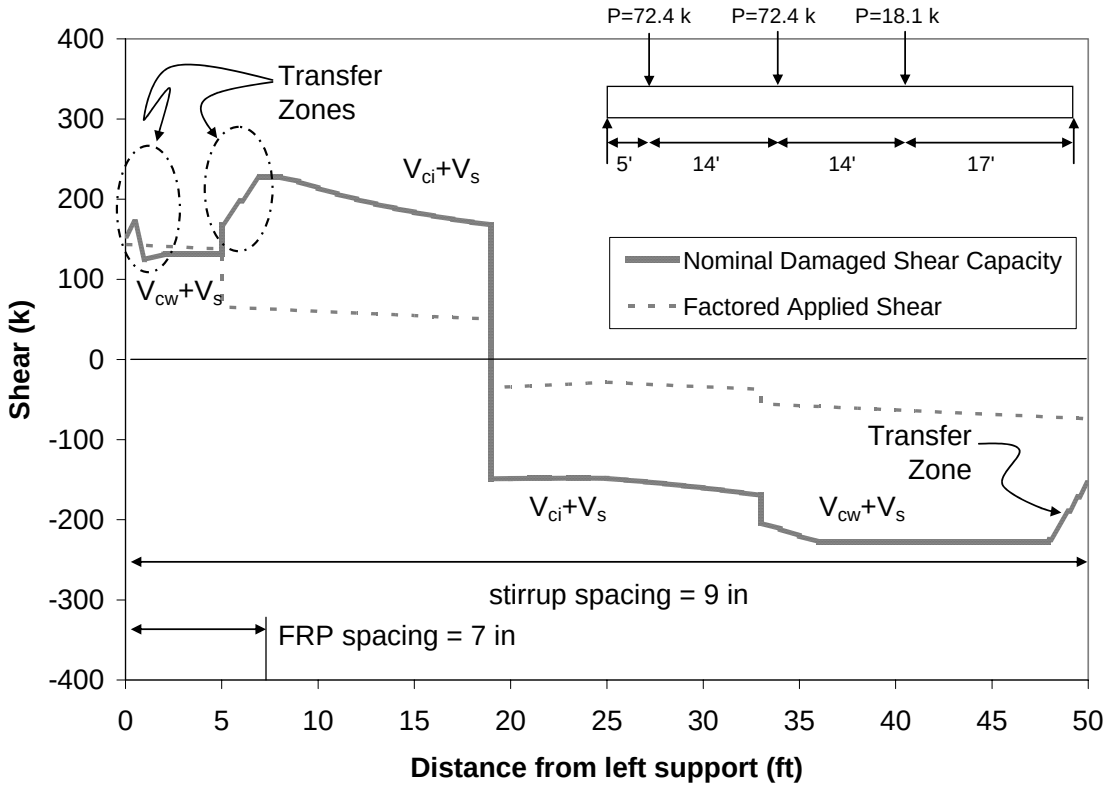

Figure B.3 Nominal damaged shear capacity of AASHTO Type II girder

B.5 Design of the Transverse CFRP

After the analysis of the undamaged and damaged sections, the next step is to choose the required amount of transverse CFRP to restore the original shear capacity at each section along the length of the girder.

Design Material Properties

The material properties provided by the manufacturer should be considered initial properties and should be appropriately reduced to account for environmental degradation. ACI Committee 440 (2002) recommends an environmental reduction factor (C_E) of 0.85 to

be applied to the ultimate tensile strength (f_{fu}^{*}) and rupture strain (ε_{fu}^{*}) provided by the manufacturer for CFRP materials subjected to exterior exposure. Therefore, the design ultimate strength (f_{fu}) and rupture strain (ε_{fu}) can be calculated as:

$$f_{fu} = C_E f_{fu}^{*} \tag{B.7}$$

$$= 0.85 \cdot (143)$$

$$= 121.5 \text{ ksi (838 MPa)}$$

$$e_{fu} = C_E \varepsilon_{fu}^{*} \tag{B.8}$$

$$= 0.85 \cdot (0.01)$$

$$= 0.0085 \text{ in/in}$$

using the reduced properties, the elastic modulus of the CFRP (E_f) can be calculated:

$$E_f = \frac{f_{fu}}{\varepsilon_{fu}} \tag{B.9}$$

$$= \frac{121.5}{0.0085}$$

$$= 14{,}300 \text{ ksi (98.6 GPa)}$$

Design of the Transverse CFRP

The task of this step is to determine the amount of CFRP required to restore the nominal shear capacity at each section along the girder. Again for this example, we will analyze the same section, 3 ft (914 mm) from the left support, which was previously analyzed in the undamaged and damaged example. From these previous examples, analysis of the undamaged and damaged sections yielded nominal shear capacities of 227 k (1010 kN) and 132 k (587 kN), respectively. For this particular section, we need to add sufficient CFRP

to increase the shear capacity by 227 – 132 = 95 k (423 kN). At this point, the ACI Committee 440 (2002) recommendations for shear contribution of CFRP are used. After several trials, it was found that 1 layer of 6 in (152 mm) wide CFRP sheets, with a 1.0 in (25.4 mm) space between sheets, oriented at 45 degrees to the left of horizontal would provided a shear contribution of 101.4 k (451 kN), which exceeds our deficit of 95 k (423 kN). The steps involved using the ACI Committee 440 (2002) guidelines are as follows. First, an area (A_{fv}) of transverse CFRP is chosen, which is calculated as follows:

$$A_{fv} = 2nt_f w_f \tag{B.10}$$

$$= 2(1)(.04)(6)$$

$$= 0.48 \text{ in}^2 \text{ (310 mm}^2\text{)}$$

where n is the number of layers, t_f is the thickness of each layer, and w_f is the width of each layer of CFRP. The next step is to find the active bond length of the FRP (L_e), which is the length over which the majority of the bond stress is maintained. The active bond length is calculated as shown:

$$L_e = \frac{2500}{\left(nt_f E_f\right)^{0.58}} \tag{B.11}$$

$$= \frac{2500}{\left((1)(.04)(14{,}300)(1000)\right)^{0.58}}$$

$$= 1.14 \text{ in (30.0 mm)}$$

where E_f is the modulus of elasticity calculated using Equation B.9. The next step is to calculate the bond reduction modification factors k_1 and k_2. k_1 accounts for the concrete

strength while k_2 accounts for the wrapping scheme used, which in our case is U-wraps. These factors are calculated as shown:

$$k_1 = \left(\frac{f_c'}{4000}\right)^{2/3} \tag{B.12}$$

$$= \left(\frac{6000}{4000}\right)^{2/3}$$

$$= 1.31$$

$$k_2 = \frac{d_f - L_e}{d_f} \text{ for U-wraps} \tag{B.13}$$

$$= \frac{28 - 1.14}{28}$$

$$= 0.96$$

where f_c' is the compressive strength of the concrete and d_f is the depth of the FRP shear reinforcement taken from the centroid of the tension steel to the top of the transverse sheet. After determining the modification factors, the next step is to determine the bond reduction factor (k_v) as shown:

$$k_v = \frac{k_1 k_2 L_e}{468\varepsilon_{fu}} \le 0.75 \tag{B.14}$$

$$= \frac{(1.31)(0.96)(1.14)}{(468)(0.0085)}$$

$$= 0.36$$

where ε_{fu} is found using Equation B.8. The next step is to determine the effective strain in the FRP at failure (e_{fe}), as follows:

$$\varepsilon_{fe} = k_v \varepsilon_{fu} \le 0.004 \tag{B.15}$$

$$= (0.36)(0.0085)$$

$$= 0.00306 \text{ in/in}$$

After finding the effective strain, the next step is to find the effective stress at failure (f_{fe}) as shown below:

$$f_{fe} = \varepsilon_{fe} E_f \tag{B.16}$$

$$= (0.00306)(14,300)$$

$$= 44.0 \text{ ksi } (303 \text{ MPa})$$

The final step is to determine the unreduced nominal shear strength (V_f) provided by the transverse FRP, as shown:

$$V_f = \frac{A_{vf} f_{fe} (\sin\alpha + \cos\alpha) d_f}{s_f} \tag{B.17}$$

$$= \frac{(0.48)(44.0)(\cos(45) + \sin(45))28}{7}$$

$$= 119.4 \text{ k } (531 \text{ kN})$$

where α is the angle of inclination of the FRP (in degrees), and s_f is the spacing of the transverse FRP reinforcement.

Lastly, V_f must be reduced by $\psi = 0.85$ to account for any uncertainties in the material properties, therefore ψV_f = 101.4 k (451 kN). Figure B.4 shows the repaired shear capacity along with the undamaged shear capacity at each section of the girder; for comparative purposes. The factored applied load is also shown in Figure B.4 It is evident

that the repaired capacity is higher than the original capacity throughout the entire member length.

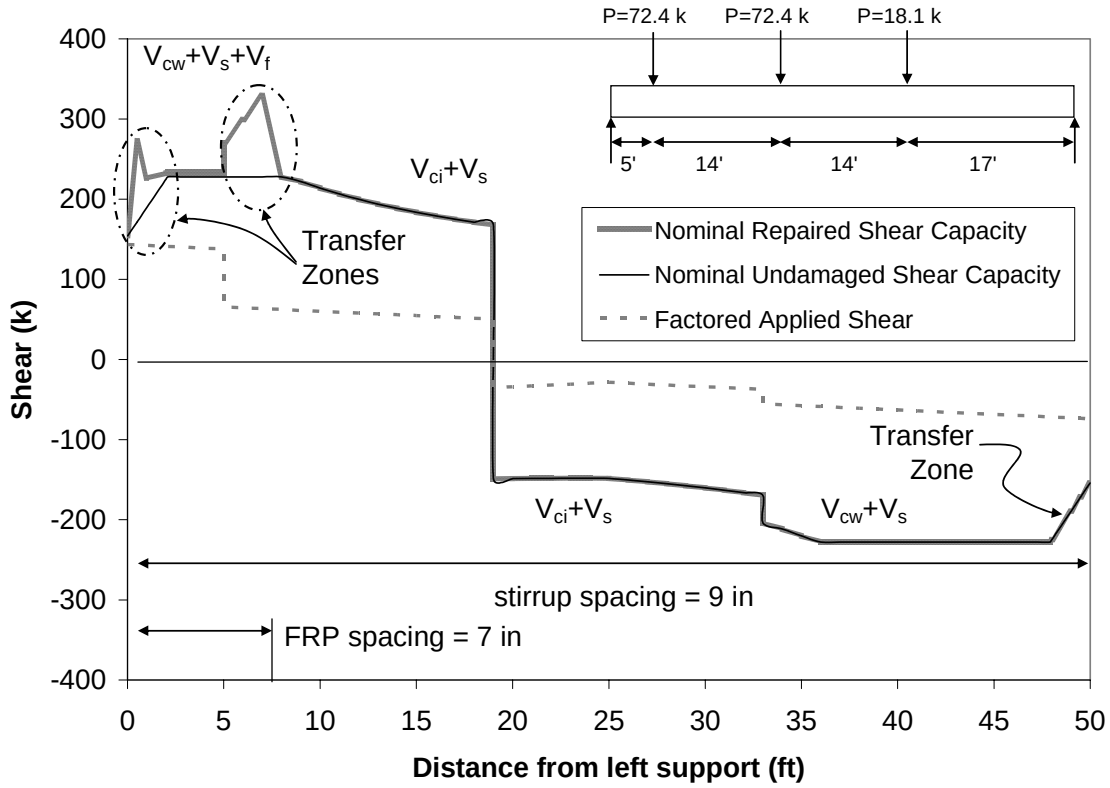

Figure B.4 Nominal shear capacity of undamaged and repaired girder

B.6 Design of the Longitudinal CFRP

The design of the longitudinal CFRP to restore the flexural capacity of the section should be performed in the same manner as previously described in Appendix A. The design calls for two layers of 16 in (406 mm) wide sheets to restore the flexural capacity. These longitudinal sheets should begin at the left support and extend for a minimum of 8 ft (2.44 m), according to the CFRP detail recommendations provided.

B.7 CFRP Detailing

The following details, in conjunction with the details laid out in Appendix A for flexural repairs using CFRP materials, should be included to ensure full effectiveness of the individual CFRP sheets and CFRP repair system as a whole:

1) The diagonal CFRP struts should be continuous from the top flange on one face to the opposite side of the bottom flange, forming a crossing pattern on the bottom with the strut on the opposite face.
2) To further control plate-end type debonding, one 12 in (305 mm) wide transverse CFRP U-wrap should be provided at the centermost termination point of the bottom layer of the longitudinal CFRP. The U-wrap should extend to the top flange on both sides of the girder.
3) To account for the outward forces created, one longitudinal layer of CFRP should be provided on each side of the girder at the intersection of the bottom flange and bottom of the web.